KTH Royal Institute of Technology
AVL MTC Motortestcenter AB

Battery Testing for Emerging Battery Applications in Industrial and E-mobility Sectors

Francisco Javier Carreras

Degree Project in Energy Technology
Second Cycle 30 credits
Stockholm, October 24, 2023

Department of Energy Technology
KTH Royal Institute of Technology

Examiner: Justin Chiu

KTH Supervisor: Taras Koturbash

Industrial Supervisor: Filippa Bengtsson

Industrial contact person: Filippa Bengtsson

AVL

Master of Science Thesis
Department of Energy Technlogy
KTH 2023

Improved testing strategies from Standards for New Growing Battery Applications in the Industrial and E-Mobility Sectors

TRITA-ITM-EX 2023:136

Francisco Javier Carreras

	Examiner	Supervisor
Approved	Justin Chiu	Taras Koturbash
	Industrial Supervisor	Industrial Contact person
	Filippa Bengtsson	Filippa Bengtsson

Resumen

En los actuales retos energéticos, relacionados tanto con el cambio climático como con la repentina subida de los precios de la energía, las baterías desempeñan un papel clave en el suministro y almacenamiento de energía. Previo a su comercialización, las baterías se someten repetidamente a distintos tipos de pruebas, ya que es de crucial importancia garantizar el rendimiento y la seguridad de estas tecnologías en las distintas aplicaciones.

Este trabajo de fin de máster está enfocado a mejorar las metodologías de ensayo de baterías para hacer frente a la creciente demanda de baterias en los sectores industriales y de transporte. Al identificar y entender las brechas existentes en las Normas Estándar Internacionales, este trabajo pretende mejorar el vínculo entre las pruebas de baterías y su uso práctico en las distintas aplicaciones, con el objetivo final de desarrollar un marco de pruebas adaptable para AVL MTC Motortestcenter AB, una empresa líder en ingeniería y sistemas de propulsión.

El estudio presentado investiga los mayores factores detrás de los ensayos de baterías, el impacto de las diversas aplicaciones en las características nóminales de las baterías y busca optimizar las estrategias de ensayo en cuanto a tiempo, dificultad y coste. La metodología incluye un estudio exhaustivo de la operación de las baterías, una revisión de sus parámetros de rendimiento y un análisis de los procedimientos de ensayo actuales en distintos Estándares Internacionales.

El resultado es el desarrollo de un algoritmo que genera ciclos de trabajo sintéticos adaptables y reales, junto con nuevos procedimientos de ensayo para pruebas de capacidad y ciclo de vida útil. La optimización de los procedimientos de ensayo permite a AVL asumir un papel destacado en la electrificación industrial y en los ensayos de prueba de baterías, ofreciendo soluciones más precisas, eficaces y reduciendo su coste. Por último, este trabajo contribuye al desarrollo de una industria más sostenible al facilitar el uso seguro y eficiente de las tecnologías de baterías en aplicaciones emergentes, especialmente dentro del sector de transporte.

Abstract

In the current energy challenges, related to both climate change and the sudden rise in energy prices, batteries plays a key role in providing and storing energy. Before batteries are sent to market, the batteries are repeatedly subjected to different types of tests since it is crucial to verify that the performance and safety of these technologies are ensured in the different applications.

This master's thesis is dedicated to improving battery testing methodologies to address the growing industrial and e-mobility sectors. By identifying and tackling gaps in existing international standards, this research aims to enhance the link between battery testing and real-life operation of batteries, with the final objective of developing an adaptable testing framework for AVL MTC Motortestcenter AB, a leading powertrain systems company.

The study investigates the factors driving battery testing, the impact of diverse applications on battery characteristics, and the need for refined testing strategies. The methodology includes a comprehensive background study of battery behavior, a review of battery performance parameters, and an analysis of prevailing testing procedures.

The research results in the development of an algorithm for adaptable synthetic duty cycles, along with new testing procedures for capacity and cycle lifetime tests. The optimization of testing procedures enables AVL to take a prominent role in electrification and battery testing, offering more accurate and effective testing solutions. Ultimately, this contributes to a more sustainable industry by facilitating the secure and efficient use of battery technologies in emerging applications, particularly within the transport sector.

Contents

List of Figures

List of Tables

1 Introduction

1.1 Emissions

The Paris Agreement, agreed upon by 195 nations in 2015, aims to limit the rise of global temperature to no more than 2°C above pre-industrial levels, and even pursue efforts to limit it to 1.5°C. It also aims to strengthen countries' abilities to deal with the impacts of climate change (European Commission, 2023). The European Union (EU) Green Deal, inspired by the Paris Agreement, is a coordinated set of policies and legislation designed to lower the European Union's global warming emissions to zero over the next 30 years. The EU has already surpassed its initial target of reducing green house gases (GHG) by 20% below 1990 levels by achieving a 34% reduction by 2020, eliminating 1,939 million tonnes CO2 equivalents as shown in Figure 1. However, this might have been largely influenced by the Covid-19 pandemic. Nonetheless, the EU has become more ambitious and is now targeting a further reduction of 60% below 1990 levels for 2030, 80% for 2040, and zero emissions by 2050 (Seront et al., 2022). It should be noted that GHG emissions are typically expressed as CO_2 equivalents, which includes all gases that contribute to global warming.

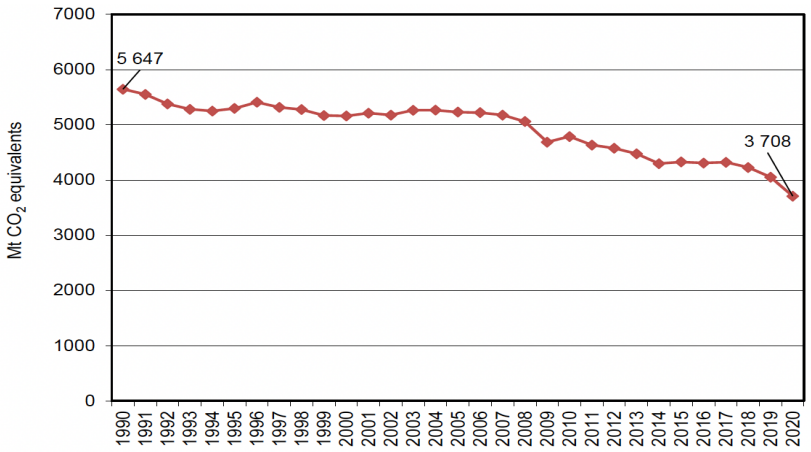

Figure 1: EU-27, the UK and Iceland indirect GHG emissions from 1990 to 2020 (Seront et al., 2022).

The decrease in EU emissions observed over the past 30 years is attributable to several factors, such as the increased use of renewable energy sources, the utilization of less carbon-intensive fossil fuels, improvements in energy efficiency, and changes in the economy's structure (IEA, 2022b). Figure 2 displays the global CO_2 emissions generated from fuel combustion by sector in 2021.

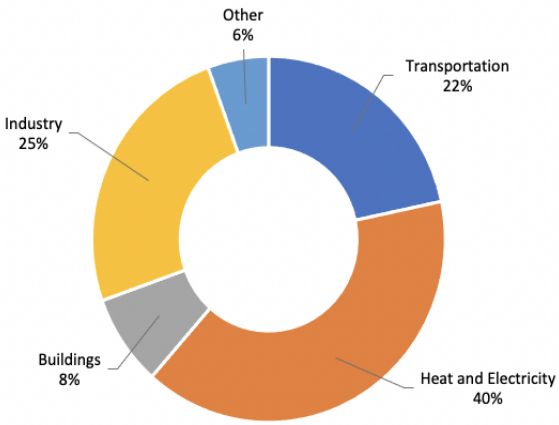

Figure 2: Global CO2 emissions generated from fuel combustion by sector in 2021 (IEA, 2022b).

The transport sector, which is highly dependent on oil, accounts for almost a quarter of global CO_2 emissions and remains one of the only sectors in the EU economy where emissions are still above 1990 levels. The European climate targets cannot be achieved without reducing emissions in this sector (Taljegard, 2017). Therefore, the EU defined the Transport White Paper, which sets out ambitious goals, including a 50% reduction of conventionally fueled cars in urban transport by 2030, phasing them out in cities by 2050, and achieving essentially CO2-free city logistics in major urban centers by 2030. Parallel to this, the Alternative Fuels Strategy was adopted in 2013, which recognized the need for a combination of several options to meet the goals set in emission reductions for respective transport mode. Amongst them, electric mobility is expected to play a significant role in achieving the set of goals imposed (Meyer et al., 2017).

The transport sector can be further divided into several sectors, each contributing differently to global emissions, as seen in Figure 3.

43.7% of the domestic transport emissions in the EU is produced by Light Duty Vehicles (LDVs), followed by heavy trucks at 18.9%. Hybrid technologies such as plug-in-hybrid-electric-vehicles (PHEVs) and hybrid-electric-vehicles (HEVs), together with battery-electric-vehicles (BEVs) have successfully lowered car overall emissions by almost 50% since 2006 (ACEA, 2022). This is mainly due to average diesel vehicles consuming 5-6 kWh/10 km, while a BEV equivalent in size would consume only 1.5 kWh/10 km, a 75% reduction. All these solutions are a result of an extensive R&D of the battery sector and currently on the rise (Campillo et al., 2017).

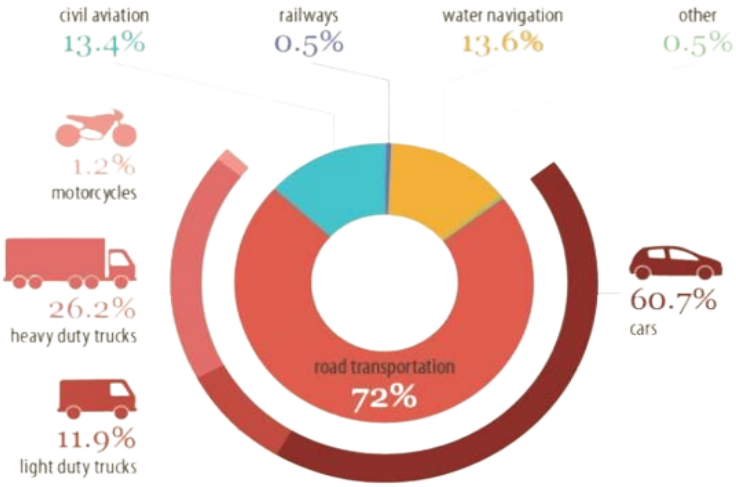

Figure 3: CO2 emissions from domestic transport in the EU in 2019 (Szymanski et al., 2021).

However, heavier vehicles have lagged behind due to higher durability requirements, cost sensitivity, and power density requirements. In fact, heavy and light-duty trucks, along with the marine sector, account for over 40% of emissions in the transport sector, and this number continues to increase (Szymanski et al., 2021).

On the one hand, heavy trucks have experienced a 36% increase in emissions between 1990 and 2010, despite some advancements in their fuel efficiency. Another significant rise in emissions is expected from 2010 to 2030. The success in the electrification of cars is inspiring the potential electrification of Heavy-duty-vehicles (HDVs). In fact, the transition towards electric trucks has already begun, when the EU launched its first HDV strategy in May 2014 (Meyer et al., 2017). Since then, Electric buses and heavy-duty truck sales are increasing every year. In 2021, electric bus and heavy-duty truck registrations rose by 40% and 200%, respectively, compared to 2020 volumes (IEA, 2021).

In the case of the shipping industry, it is responsible for over 3% of all anthropogenic CO2 emissions worldwide, with regulations currently in place to reduce emissions from burning fossil fuels. Electrified drive trains have already been introduced in vessels operating on short journeys and recent advances in battery technology are allowing bigger ships to travel longer distances using fully electric or hybrid-electric power (Meyer et al., 2017). According to Erno Tenhunen, marine director of Danfoss Power Solutions', "the maritime sector recognizes that electrification is the future of the industry" as the sector finally identifies a tremendous opportunity for zero-emission shipping by using fuel cells and/or renewable sources (Danfoss, 2022).

On the other hand, the aviation industry aims to reduce CO_2 emissions by 75% and NOx emissions by 90% by 2050 through better aerodynamics and using cleaner biofuels. Electrification of this sector seems to be a promising solution for eventually making aircrafts emission-free, but this is not currently viable in the short-term due to high power and low weight requirements in the existing battery packs (Meyer et al., 2017; Laestander, 2017). Since this thesis aims to study new growing battery applications in the upcoming years, batteries in aviation will not be considered for the scope of this project.

1.2 Battery market

From the scenario described so far, it is clear that a change in the propulsion technologies used in the transport sector is necessary in order to comply with climate targets. This is developing a pressing need and market opportunities to find ways to reduce emissions in the sector. There are many alternative technology proposals that could cut emissions and bring us closer to the Net-Zero-Emission (NZE) target, including hydrogen engines, biomass and many others. Among all technologies, the most advanced and promising is the use of batteries as a propulsion system, given their rapid development in recent years. The NZE scenario predicts a substantial increase in annual battery demand, from 340 GWh in 2021 to 5,600 GWh by 2030 (IEA, 2022d).

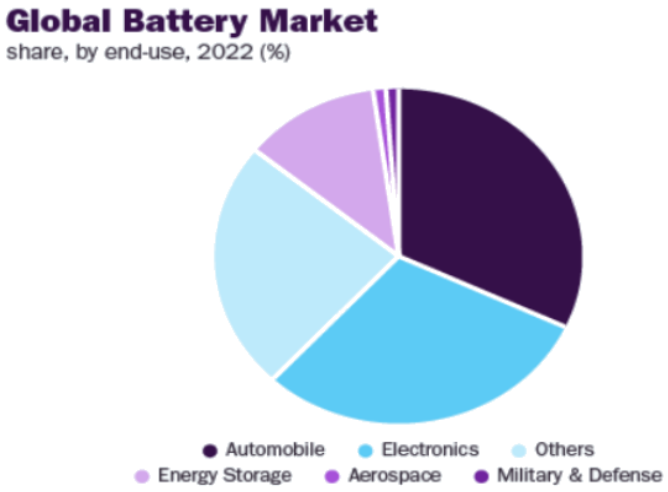

Figure 4: Global Battery Market share for different industrial sectors, 2022 (Grand View Research, 2023).

As it is shown in Figure 4, the automotive sector is leading this growth with a market share of 32,37% in 2022 (Grand View Research, 2023). Within the automotive sector, electric cars account for three-quarters of the projected total by 2030 (IEA, 2021). This large market share

can be explained by several reasons that follow a causal effect:

1. The large potential to reduce GHG and energy consumption in the transport sector, heavily associated to the recent increase in oil prices (Szymanski et al., 2021).

2. The numerous legislation's and regulations issued to achieve the goal of NZE and more sustainable mobility have pushed Original Equipment Manufacturers (OEMs) to announce emission-reduction targets through the development of new engine technologies (Fleischmann et al., 2023).

3. The benefits of electrifying the various transport modes (Szymanski et al., 2021):

    - Electric powertrains are more energy efficient than conventional ones.
    - Electricity can make direct use of energy from renewable sources.
    - Batteries of electric vehicles could stabilize the grid and facilitate the integration of renewable sources.

Beyond that, electronics are the second-largest segment of battery demand, with wide-ranging applications in portable consumer electronic devices. The remaining end-use segments include industrial, medical, construction, mining, with most of these industries utilizing batteries for supplying backup power to critical machinery and equipment. To meet this increasing annual battery demand, that will reach 5600 GWh by 2030, an additional output of around 150 gigafactories of 35 GWh annual production capacity operating at full capacity is required. Nevertheless, the industry is well-prepared to respond to this surge in demand, having undertaken strategic early investments in battery plant capacity (IEA, 2022d). Battery production capacity is mainly concentrated in China, although more investments are now being planned in other regions. A quarter of battery production capacity is expected to be in Europe and the United States by 2030, as they look to become more independent by establishing a local eco-friendly supply chain of batteries (IEA, 2021; Cole, 2019).

Among all the technologies, Lead-based and Li-ion batteries will remain the most important ones in the market, and, compared with 2020, they are expected to increase in capacity 20% and 274%, respectively, in 2030 as is shown in Figure 5. On one hand, lead-based batteries will remain dominant in auxiliary applications (12V) in the battery system of cars, but will only make up a very small global market share (3%) in the battery industry by 2030 (Pillot, 2020).

On the other hand, Lithium-Ion will remain the main battery technology used in powertrain for mobility because of their better energy density, lifetime and capacity.

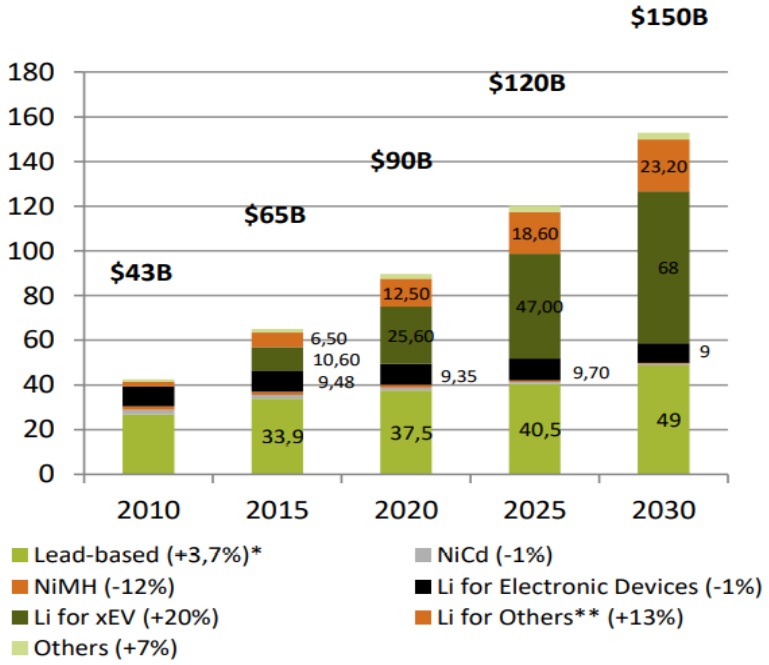

Figure 5: Battery Market value among different battery technologies (Pillot, 2020)

.

For Lithium-ion battery, it can be noticed how its development is going to be consistent throughout the coming years. This growth is driven not only by the increasing demand for electric cars and other transportation sectors, but also in various of its different applications like portable electronic devices and backup power for critical machinery and equipment. The entire market value of the Li-Ion batteries is expected to reach in 2030 a market value of about $100b which will represent 66% of the total battery market value of $150b (Pillot, 2020).

1.3 Battery testing

As the battery market is expected to have significant growth in the coming years, it becomes important to focus on one of the main aspects of batteries, such as testing battery performance. The global battery testing equipment market is expected to grow with a Compound Annual Growth Rate (CAGR) of 5% between 2022-2030. It was valued at USD 11,2 million in 2021 and is expected to generate 16,7 million by 2030.

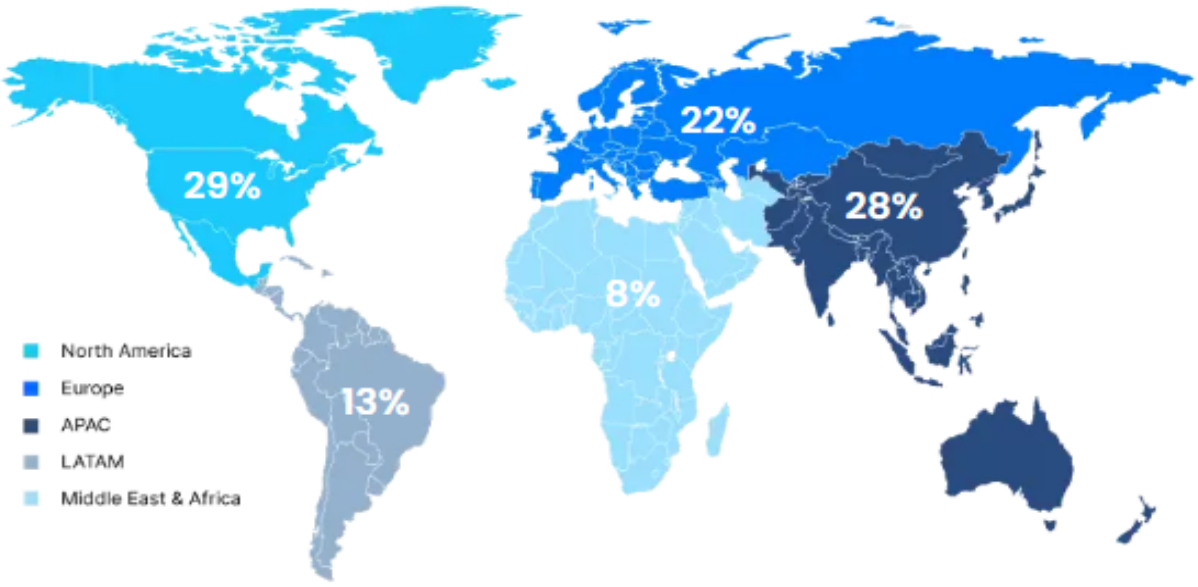

Figure 6: Battery Testing Market value in the world in 2021 (Straits Research, 2022)

.

In 2021, the biggest market share in the world for battery testing equipment was held by North America with a market value of USD 3,1 million, as shown in Figure 6. In 2030, it is expected to grow to USD 4,1 million, with a CAGR of 3%, due to the large amount of government and corporate investments taking place in these countries in the electronic industry. This growth shows, once again, the gaining importance of batteries in the industry. In second place was Asia-Pacific with a value of USD 2.998 million, with China and India leading the way due to the increase in certain factors, such as the growth in the use of electric vehicles. Europe also played an important role with a market value of USD 2,374 million in 2021, with France and Germany holding the largest share of the market. Due to the presence of large lithium reserves and the low cost of extraction and labour, Central & South America and The Caribbean foresee great market growth, as they could become a strategic centre for the production of rechargeable batteries, starting from a current value of USD 1,392 million. Finally, the Middle East & Africa close the classification with a market value of USD 864 million, which is also expected to increase in the coming years due to the great development of these countries recently (Straits Research, 2022).

Rigorous testing is necessary to ensure batteries meet government-mandated safety requirements and perform well under specific environmental stresses. By subjecting batteries to testing and certifying them according to globally recognized standards, it can be assured that reliable

products that will perform as expected are received. However, testing can be time-consuming and expensive, and new advances are needed to simulate the most realistic scenarios possible in a shorter period of time and at a lower cost. This is how the accelerated charge/discharge test to measure the lifespan of a battery was established, to avoid running the test for as long as the desired lifespan of the battery (i.e. 15 years). But, important factors have to be considered in order to realistically obtain reliable battery testing results, such as time degradation mechanisms in this example. Identifying these factors is the hardest part and various analytical methods are necessary to evaluate batteries and battery components at different scales. In addition, with new products and growing applications for batteries, new battery developments are going to be necessary to meet the different requirements of the application. Since each battery is unique in composition and has its own use and purpose, companies must learn how to adapt established testing methods to new performance standards for these applications. For this, it is important to fully understand the nature of battery testing in order to comprehend how differences between batteries can affect testing conditions and strategies. Only then will it be possible to develop new standards on effective and efficient testing methods for new applications.

1.4 The company: AVL MTC Motortestcenter AB

AVL is one of the world's leading mobility technology companies for development, simulation, and testing in the automotive industry, and in other sectors by providing concepts, solutions, and methodologies for a greener, safer, and better world of mobility. The objective is to expand their portfolio of high-end methodologies and technologies in the areas of vehicle development and testing. With a holistic approach from ideation phase to serial production they cover vehicle architectures and platform solutions including the impact of new propulsion systems and energy carriers for all applications, from traditional to hybrid to battery and fuel cell electric technologies. As a global technology provider, the offerings range from simulation, virtualization, and test automation for product development to ADAS/AD and vehicle software. AVL's mission is to move towards a safe and comfortable driving experience for everyone by finding more efficient and greener solutions to improve the mobility. Scandinavia is an important and strategic area for the global automotive industry, thus AVL presents different offices in the area which all are included under the Swedish affiliate of AVL MTC.

Figure 7: AVL MTC in Haninge, location where we performed this thesis

.

1.5 Purpose

The purpose of this master thesis study is to analyze and understand the nature of battery testing and battery behavior, with the final objective of developing an adaptable and improved battery testing methodology for AVL MTC, a leading company in development, simulation and testing of powertrain systems in different industries. This methodology will be built based on gaps that we have found on the most known international standards.

More specifically, this thesis will try to answer the following research questions:

1. What are the driving factors behind battery testing, including the reasons for testing a specific parameter and the reason for doing it in a certain way?

2. What are the characteristics that differentiate batteries for different applications, and how do these translate into differences in testing conditions and strategies?

3. What is lacking in current international standards and how can these gaps be tackled?

4. How can AVL MTC adapt their testing strategy to fill these gaps and keep up with advancements in battery technology, while ensuring the safety, reliability, and efficiency of the batteries for their intended applications?

By addressing these questions, this thesis aims to provide AVL MTC with a comprehensive understanding of battery testing and eventually help them develop an adaptable and robust testing framework for new batteries of varying characteristics. This will enable AVL MTC to

take the lead in the field of electrification and battery testing, while providing clients with more accurate and effective testing solutions. Furthermore, it may contribute to the development of new business models (i.e. Testing x consulting packages) that can benefit the company in the short and long run. Ultimately, this thesis will contribute to the development of a more sustainable and environmentally friendly industry, particularly in the transport sector, by enabling the safe and efficient use of battery technologies in new growing applications.

1.6 Methodology

The methodology for this thesis is illustrated in Figure 8 and described below:

1. Introduction:
    - Provide an overview of the research problem and the limitations of the thesis.
    - Clearly state the research objectives and research questions.
2. Background Review:
    - Conduct a comprehensive background study on batteries to gain a basic understanding of battery behavior, operation, and factors affecting performance.
    - Conduct a state-of-the-art review on the most important battery performance parameters.
    - In parallel, research growing applications for batteries in the industry, especially in the transport sector, and study their market size in the near future and potential for battery implementation in the application.
    - Out of the entire market study, select two applications which seem more promising in the near future and more relevant for AVL MTC.
3. Literature Review:
    - Literature review of current testing procedures in 6 internationally reknown standards with regards to main performance parameters analyzed in the background review with respect to both selected applications
    - Analyse and investigate the gaps missing in the standards and how could they potentially be improved to better reflect real-life usage of the battery.
4. Analysis and Optimization of existing testing procedures:

- Analyze and compare the effect of different parameters which are not considered in current standards for both applications.
- Modify a robust algorithm that can help generate synthetic duty cycles that can adapt to the different applications and generate more accurate and reliable test results.
- Optimization of existing testing procedures to better represent real-life conditions by including the main gaps missing.

5. Testing Validation:

   - Construction of two battery modules from scratch, to gain comprehensive knowledge of the required materials and subsequently assess the effectiveness of our modified procedures by conducting tests on these modules.
   - In case this is not possible due to time limitations, validate results with data provided to us and data from the literature.

6. Analysis of Results:

   - Analyze the results from real-life testing and/or simulations and compare them to the existing testing procedures.
   - Evaluate the effectiveness of the testing procedures and identify areas for improvement.

7. Conclusion and Future Work:

   - Summarize the key findings and contributions of the thesis.
   - Highlight the practical implications of the research and potential future work in the field.
   - Conclude the thesis with recommendations for AVL MTC and other battery testing companies.

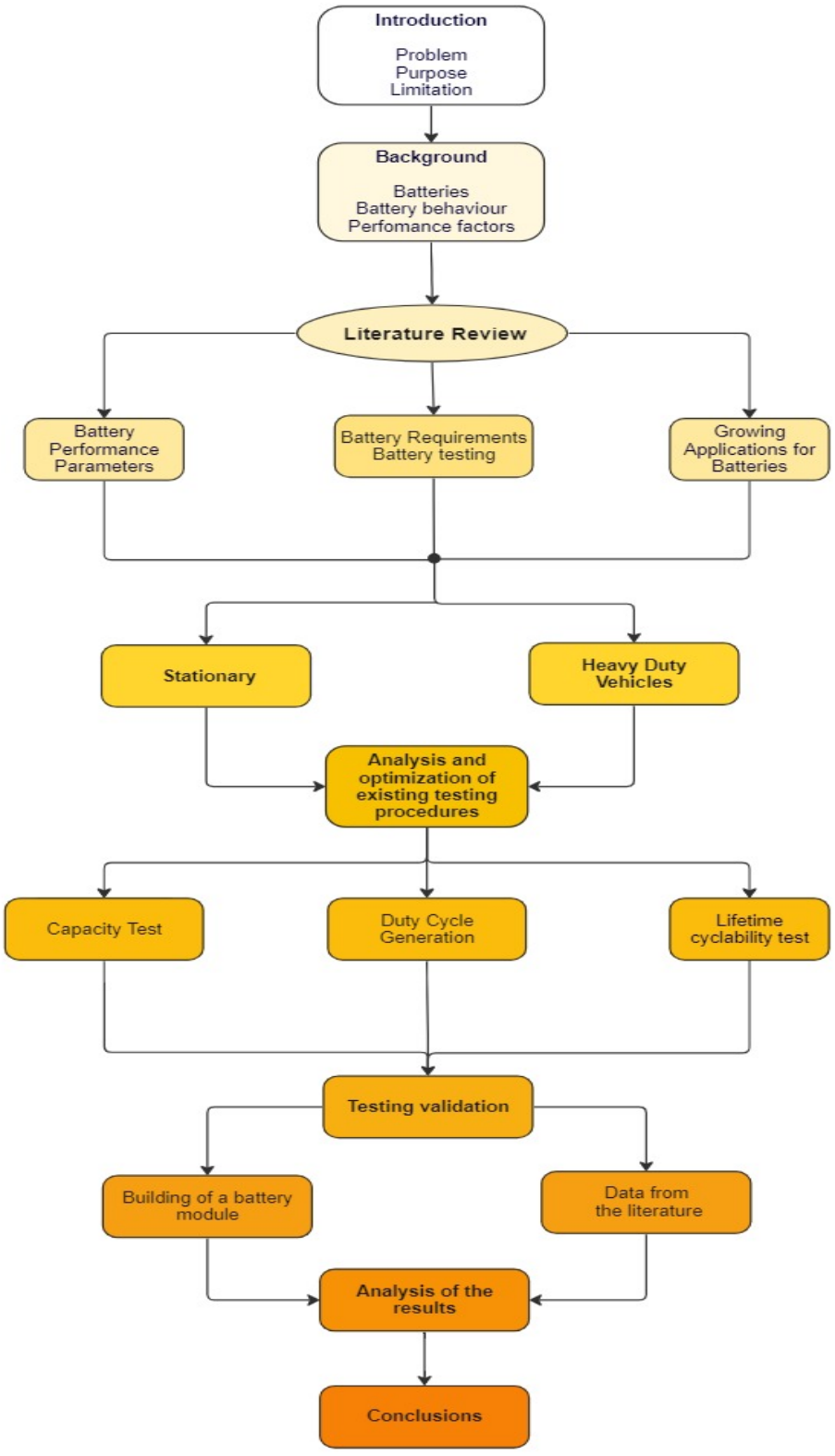

Figure 8: Flowchart of the working path.

2 Background

2.1 Batteries

Batteries are an efficient energy storage system, which can be used to power electronic devices in vehicles, including the engine itself. Battery systems are made up a number of cells connected in series or parallel that provide the right amount of energy and power to the target application (Cameron, 2019). A single cell is made up of two electrodes: a negative one (anode), which has an excess of electrons; and a positive one (cathode), with a deficit of electrons. Both these electrodes are separated by a porous material (separator) and are immersed in an electrolyte, which serves as a medium for the movement of charge carriers within the cell. Charge carriers, as their name implies, are particles that carry a charge and can move freely (i.e. ions). An electrode has the capacity of storing electric energy via these charge carriers (EUCAR, 2019). This internal movement of charge is part of the primary or internal circuit of a cell. The secondary or external circuit is formed when a conductor is connected to both electrodes and electrons can flow back and forth depending on the cell mode (Laestander, 2017). This configuration can be seen in Figure 9.

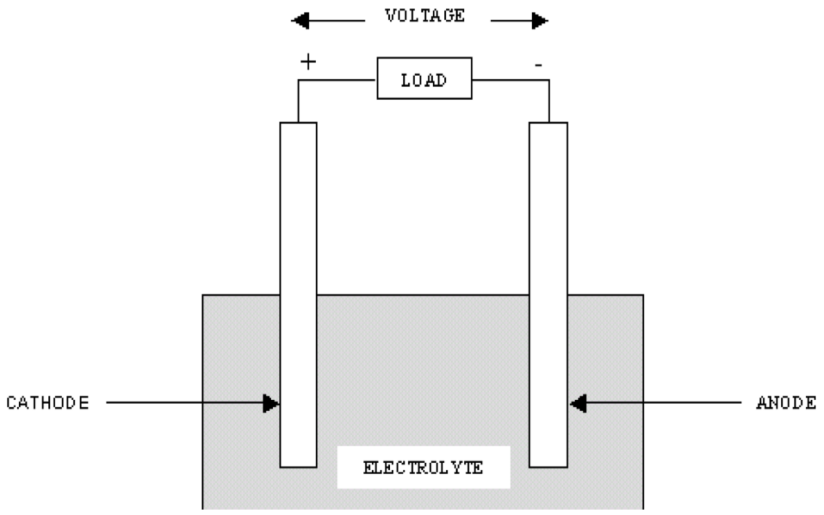

Figure 9: Basic components of a battery (Cameron, 2019).

The charging and discharging process will be discussed in further detail in Chapter 2.3, but in simple terms: when a battery is being used, electrons move from the negative electrode to the positive one through the external circuit, creating a flow of current that is used to run the connected device. At the same time, positive ions move through the separator to the positive cathode through the internal circuit. This process continues until the electrons and ions are

depleted, which is when the battery is completely discharged. When being charged, an external power source is connected and the opposite occurs (Laestander, 2017).

The selection of the electrode materials is key to determine the maximum voltage that can be produced across the cell. This voltage is determined by the spontaneity of electrodes to react with the electrolyte and the standard electrode potentials (UT Austin, 2013). The standard reduction potentials per material can be found in the Appendix 10. The greater the difference in voltage potentials between electrode materials, the more prone the electrons will be to move across the cell, thus the higher the overall potential energy of the cell.

Batteries can be broken down into two main categories: primary and secondary batteries. This division is mainly based on the chemical nature of the batteries. The chemical reactions occurring inside a primary battery are irreversible, meaning they can only be used once and then must be discarded. On the contrary, secondary batteries have reversible processes and thus can be used several times through recharging (Liu et al., 2019). Since the focus of this study is testing battery performance for diverse applications in the industry (mainly the transport sector), only secondary batteries will be considered as primary batteries are not really suitable for these applications.

2.2 Established technologies

For the electrification of the transport industry to occur, secondary batteries with different parameter performance requirements are needed depending on the intended end-use. As a general rule though, a battery with a long lifetime cycle, minimal energy loss, high power and energy density and an adequate safety level is preferred for most applications. (Liu et al., 2019).

- Batteries with a longer cycle life can maintain acceptable battery performance standards for a longer period of usage, reducing the need for replacing the battery and thus lowering the costs (SparkFun Electronics, 2018).
- Small energy losses improve the overall efficiency of the system by maintaining the energy for longer periods of time when not using the battery (SparkFun Electronics, 2018).
- Power density refers to the capacity of a battery to provide a high amount of current for a specific amount of time, and it represents the maximum amount of power that can be

provided at any given moment. It is an essential feature for applications that require a lot of power such as starting an engine or accelerating an electric vehicle (EUCAR, 2019).

- Energy density refers to the capacity of a battery to provide continuous current flow over time. It represents the maximum amount of energy that can be delivered by a fully charged battery. It is a key characteristic for applications that require continuous energy delivered for a long period of time such as for an electric vehicle travelling long distances (EUCAR, 2019).

Currently, only a limited number of batteries are established in the market and commercially available, with the most common used being Lead Acid battery (LAB), Nickel-Cadmium (Ni-Cd), Nickel-Metal Hydride (Ni-MH) and Lithium-ion battery (LIB) (Liu et al., 2019). These will be described below.

2.2.1 Lead-Acid Batteries (LAB)

Lead-acid batteries use lead dioxide (PbO_2) as their cathode and lead (Pb) as their anode, both immersed in sulfuric acid which acts as the electrolyte (Veneri, 2017). The overall reaction of the cell is:

$$Pb + PbO_2 + 2H_2SO_4 \underset{discharge}{\overset{charge}{\rightleftharpoons}} 2PbSO_4 + 2H_2O \quad (1)$$

LABs have been widely utilized in various applications, mainly as back-up power systems for data centers and telecommunications, but also for traction in battery-powered trucks as they can deliver a high current for a short period of time. In the transport sector, the use of LABs has been mainly in start, lighting and ignition (SLI) operations in most Internal combustion engine (ICE) vehicles, mainly because of their wide availability, low cost per unit of energy and their high charge retention, allowing vehicles to sit for extended periods of time between use (Veneri, 2017). In fact, according to a report by Grand View Research in 2023, LABs accounted for approximately 40% of the global battery market in 2020 (Grand View Research, 2023). However, they also have important limitations such as requiring periodic maintenance, having a relatively low cycle life and being heavy, making it difficult to transport them (Veneri, 2017). With these limitations and with the widespread adoption of other battery technologies, such as LIBs, it is expected that the total share of LABs will decrease in the following years (Grand View Research, 2023).

2.2.2 Nickel-Cadmium Batteries (Ni-Cd)

Nickel-Cadmium (Ni-Cd) batteries were developed around the same time as LABs. The cathode is usually made of nickel oxide hydroxide (NiO(OH)), while the anode is made of cadmium. The electrolyte medium used is a potassium hydroxide (K(OH)) solution (Laestander, 2017). The overall reaction of the cell is:

$$2NiO(OH) + 2H_2O + Cd \underset{discharge}{\overset{charge}{\rightleftharpoons}} 2Ni(OH)_2 + Cd(OH)_2 \tag{2}$$

They have two main configurations: unsealed and fully sealed, where the first one is used in traction applications and the second one is more suitable for portable power applications. The advantages of these batteries are their reliability and long lifespan which are two key features for transport and storage applications. However, they have a voltage suppression, also called 'memory-effect', which means they can only provide the same energy as the previous charging/discharging cycle (Veneri, 2017). Therefore, to fully take advantage of these batteries, they should be fully discharged before recharging. This is a big issue for transport modes since charging points are limited and it is not always feasible to wait until the vehicle's battery is drained to charge it again. In addition, cadmium is an environmentally hazardous material, complicating its disposal and making this option less attractive for the future of sustainable transport (Campillo et al., 2017).

2.2.3 Nickel-Metal Hydride Batteries (Ni-MH)

Nickel-Metal Hydride (Ni-MH) batteries use the same cathode and electrolyte as Ni-Cd batteries, but use metal hydrogen alloys (MH) instead of cadmium for the anode (Laestander, 2017). The overall cell reaction is:

$$2NiO(OH) + MH \underset{discharge}{\overset{charge}{\rightleftharpoons}} 2Ni(OH)_2 + M \tag{3}$$

Compared to Ni-Cd batteries, Ni-MH overcome some of the previously mentioned limitations by not having memory-effect and being more eco-friendly by not using cadmium. Also, Ni-MH batteries have a high energy and power density, allowing them to travel longer distances and more suitable for heavier transport modes. They have already been implemented in some HEV (i.e. Toyota Prius) due to their high power density which has helped them gain a more important position in the transition towards electrifying the transport sector (Veneri, 2017). Nevertheless,

these batteries also present important drawbacks which make them not ideal for transportation. For instance, their charging time is long and their capacity to retain charge is low. Additionally, they also have a shorter lifetime when discharged at high-current levels which limits their range of applications (Iclodean et al., 2017).

2.2.4 Lithium-Ion Batteries (LIB)

Lithium-ion batteries represent an entire family of secondary batteries which vary in chemistry, performance, cost and safety among their several types (Bini et al., 2015). Their cathode is characterized for having Lithium, which is an ideal material as it has the lowest negative electrochemical potential possible (Appendix (10)), thus these batteries can present the highest cell voltage. The anode is primarily composed of graphite or lithium titanate ($Li_4Ti_5O_{12}$), but recent developments are introducing new anode materials like Li-metal or Li(Si) alloys which present promising features. The electrolyte must be non-aqueous to prevent violent reactions with water. The most common electrolyte used consists of a mixture of lithium salts (i.e. $LiPF_6$) and an organic solvent (i.e. diethyl carbonate) to facilitate ion transfer (Miao et al., 2019).

The general chemical reaction involved in typical LIB is shown below, where lithium carbon (LiC_6) reacts with metal oxide (MO_2) to form carbon and lithium metal oxide.

$$LiC_6 + MO_2 \underset{discharge}{\overset{charge}{\rightleftharpoons}} C_6 + LiMO_2 \tag{4}$$

An overview of both current and future electrode chemistry materials is shown below.

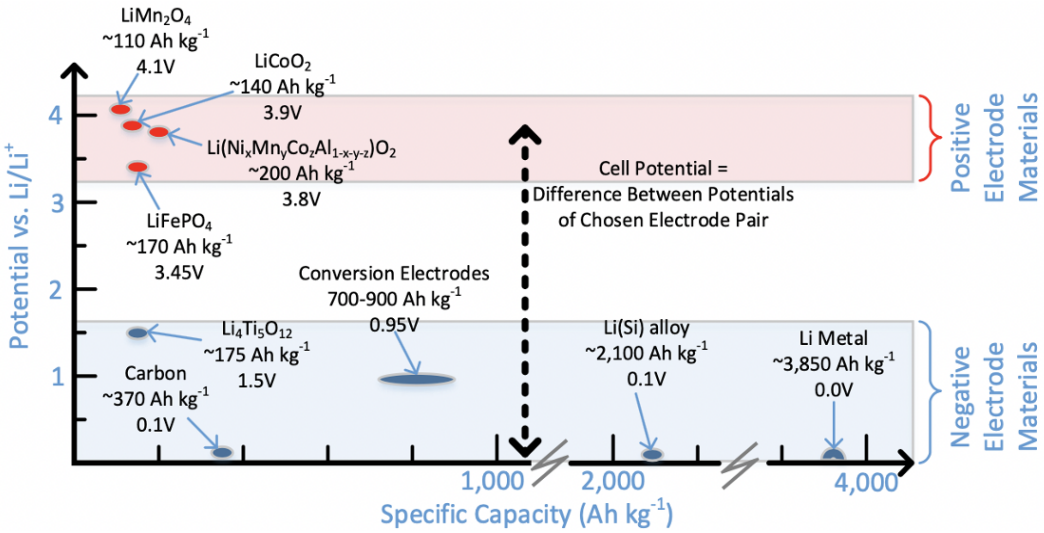

Figure 10: Current and near-future electrode alternatives for lithium-ion batteries (Miao et al., 2019).

It is important to note that some of the proposed energy capacities in Figure 10 are based on theoretical values that are most likely going to be reached in the near future (upcoming 5-10 years). In the case of the anode Li(Si), the value shown is actually 50% of its theoretical capacity due to the fact that approaching 100% value is not realistic in the upcoming 10 years. The combination of cathode and anode materials in LIB may vary per end-use application. As aforementioned, the cell voltage is the difference in voltages of the chosen pair of electrode materials (approximated value since cell losses, such as internal resistance, must also be taken into account) (Miao et al., 2019). It is calculated following equation 5.

$$V_{\mathrm{OC}} = V_{\mathrm{cathode}} - V_{\mathrm{anode}} \tag{5}$$

Likewise, the cell capacity is determined based on the specific capacities of the electrode materials, such as the ones observed in Figure 10. As an example calculation (Miao et al., 2019), consider the cathode $LiMn_2O_4$ (energy density of 110 Ah/kg), paired up with a carbon anode (energy density of 370 Ah/kg) in a way that's proportional to their individual capacities. The cell voltage would be:

$$V_{\mathrm{OC}} = 4.1 - 0.1 = 4V$$

The ideal weight ratio of electrode materials would be:

$$110 : 370 = 0.297$$

This means that in order to obtain a battery with 110 Ah capacity made up of these materials, 1 kg of $LiMn_2O_4$ would be needed while only 0.297 kg of graphite would be needed. Assuming 15% additional weight coming from the other materials of the battery, the specific cell capacity would then be:

$$\frac{110}{[(1 + 0.297) \cdot 1.15]} = 73.7 \frac{Ah}{kg}$$

The specific energy of the cell is then the result of the specific cell capacity multiplied by the cell voltage, as shown below:

$$73.7 \cdot 4 = 294.8 \frac{Wh}{kg}$$

Generally, LIB offer a significant advantage over other battery technologies by having a higher cell voltage and energy density which translates into a smaller and lighter battery, ideal for storage and transport applications. Additionally, they can optimally present one of the highest

Coulombic Efficiency (CE), 99%, which is the ratio of energy output with respect to energy input into the battery in one full cycle. There are several combinations of existing LIBs which present different characteristics and that can be suitable for different applications depending on their end-use (Bini et al., 2015). The most common ones are compared below in Figure 11, followed by a brief description of the most important characteristics of each LIB chemistry.

It is important to note that in Figure 11, there is a criterion followed for classifying the different LIBs in the way they are. Cost is a function of $ per kWh of energy produced from a battery, where the cost of the entire manufacturing chain of the battery is considered, including the cost of extracting raw materials. Specific energy is the total stored energy in one cycle of the battery and specific power refers to the maximum amount of power that can be provided at a given point. The lifespan parameter accounts for: the total number of cycles a battery can undergo before reducing its initial energy capacity below 80%; and the expected number of years a battery can remain useful. The safety and performance parameter are qualitative parameters and therefore more subjective. In the case of safety: factors such as the toxicity of battery components and risks associated to using the battery, such as thermal runaway (leading to explosions) or short-circuits (leading to fires) are taken into account. Performance refers to how well a battery can serve its purpose without failing, so thermal, electric and mechanical resistances are all included in this parameter, as well interesting characteristics such as Fast Charging (Bisschop et al., 2019; BCG, 2020).

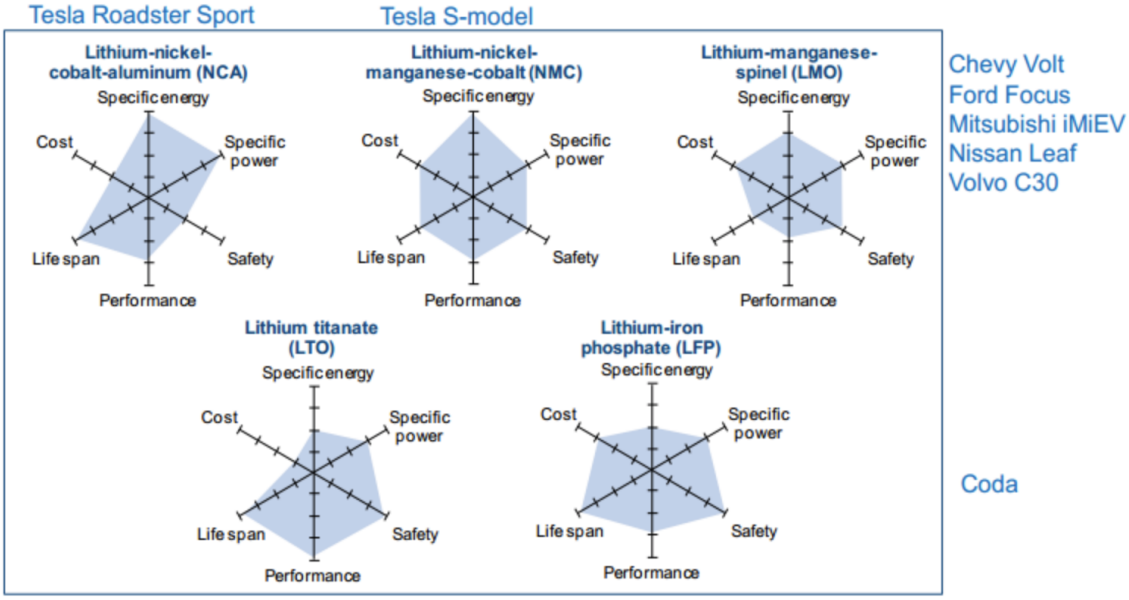

Figure 11: Parameter comparison of different LIB chemistry used in industrial and automotive sector (BCG, 2020).

Lithium-Nickel-Cobalt-Aluminum (NCA) battery

NCA share several similarities to NMC battery's, including high specific energy, power and a long cycle life. But, they are not as safe as other LIB and usually require additional safety monitoring systems (Marsh, 2019). Furthermore, the manufacture of these batteries is costly mainly due to the presence of cobalt, which is a scarce material. At the moment, only Tesla has used this cathode chemistry for some of its EV models such as the Tesla Roadster and Model X, where they even claim to use less cobalt than in NMC-811 batteries (Miao et al., 2019).

Lithium-Nickel-Manganese-Cobalt-Oxide (NMC) battery

NMC battery's were selectively designed to provide high specific energy or high specific power, while maintaining thermal stability (Bini et al., 2015). The combination of cobalt, nickel, and manganese is key in achieving these traits since they all complement eachother. Cobalt offers good thermal stability and high energy density, while nickel provides high specific power but poor stability, and manganese has the opposite characteristics of Nickel. In order to obtain a high performance battery with desired characteristics, the ratio of these metals can be balanced in such a way that suits the applications requirements. Recent developments have focused on increasing nickel and reducing cobalt due to its toxicity and high cost (Miao et al., 2019). In fact, the NMC-811 battery, with a ratio of 8:1:1 of nickel, manganese, and cobalt respectively, is currently the most suitable Li-ion system for EV powertrains and has been used by car manufacturers such as Nissan and BMW (Cameron, 2019).

Lithium-Manganese-Oxide (LMO) battery

LMO battery's are known for having low internal resistance which enables fast charging and high current discharging of up to 30A. While they have better thermal stability compared to LCOs, they have about a third less energy capacity and lifespan. To improve this, LMOs are usually blended with NMCs as it has been successfully seen in EVs like the Nissan Leaf or Chevrolet Volt (Miao et al., 2019; Marsh, 2019).

Lithium Titanate (LTO) battery

LTO battery's differ from the previously mentioned ones as they use this chemistry for the anode and not the cathode. Lithium titanate is highly valuable because it maintains the volume of the electrode constant during lithiation, which is the process where a lithium ion replaces a hydrogen atom from an organic compound, leading to a longer lifetime of the battery (Miao

et al., 2019). They also have a characteristic long plateau charge and flat discharge curve which prove that they are one of the safest battery's in the market. The downside of this battery is its low conductivity, which results in poor performance at high power levels. Nevertheless, studies have successfully improved this by reducing Li-ion transport paths through nano-structuring and through doping with better electric conductors (Laumann et al., 2011). This improvement seems promising for the future of this battery chemistry, which is already being used in some Mitsubishi and Honda EVs. It is also starting to be considered for marine applications and stationary applications, such as UPS systems (Meyer et al., 2017).

Lithium-Iron-Phosphate (LFP) battery

LFP battery's are very popular and widely used due to their good electro-chemical performance with low resistance, high power-to-weight ratio, high current rating and long lifespan. The key for their high performance is the presence of phosphate which stabilizes the electrodes against overcharging and increases resistance to thermal runaway. They also have a high reliability as they are capable of operating at a wide range of temperatures (-30 to 60 ^{o}C). These battery's were implemented in the first all-electric motorhome, the Iridium E Mobil. The downside of LFPs is that they are vulnerable to moisture, which can significantly reduce their lifespan. They also have a relatively higher self-discharge rate that increases with aging, but this can be mitigated with expensive control systems (Miao et al., 2019).

Lithium-Cobalt-Oxide (LCO) battery

LCO battery's are mainly used in personal electronic equipment, such as laptops and cameras (BCG, 2020). They are ideal for these applications since they are easily manufactured, offer high energy density and a long cycle life (Miao et al., 2019). However, these batteries are also very reactive which may lead to thermal stability issues. As a result, they require adequate thermal management systems to ensure safe operation (BCG, 2020). In addition, the limited availability of natural cobalt leads to political issues and higher prices, which hinders the large-scale deployment of these batteries (Miao et al., 2019).

2.2.5 Comparison of Established Battery Technologies

Table 1 illustrates a summary of the most important characteristics of the established batteries previously discussed above

Table 1: Summary of the most important parameters of mature battery technologies (Liu et al., 2019).

Parameter	**Li-ion**	**Lead Acid**	**NiCd**	**NiMH**
Lifespan (cycles)	600-3000	200-300	1000	300-600
Nominal Voltage (V)	3.2-3.7	2.0	1.2	1.2
Energy Density (Wh/kg)	100-270	30-50	50-80	60-120
Power Density (W/kg)	250-680	180	150	250-1000
Charging Efficiency (%)	80-90	50-95	70-90	65
Self-discharge rate (%/month)	3-10	5	20	30
Charging Temperature (^{o}C)	0-45	-20-50	0-45	0-45
Discharging Temperature (^{o}C)	-20-65	-20-50	-20-65	-20-65

As it can be seen, LIB have significant advantages with respect to other battery technologies in terms of key performance parameters:

1. Energy densities are highest for some Li-ion chemistry's, such as NMC or NCA, with only Ni-MH battery obtaining competitive values. Because of this higher energy density, these batteries can charge and discharge quicker than the rest, offering more stable charge cycles.

2. Cell voltages are high, with average operating voltages at around 3.7 V using carbon anode; these are around three times more than the cutoff voltage of Ni-Cd and Ni-MH batteries. As a result, these batteries are able to deliver rapid surges of electricity on-demand, which is very attractive for current industrial applications.

3. Cyclability characteristics are excellent as any LIB chemistry can be put through a minimum of 600 cycles, while some chemistry's can reach values of 3000 cycles, ten folding the lifespan of a Lead Acid battery (LAB).

4. Charging and Coulombic Efficiency (CE) are very high and self-discharge is minimal, at under 10% per month, making these batteries especially suitable for storage and transport applications. Other batteries might have good efficiencies or low self-discharge but difficult to have both.

5. LIB have no memory effect such as that in Ni-Cd and Ni-MH batteries (SparkFun Electronics, 2018).

Nevertheless, A lot of attention has to be put in to control the voltage levels when charging these batteries since even a slight over-voltage can damage the battery, thus proper cell equalization is needed to ensure years of safe operation. Also, thermal management is key for these batteries because hot and cold temperatures accelerate significantly the aging and battery performance is largely affected in cold conditions (Lajunen et al., 2018). This will be further discussed in Chapter 2.4

2.2.6 Form Factor

Besides the different available battery chemistry's, there is another category known as the form factor, which broadens the use of batteries. This refers to the different shapes a battery cell can be put in, where each shape has different features that can heavily influence the suitability of a battery in different applications. The most common form factors are cylindrical, prismatic and pouch cells; and they can be used in several applications ranging from power tools to EVs to energy storage systems (Cameron, 2019). Cylindrical and prismatic batteries have their cathode and anode sheets wounded together in a spiral shape and packed into a cylinder-shaped and cubic-form pack, respectively. Between the electrodes, there is a polymer separator film sheet wounded which obstructs the micro-pores and interrupts the reaction of the cell in case of excessive rise of temperature inside the cell. Pouch cells on the contrary have the electrode and separator layers stacked together and do not have a rigid enclosure for the cell container, but use rather a flexible foil (SparkFun Electronics, 2018).

Table 2: Qualitative comparison of different form factors for batteries (Miao et al., 2019).

Shape	**Cylindrical**	**Prismatic**	**Pouch**
Diagram	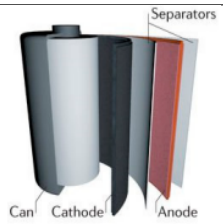	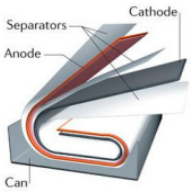	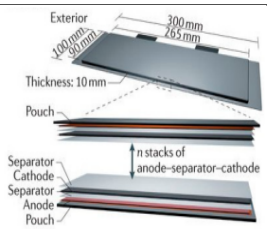
Electrode Arrangement	Wound	Wound	Stacked
Mechanical strength	↑↑	↑	↓
Heat management	↓	↑	↑
Specific Energy	↑	↑	↑↑
Energy Density	↑	↑↑	↑

The design and some qualitative information of these three forms can be seen in Table 2. Note that an *upward-arrow* means good performance while a *downward-arrow* refers to poor performance.

The cylindrical configuration is the most commonly used form and it is produced in large quantities. This results in lower manufacturing costs due to economies of scale. These cells have high mechanical stability: they tolerate high internal pressures without deforming due to their circular geometry which allows an even distribution of pressure from side reactions over the cell circumference. However, when combining cells into battery packs this geometry is not ideal as it limits the use of available spacing thus lowering the energy density of the pack. Furthermore, there is low heat transfer from the cell center to the outside, which poses serious thermal risks to the battery pack. Although this can be alleviated with refrigerants circulating through the space cavities formed (Arar, 2020). Besides being widely used in portable applications, power tools and even in EV applications, such as several Tesla models, this configuration seems to have reached its maximum potential in terms of energy density and poses serious questions about its potential use in next-generation batteries (Cameron, 2019).

The prismatic form is still not widely produced and is more expensive to manufacture than its cylindrical counterpart. When combining prismatic cells in battery packs, their squared shape enables optimal space use leading to increased energy density. This form factor is mainly used in portable electronics such as laptops and phones but is also suitable for electric power-train applications and energy storage systems. However, the parts of the electrode and separator sheet that are located near the corners of the cell experience more stress, resulting in lower mechanical resistance and increased risk of damage to the electrode coating. Nevertheless, the prismatic cell is promising for applications where space optimization is crucial (Arar, 2020).

Finally, pouch cells are a cost-effective and lightweight configuration that still lack a lot of R&D and improvement. Currently, the main drawback this form has is the soft construction of the cell which reduces its mechanical strength and requires additional support structures. On the other hand, the layers are stacked in this configuration, achieving 90-95% packaging efficiency, the highest out of all forms (Arar, 2020).

However at the moment, there is still some cell swelling (around 8% after 500 cycles) that causes some space to be left unused for safety reasons (Arar, 2020). There is still room for

improvement in this aspect. Despite this, pouch cells seem very promising for emerging technologies, especially some that can only work with pouch cell format such as solid-state LIB. This configuration can be used in the same applications as the prismatic cell: from small portable technologies to EVs and energy storage systems (Cameron, 2019).

While it is not clear yet which form factor will become the standard for storage applications and the transport industry, it seems that cylindrical cells are the most mature configuration but have reached their maximum limit in terms of performance; prismatic cells already competing with cylindrical cells in some applications and have still not reached their optimum performance; and pouch cells are still in the early stages of development and are already producing promising results.

2.3 Operation/behaviour of batteries

The life cycle of a battery mainly depends on three factors:

1. **Depth of Discharge (DoD)**, i.e how much the battery is discharged
2. **Charging**, overcharging or undercharging can reduce the capacity of the battery.
3. **Temperature**, the capacity of the battery can be reduced at low-temperatures while high temperatures reduce the life time of the battery (Jain, n.d).

The process of charging and discharging a battery occurs through the movement of lithium ions between the cathode and anode and that of electrons through a process of doping and de-doping. This process is exemplified, with an example of a LIB, in Figure 12.

Specifically the cathode, usually formed by a lithium-containing compound, is de-doped during the charging process. In contrast, during discharging the compound layers are doped. As for the anode, however, the process is reversed. Therefore, the carbon interlayers present will be doped with lithium during the charging process and de-doped during discharge.

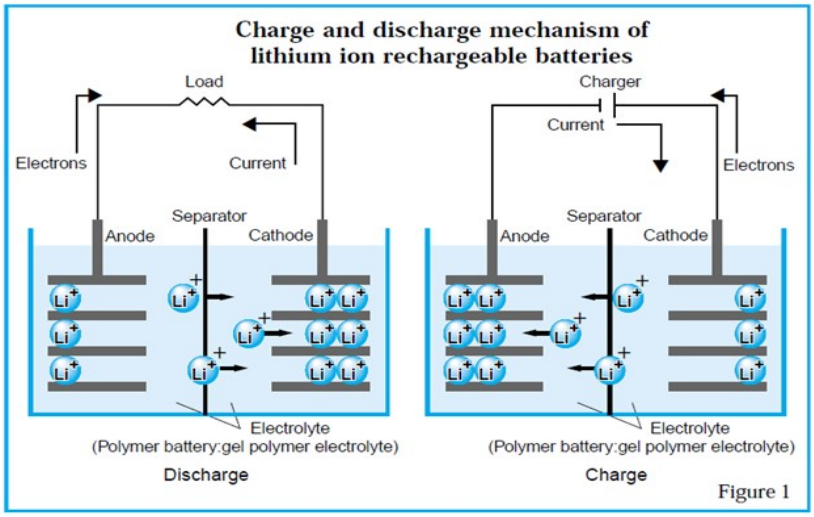

Figure 12: Charging and discharging mechanism of a rechargeable LIB (SparkFun Electronics, 2018).

2.3.1 Charging

The process of charging a battery can be very complex and difficult to perform optimally because of the numerous criteria to meet, such as SoC and voltage, and it is very easy to damage the battery. Different main processes take place within the cell during the charging process, each with a different time constant:

- **Charge Transfer**, the actual chemical reaction that occurs in the electrodes fairly quickly, in about a minute or less from the beginning of the process.
- **Mass Transport or diffusion**, in which the materials produced by the chemical reaction move from the electrode where they were produced to the other. This happens until all the materials have been transported and therefore can take up to hours, depending on how large the cell capacity is.

  Other significant effects, such as the **Intercalation process**, where ions are inserted into the crystal lattice of the electrode and which time constant varies depending on the battery components and electrolyte.

Another phenomenon that inexorably occurs when it comes to electric charges, is the hysteresis process and it should be taken into account when estimating the time required for charging and discharging. During this process, there is a delay that occurs between the chemical reaction and the load applied to the battery, in the case of a discharge process, which additionally also leads to energy losses. Therefore, it is preferred to have resting periods during both charging

and discharging processes for the chemical reactions to end and reduce the voltage gap due to hysteresis. In the Figure 13 below is showed an example of the hysteris process of a LIB.

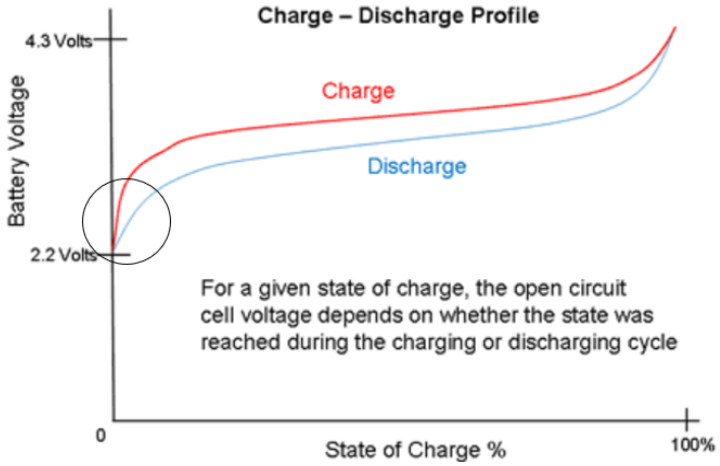

Figure 13: Hysteresis effect on a LIB (Electropedia, n.d).

In particular, from the bending of the curves at the starting points, it can be noticed the big delay in State of Charge compared to the rapid increase in voltage levels for both charging and discharging processes. This time required to overcome the hysteresis effect is one of the main problems that might occur during fast charging. In fact, pumping energy into the cell faster than the occurrence of the chemical reaction can cause local overcharge conditions, damaging the cell with phenomena such as polarization, overheating, and unwanted chemical reactions in the electrodes (Electropedia, n.d).

2.3.2 Termination Methods

When charging a battery, it is very important to end the charge at the right time. Failure to do so could result in an undercharged battery, which would mean not taking advantage of the battery's maximum capacity. For example, for LIBs, when the battery is undercharged by even a slight 100mV, up to 10% of the battery capacity can be lost, as shown in Figure 14. This is why it is very important to precisely measure and control the final voltage for these type of batteries when charging.

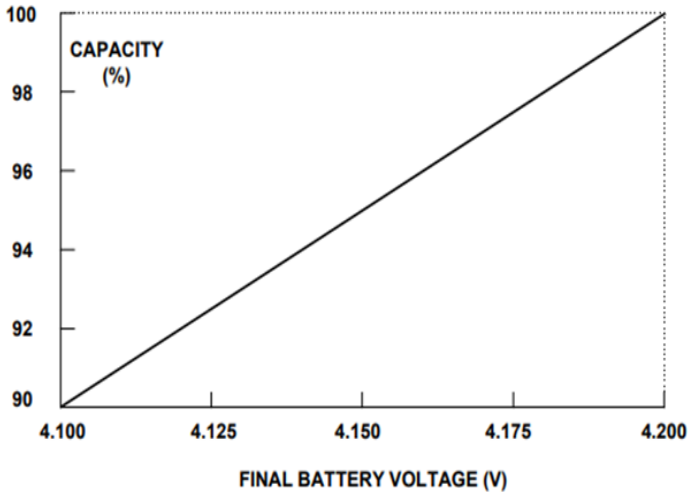

Figure 14: Effect of undercharge on LIB capacity (Kester and Buxton, 2015).

Another problem that could arise is overcharging the battery. This could damage the battery and be very dangerous, especially in the case of a battery with high energy density. It could in fact lead to over-gassing of the cell, especially in liquid electrolyte cells, and thus to an increase in the volume of the individual cell, which is not tolerated in a rigidly assembled pack. Furthermore, overheating of the cell could occur, which could cause the pack to catch fire or, even worse, explode, especially in Lithium-based batteries, due to the high reactivity of Lithium. It is therefore important to choose the most suitable termination method, depending on the application and the environment in which the battery is used. There are several methods that can be used and taken into account:

1. **Time**: in this case the the charging process is stopped after a predetermined time period has elapsed. it is not expensive and it is generally used as a backup for fast charging or regular charging for some batteries. The problem arises when the battery capacity decreases over time, in which case the time should be adjusted according to the reduced battery capacity to avoid overcharging. Therefore, the charger would not work efficiently for new batteries and this leads to a reduction in battery lifetime.

2. **Voltage**: in some applications it is preferred to pre-define an upper voltage limit, called the termination voltage. In these cases, the battery is charged until this limit is reached, in order to avoid temperatures beyond the safe limit and thus damage the battery. This is especially important for fast charge processes, where energy is sent to the battery faster than in the standard charging process. Although, this method has its drawbacks, such as obtaining the actual open circuit voltage value instants after the battery has been

disconnected from charging. This is because, as mentioned above, chemical reactions need a certain amount of time to stabilise.

3. **Voltage drop**: when a battery is almost fully charged, oxygen starts to accumulate inside the battery, lowering its voltage. In some batteries this voltage drop occurs within a certain allowable time and is a good indicator to terminate the charging process. For example, in Ni-Cd batteries, the voltage drop is significant enough to stop charging and avoid the 'Fail safe charge time zone', as shown in Figure 15. However, in other technologies, such as Ni-MH, the voltage drop is not fast enough to be reliable and is therefore not recommended to be used as a termination method. The plot voltage-time for a battery should be studied prior to using this method.

4. **Cell Temperature**: when temperature rises in a battery, especially in the cells, it indicates battery over-voltage, meaning that the battery is fully charged. This can therefore be a reliable termination method, but temperature sensors must be added to the battery, which can significantly increase the cost (Campillo et al., 2017).

The use of various combinations of termination methods, are mainly required in fast charging, where a primary and a secondary method are selected, with the latter mainly used as a backup for safety reasons. For example, for Ni-Cd and Ni-MH batteries, the most commonly used methods are battery voltage and temperature. Figure 15 shows how these two parameters vary as a function of charging time.

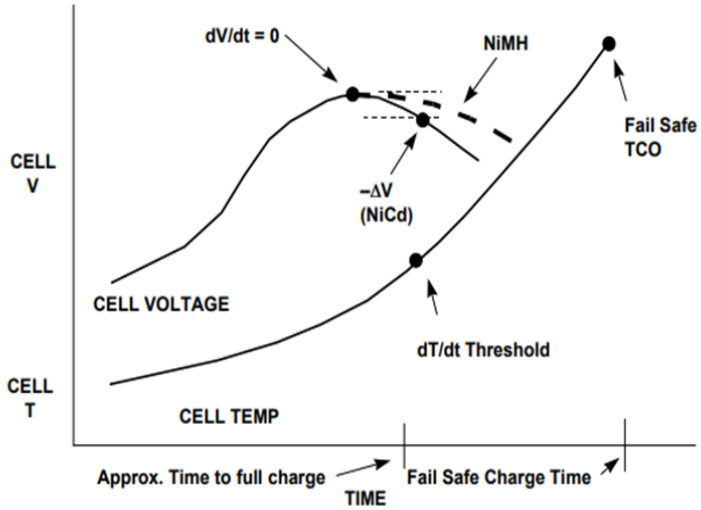

Figure 15: Ni-Cd/Ni-MH battery temperature and voltage charging characteristics (Kester and Buxton, 2015).

An example is the voltage drop ($-dV$), in which the charge ends when the cell voltage drops between 10 and 20 mV after reaching its peak. In particular, it is important to note that the peak for Ni-Cd batteries is more pronounced than for Ni-MH batteries, which is why it is preferable to use the change in temperature with respect to time (dT/dt) as the primary method for Ni-MH batteries.

With regard to slow charging, the termination method used for LIBs is the Termination voltage, while for Ni-MH time is considered. For other battery technologies it is recommended to trickle charge the battery, which means to inject a small current into the battery, such that the life cycle of the battery is not reduced, in order to keep the battery at full charge state and thus avoid self-discharge (Kester and Buxton, 2015).

2.3.3 Charging Strategy

In order to get the best charge, there are different charging strategies depending on the chemistry of the battery. In general, the most commonly used charging methods are explained below.

On of the most used charging method is called **Constant Current (CC)** in which the current is kept constant (with a very low variation), by varying the voltage through control strategies to terminal conditions, depending on the battery type and manufacturer. It can be carried out using:

1. **Single Rate Current**, applying only a predefined current to the battery
2. **Split Rate Current**, varying current rates according to charge time and voltage. This method is more accurate but requires the use of backup circuits (Campillo et al., 2017).

In general, the CC strategy is very easy to implement, but at the same time it is challenging to find the best current rate for balancing battery charge rate and capacity utilisation. If the current rate is too high, it can improve the charging time rate but at the same time decrease battery life. If it is too small, it will have the opposite effect, resulting in a better capacity utilisation but a slower charging rate, which is inconvenient in the case of electric vehicles. CC strategy is mainly used for Ni-Cd, Ni-MH and LIB technologies.

The second most common method is **Constant Voltage (CV)** in which the battery is charged with a fixed voltage, usually predefined by the manufacturer, while varying the current to levels according to the battery capacity. This method is also easy to implement and has a stable terminal voltage, therefore avoiding irreversible reactions and over-voltage. However, it also has

some disadvantages. For instance, in order to maintain a constant terminal voltage in the initial stages, it is necessary to use very high currents, which may cause the battery to collapse. It is also hard to select an adequate value for constant voltage which can balance a good charging speed, while avoiding electrolyte decomposition and bad capacity utilization.

Using beyond acceptable charging currents could cause the battery lattice frame to collapse and aggravate the pulverisation of the active substance in the battery pol e(Liu et al., 2019). Therefore, currents are varied from high to low, impacting the charging rate. Usually the charging rate increases when the SoC is between 0.15 and 0.8 while it decreases when it reaches 0.9. This method is generally used for LABs and LIBs. For LIBs in particular, the voltage limits are between 4.2 V / -50 mV (Campillo et al., 2017).

The **Constant Current and Voltage (CCCV)** method is mainly used for LABs and LIBs. It is divided in two phases, a first phase in which the battery is charged with constant current and a second phase in which constant voltage is used instead. Figure 16 below shows an example of CCCV charging for a Li-ion cell.

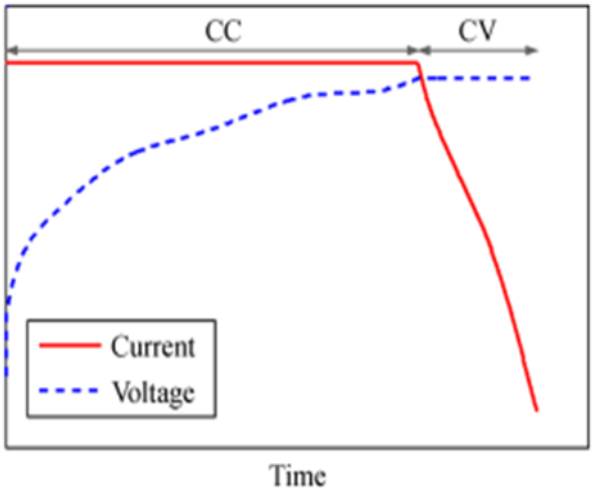

Figure 16: Charging curve with the CCCV method (Liu et al., 2019).

As it can be seen from the diagram, one starts with CC until the cut-off voltage is reached. Then, the second phase begins with CV and the current falls until it reaches 0.05C. When at least one cell reaches full charge, the voltage will indicate that the battery is charged, even if the SoC is not exactly 100%. In this case, the Trickle Charge mode can be used where a reduced charge current charges the remaining battery capacity slowly while balancing the cells (Bollini, 2022). Here again, the main challenge is to find the most accurate current rate and voltage

values. If in fact the current is too high, this can cause lithium plating phenomenon, in LIBs, which leads to low energy conversion efficiency and a rise in temperature beyond the permitted limits. If the current is too low, it may decrease the charging rate and thus be inconvenient for some applications. The combination of these two methods can bring advantages since the loss of capacity caused by CC due to extensive electrochemical polarisation can be subsequently compensated with CV. Furthermore, this method has a high capacity utilisation and stable terminal voltage.

Since this method has more advantages than the methods mentioned so far, it is generally used as a benchmark for comparing the new models tested for battery charging (Liu et al., 2019).

Finally, another often used method is **Multi-stage Constant Current (MCC)** in which several constant currents are used in steps during the charging process, as seen in the graph in Figure 17.

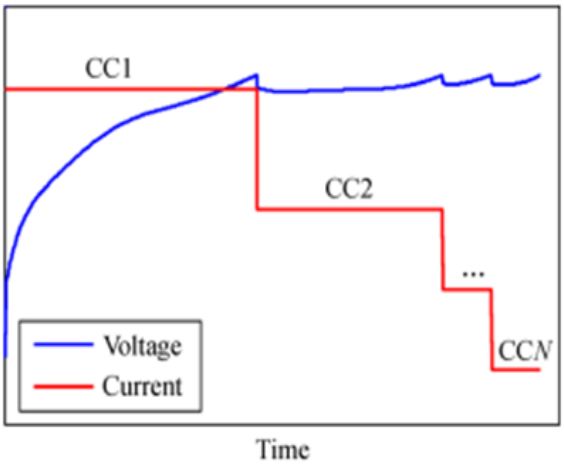

Figure 17: Plot of MCC charging method (Liu et al., 2019).

The order of current intensity decreases as the charge progresses, so each current will always be less than the previous one. More specifically, during each step, when the voltage reaches a certain predefined threshold value, the current is switched to the next constant current stage. This will happen until the battery terminal voltage reaches the last default voltage threshold under the condition of minimum current. This method is slower than CCCV and there can also be difficulties in balancing different parameters such as charge rate, capacity utilisation and battery lifetime. This MCC strategy is used for several battery types, including LAB, Ni-MH and LIB (Liu et al., 2019).

2.3.4 Discharging

As for the charging process, it is important to determine the proper conditions for the discharging process, as it can impact its performance and efficiency. The graph in Figure 18 shows typical curves of a discharge process with 0.2C rate for different cells with different chemical characteristics. As it can be observed, each cell is characterized by a different nominal voltage and discharge curve.

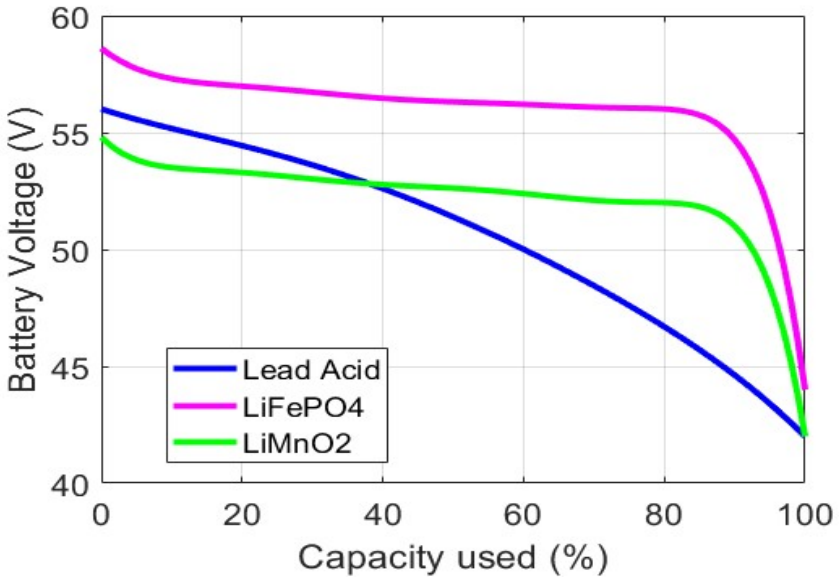

Figure 18: Discharging curves for different battery technologies. (Shepard, 2021)

In general, as the graph also shows, two types of discharge curves can be highlighted: flatter and with a more pronounced slope. In the case of a sloping discharge curve, such as that of LABs, the power delivered by cells falls progressively throughout the discharge cycle. In particular, if these batteries are used in low power applications, a regulator may be required to ensure a stable supply voltage. However, this device is not very recommended for high power applications, as the losses in it would draw too much power from the batteries, which may already need over-sizing to support the requirements of the distinct applications.

On the other hand, batteries with a flatter curve, such as LIBs, are better since the voltage supplied is more uniform during the discharge cycle and therefore its applicability is also easier. Nonetheless, a drawback associated with this curve is that the battery pack might not be able to achieve a complete 100% DoD. This limitation arises because the battery is designed to shut off once a single cell within it reaches its lower cut-off voltage.

Finally, in sloping curves, it is very easy to evaluate the SoC, since the battery voltage is

closely related to the remaining charge. Flat curves, however, require more complex methods such as Coulomb counting that measures the discharging current of a battery and integrates the current over time to estimate SoC.

In addition, during the discharge process it is important to take into account how this occurs at different temperatures or under different charging rates.Below, the behaviour of the LIB in these two situations will be assessed.

First, regarding discharging with different c-rates in Figure 19, it can be mentioned the phenomenon of charging off-set, which also occurs in other battery technologies. As a general rule, the more the battery is discharged at higher c-rates, the quicker the charging time but the more the capacity is reduced and vice versa.

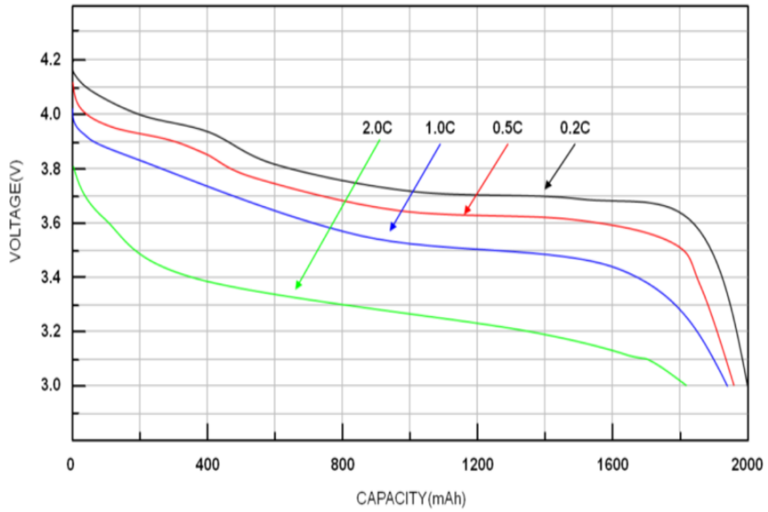

Figure 19: Discharge curves of LIB for different charging rates. (Shepard, 2021).

Secondly, regarding the effect of temperature on the battery in Figure 20, the further the temperature is from ambient conditions, the greater the degradation of the battery's cycle life.

At low temperatures, the battery will deliver less voltage and have a lower capacity, as shown in Figure 20, consequently delivering less energy. In extreme cases, batteries with aqueous electrolytes may freeze, leading to complete failure of the battery. In these cases, a lower temperature limit is defined by the manufacturer. In the case of LIBs, these may suffer from the phenomenon of lithium plating of the anode, which occurs when Li-ions exceed the rate at which the anode can take them in, causing a permanent capacity reduction (Laestander, 2017).

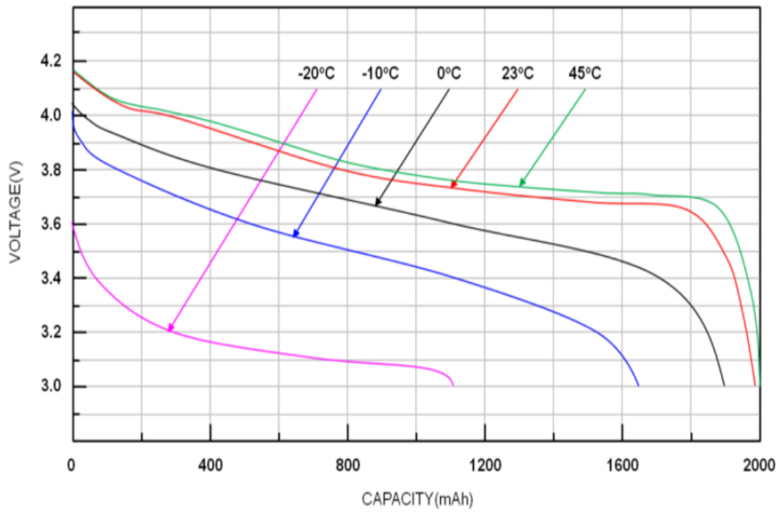

Figure 20: Discharge curves of LIB for different temperature (Shepard, 2021).

At higher temperatures, on the other hand, batteries deliver higher voltage and higher capacity, resulting in a better flow of electrons and thus in more delivered energy. However, these benefits come at the expense of reducing the cycle life of the battery. In extreme high temperatures, the active chemicals may break down destroying the battery and leading to dangerous risks such as exploding or starting a fire. Either way, the battery will be prone to failure under these conditions.

2.4 Factors affecting performance (degradation)

Battery degradation is a very complex phenomenon that can negatively affect the performance of batteries. It is also known as ageing and is most significant when the battery is used at conditions different than the ones recommended by the manufacturer (Miao et al., 2019). The cause of it can be both chemical or mechanical, although it is generally difficult to notice the real consequences on the battery itself as it can take place in different parts of the cell (Gräf et al., 2022). The effects of battery degradation can be made explicit through two performance parameters:

- **Capacity fade**, the reduction of usable energy provided by the battery in a life cycle, generally manifested through a reduction in the number of cyclable lithium available to move back and forth between both electrodes (Joshi, 2016).
- **Power fade**, the reduction of the maximum power that can be provided by the battery at any given moment, mainly caused by an increase in cell resistance, as shown in the

following equation (Joshi, 2016):

$$P_{\mathrm{Max}} = \frac{{V_{\mathrm{OCV}}}^2}{4 \cdot R_{\mathrm{cell}}} \tag{6}$$

where

P_{max} is the maximum power provided by the battery;

V_{OCV} is the open circuit voltage;

R_{cell} is the cell resistance;

There will be a reduction in capacity when the active material is transformed into inactive material due to parasitic chemical reactions. This parasitic reactions will lead to the conversion of battery material into something different than before, increasing the internal impedance of the cell and thus reducing the operating voltage at each discharge rate and increasing the resistance of the cell (Miao et al., 2019).

The degradation phenomenon can be divided into several stages, as shown in Figure 21. The effects discussed above are a consequence of degradation mechanisms that are triggered by different factors. Additionally, there are degradation modes which englobe these mechanisms according to their impact on the thermodynamic and kinetic characteristics of the cell (Laestander, 2017). The following four modes have been identified in the literature:

1. **Loss of active material (LAM)**, occurring in both positive and negative electrodes. This mode groups mechanisms which lead to a reduction in the material available for electrochemical activity (Edge et al., 2021).

2. **Loss of lithium inventory (LLI))**, this mode groups mechanisms which cause a reduction in the amount of cyclable lithium ions available for transport between electrodes which lowers the battery's capacity (Joshi, 2016).

3. **Stoichiometric drift**, mostly associated with LLI, where the electrodes become imbalanced relative to each other (Edge et al., 2021).

4. **Impedance change**, it arises through the degradation of the electronic conduction pathways in the cell that cause a reduction in lithium-electrode interaction, consequently leading to LAM (Edge et al., 2021; Joshi, 2016). This parameter mainly affects the power as the increased resistance prevents some electrochemical activity from happening.

In this chapter the focus will be only on the most important factors that may lead to degradation and the consequences they may have on the functionality of the battery. Therefore, the internal mechanisms that lead to these irreversible effects on the battery will not be explained.

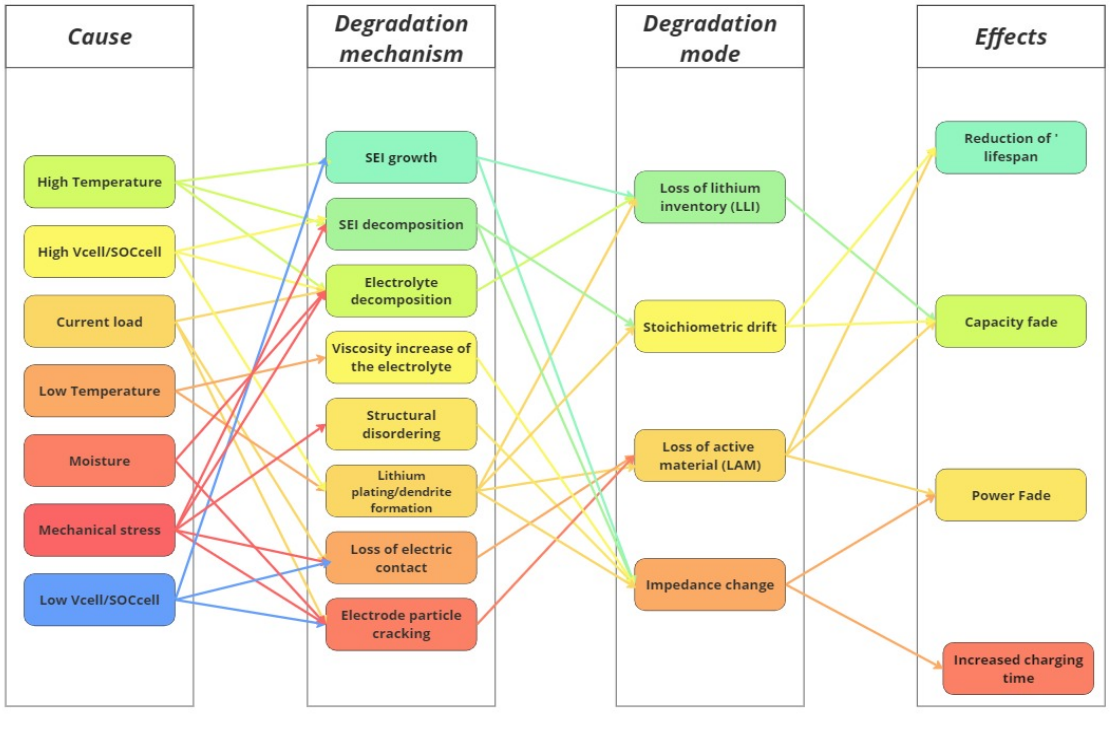

Figure 21: Causes and effects of degradation mechanisms and modes (Laestander, 2017).

TEMPERATURE

Most of the effects related with temperatures are linked to the materials and chemical reactions taking place in batteries, which follow the Arrhenius equation, according to which a change in temperature can lead to a change of electrochemical reaction rate in batteries (Ma et al., 2018). It is therefore advisable to use the battery in the temperature range recommended by the manufacturer, which varies according to the chemistry of the battery, but is usually around room temperature. For instance, the optimal temperature range of LIB is between 15 °C - 35 °C (Momidi, 2019).

If the battery operates at low temperatures, the viscosity of the electrolyte will increase, reducing the ionic conductivity and thus increasing the impedance in the battery by slowing down lithium-ion intercalation into the anodes (Ma et al., 2018). All this leads to a longer time

required to charge the battery and to lithium-ion deposition on the electrode surface, which will result in the reduction of battery capacity (Momidi, 2019). For example, for LIBs, it has been shown that when the operating temperature drops from 25°C to -15°C the SoC decreases by 23%. Furthermore, the lithium plating exists in the form of dendrite, which may penetrate the separators, and result in the Internal Short-Circuit (ISC) (Ma et al., 2018).

On the other side, the effects of operating at high temperatures are far more complex compared to low temperature operation (Ma et al., 2018). High temperatures can lead to accelerated ageing of the battery, reducing its performance and its lifetime. In this case, what happens inside the battery is the decomposition of conductive salt into electrolytes and the increase of the inorganic compounds at the Solid Electrolyte Interface (SEI). The SEI is a stable layer formed on the surface of the electrodes, which in the right measure, enhances the performance and lifetime of cells by preventing electrolyte decomposition. However, when grown excessively, it leads to an increase in the internal impedance and thus to an increase in the internal temperature of the battery. This can degrade the battery or, in the worst cases, lead to thermal runaway (Momidi, 2019). Even if a single cell reaches thermal runaway, it can cause a chain reaction that could reduce the battery's properties or even cause it to catch fire (Miao et al., 2019).

To limit these problems, batteries are generally equipped with a Battery Managment System (BMS), which regulates and controls many aspects of the battery such as charging, discharging. cell equalisation and monitoring as well as controlling the overall temperature of the system (Miao et al., 2019).

VOLTAGE

When charging, as it was shown in the previous Chapter 2.3.1, the voltage of a battery increases. In case of overcharging, if the charging strategy fails or is not adequate, over-voltage will occur. In this case, the transport of Li-ions will exceed the rate at which the anode can take them in and therefore metal lithium will be plated on the electrode (Laestander, 2017). In turn, this will reduce the amount of active material in the electrode and in the electrolyte; and increase internal resistance of the battery, thus permanently degrading both the capacity and power of the battery, respectively (Joshi, 2016; SparkFun Electronics, 2018). Furthermore, the Lithium can form dendrites and break-through the separator, causing an Internal Short-Circuit (ISC), leading to increased risks of fire and explosions. At the cell level this can be controlled, however

in large battery packs this can pose a real-life threatening catastrophe (Fear, 2017).

When discharging, the voltage of a battery drops and in case of deep discharging, the voltage level could drop to very low undesirable values which could degrade the battery severely. In this sense, when a battery is discharging the anode releases Li-ions and tends to reduce its volume because of it. In the case of deep discharge, the volume reduction can be such that micro-cracks could appear in the anode (Gräf et al., 2022). This exposes the anode to electrolytes which can contribute to the formation of SEI and in turn increase the internal resistance of the battery (resulting in power fade) and consume some amount of lithium for its formation (resulting in capacity fade) (Joshi, 2016). Additionally, at extremely low voltages, unwanted electrode reactions can occur, such as corrosion, gas evolution and current collector dissolution. These mechanisms can negatively affect the capacity of the battery and in worst cases, lead to ISC and consequently fire and possible explosions (Fear, 2017).

To understand the extent of these effects on capacity fade, Malaki and Howard performed deep discharging experiments on 780 mAh Li-ion cells. The cells that were overdischarged to 0.5-2 V experienced an immediate permanent capacity loss of 2-16%; and after 100 cycles the same cells had lost 8-26% of their initial capacity. Furthermore, for Li-ion cells overdischarged between 0.5-1 V, an immediate loss of 29-38% of their capacity was observed. Lastly, the cells overdischarged to 0.0 V suffered from either severe capacity loss (over 40%) or were fully damaged (Maleki and Howard, 2006).

The effects of overcharging and discharging on capacity and power fade can be observed in Figure 22.

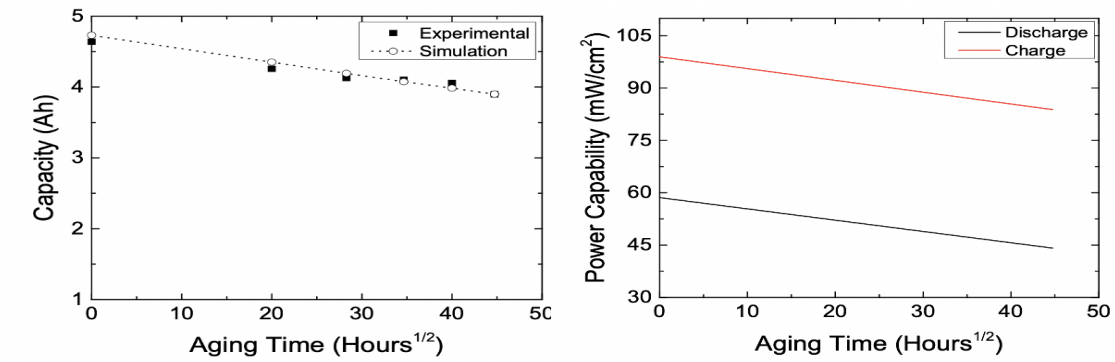

Figure 22: Capacity fade due to cyclable Lithium loss (left) and Power fade due to increasing size of the SEI attributable to more Lithium lost in the SEI (right) (Joshi, 2016).

CURRENT LOAD

A commonly experienced abuse condition for LIB is an external short circuit, in which a battery is discharged at high currents (above the recommended by the manufacturer) usually due to a fault in load management. This results in a large and rapid heat generation in the battery and the wire connected to the load. In fact, one single cell inside a battery pack can reach approximately 180°C and even cause exothermic reactions in the cell that may lead to thermal runaway. However, for this to occur, several external shorts must take place on the same battery.

To test this, Conner Fear subjected an 18650 Samsung battery cell to high discharge rates (resistance of the short read between 0.47 and 1 ohm) and observed cracking on the surface of both electrodes. This cracking resulted in permanent loss in capacity and small increase in resistance of charge transfer in the cathode. Nevertheless, in the experiment it was also concluded that it was very unlikely that one single external short incident could lead to thermal threat or complete battery failure (Fear, 2017).

MECHANICAL STRESS

Mechanical stress can be either caused by mechanical ageing or mechanical abuse.

The first one depends on the number and quality of battery cycling. During charging and discharging, lithium ions intercalate in the structure of the electrode, thus increasing its volume. This expansion causes mechanical stress, which can subsequently cause parts of the SEI or the active material to rupture or burst. This can eventually lead to an increase of the internal resistance of the battery, causing an irreversible power and capacity reduction (Gräf et al., 2022).

The latter includes extrusion, shaking and needling, which can cause mechanical deformation of the battery and lead to Internal Short-Circuit (ISC) or electrolyte leakage. Depending on the severity of the physical abuse, the battery can lose part of its energy through the ISC, producing heat (increasing risk of fire) and experiencing a significant power fade. In case of electrolyte leakage, active material is lost from the battery leading to capacity fade (Lamb and Orendorff, 2014).

MOISTURE

Moisture can lead to undesired chemical and electrochemical side reactions in the battery, causing the degradation of the cathode, the anode and the electrolyte itself. This happens because inside the battery we find the $LiPF_6$, i.e the most used lithium salt in the electrolyte, that is highly reactive with water. The hydrolysis of this salt is described in Figure 23 and can produce Lithium Fluoride (LiF), Phosphoryl fluoride (POF_3), Hydrogen Fluoride (HF).

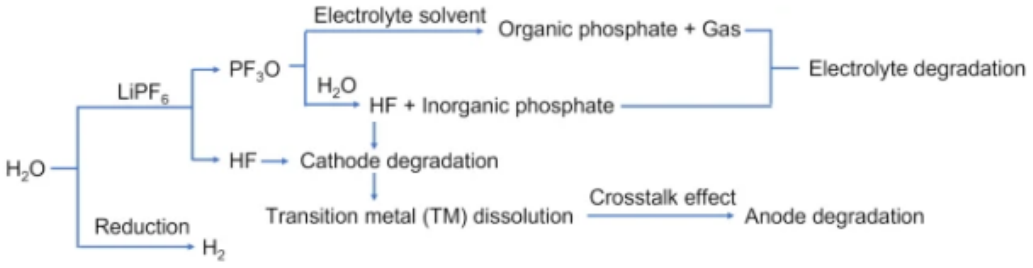

Figure 23: Hydrolysis of $LiPF_6$ that can occur in the electrolyte (Cao, 2023).

The HF its highly corrosive and can initiate Transition Metal (TM) dissolution that will lead to cathode material dissolution and, consequently, its degradation. In addition, TM could also migrate to the anode through the electrolyte, contaminating it and causing its degradation.

The LiF produced can degrade the electrolyte, producing organic and inorganic phosphate products and gases from it (Cao, 2023).

In the case of LIB, the presence of excessive moisture in the external ambient or of any trace of water can lead to battery corrosion and consequently to its degradation (Miao et al., 2019). In the literature it is also reported that high humidity condition can cause a drop of the Open-circuit voltage (OCV) and thereby a degradation of the battery capacity and power as shown in Figure 24 (Byun et al., 2016). In fact, it is shown that for a battery operating in humid conditions, the final capacity will be lower than one operating in dry conditions. Even after the capacity has stabilised, it does not deviate much from the estimated residual capacity and is therefore lower than in dry conditions.

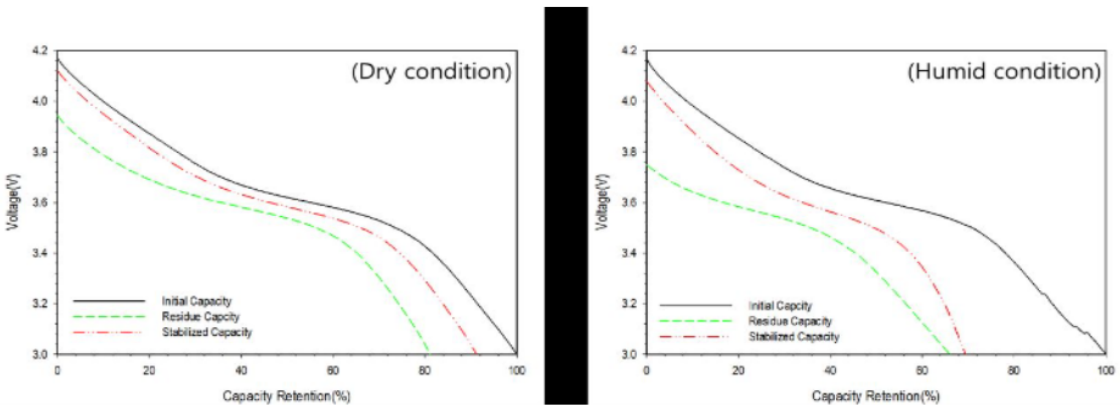

Figure 24: Capacity of a battery operating in Dry Condition and in Humid Condition (Byun et al., 2016).

3 Battery performance parameters

3.1 Parameters

Given the exponential growth of batteries in the global market and the wide array of technologies both present and forthcoming, the ability to compare and assess them based on their capabilities becomes essential. In this way, their suitability for certain applications can be determined. Therefore, a series of key parameters have been selected that measure the performance of batteries, while considering the conditions found and required by the different applications. These parameters englobe the most important features to take into account for a battery to carry out its intended purpose, but it must be also pointed out that they widely depend on the battery chemistry. In particular, in this chapter the following parameters will be considered: capacity, stored energy, power (C-rate), cycle life, self-discharge, charge rate, impedance/resistance and charging efficiency.

CAPACITY

The capacity of a battery can be defined as the total energy stored in the battery (Barai et al., 2019) and thus the total energy produced by the electrochemical reactions taking place in it, usually measured in ampere hours (Ah) (Aktas and Kircicek, 2021). Furthermore, battery capacity depends on several factors:

- **Number and size of electrodes in a cell**: the larger the number or width of these plates, the more active substances, the greater the stored energy. The capacity of the battery depends on the amount of active material present to intercalate the electrodes. If this material is reduced, the capacity will also be reduced.
- **Electrolyte density**: Choosing an electrolyte with a high density, i.e a higher concentration of ions, for the battery can also increase the capacity, but this can lead to a reduction in battery life and is therefore not always advantageous.
- **Electrolyte temperature**: As temperature increases capacity can increase, however, excessive heat can cause damage and leakage in batteries and therefore it is not recommended to expose batteries to excessive heat (Aktas and Kircicek, 2021).
- **Age**: As the battery is used over time, the capacity decreases due to degradation of the battery caused by pouring the active substance from the plates, ageing and wearing out of the elements forming the battery.

The capacity of a battery is linked to other parameters through the Peukert's law where C_p (Ah) is the capacity, usually given by the manufacturer, I_b (A) is the battery discharge current, t is the discharge time and k is the Peukert constant, with a value usually between 1.1 and 1.3 (Aktas and Kircicek, 2021).

$$C_{\mathrm{p}} = {I_{\mathrm{b}}}^{\mathrm{k}} t$$

As can be seen from the equation and the graph, the higher the discharge rate, the lower the battery capacity. This general law, mainly used for Lead Acid battery (LAB), however, is not entirely accurate, as it does not take into account the effects of temperature and age of the battery. In fact, in many studies, many improved versions of the law can be found, where the non-linear capacity characteristics of some types of battery, such as Lithium-ion battery (LIB), are taken into account (Zhang et al., 2018). Finally, this parameter is very important in the transportation sector because it defines the maximum driving range of a vehicle, while for stationary applications it means less battery autonomy to meet the required demand.

ENERGY STORED

The energy stored in a cell or a complete battery pack system is characterized by the parameters specific energy (Wh/kg), i.e energy as a function of the battery mass unit, or Energy Density (Wh/l), i.e energy as a function of the battery volume unit (EUCAR, 2019). Specific energy is the stored energy content per mass of the cell and therefore is closely-linked to the weight of a battery pack:

$$\text{Specific Energy (Wh/kg)} = \frac{\text{Rated Capacity (Ah)} \cdot \text{Voltage (V)}}{\text{Weight (kg)}} \tag{7}$$

The weight of a battery can be important depending on the application. For example, weight frequently emerges as a recurrent restriction for numerous vehicles, primarily owing to concerns about mobility. By increasing the specific energy, it is possible to reduce the total weight of the battery pack, as less cells will be required to generate the same energy. Therefore, this will also result in less fuel/energy consumption by the vehicle, as the weight transported will be reduced (EUCAR, 2019).

However, for stationary applications, the battery serves its purpose statically, therefore weight is not taken as much into account as it doesn't really affect the performance of the battery. Nevertheless, a high specific energy is still preferred since the higher the specific energy, the more capacity it has for energy storage and the longer period of time it can last solely in the event of

a power outage.

On the other hand, energy density is the stored energy per volume of a battery pack as shown in equation 8, which is closely related to the size of a battery.

$$\text{Energy Density (Wh/L)} = \frac{\text{Rated Capacity (Ah)} \cdot \text{Voltage (V)}}{\text{Volume (L)}} \tag{8}$$

This parameter is associated to the space a battery might require to comply with its applications requirements. This is an important parameter for mostly all applications as space in vehicles is highly limited and space availability for storage in buildings can also be an issue. Therefore, space should always try to be minimized. A high energy density increases the compactness of a battery, thus reducing its volume and the space needed to cover the energy requirements for the applications (EUCAR, 2019).

POWER

The power of a battery is the rate at which energy or current can be delivered by the battery. It is measured in Watts (W) but it can also be expressed in terms of Specific Power (W/kg) or Power Density (W/l). It is also often represented with the C-rate, where the higher the C-rate, the higher the Watt needed to deliver the energy required.

This parameter must not be confused with energy. For example, a system can have the capacity to store a lot of energy, but not be powerful. If the internal resistance is too high, the system will be able to store a lot of energy, but discharge it over a long period of time, and thus not be very powerful. On the other hand, a system with low energy content may be able to release all its energy content in a very short time, thus being very powerful.

Most applications do not have the same power requirements and applications within the same sector (i.e. stationary or transport) can also require different power surges. For example, in stationary applications, the power requirements of a battery depend on the load profiles, the existing generation technologies and the intended operating strategy, as observed in Figure 25 (Sun et al., 2013).

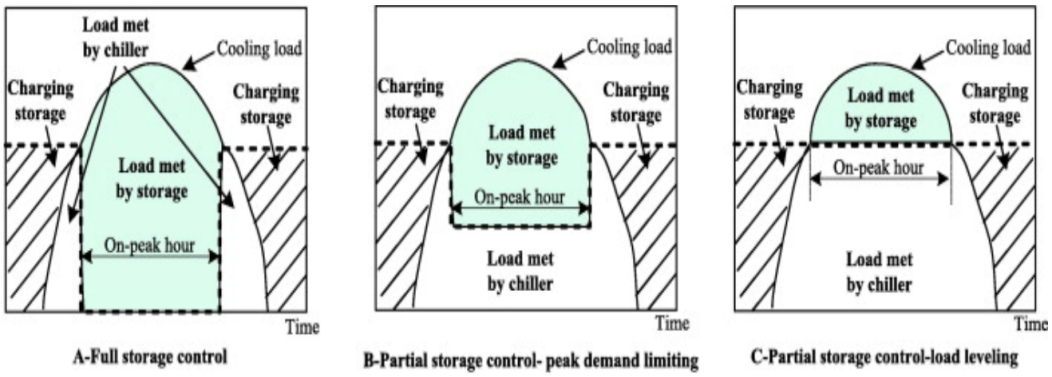

Figure 25: Different control strategies for energy storage systems (Sun et al., 2013).

In cases where operation times can be very long and the energy supply by the battery must be constant, without significant peaks, it is more relevant to be able to store as much energy as possible, than release it in the shortest possible time. This is the case for renewable integration, micro-grids, peak shaving and load-levelling scenarios. In these scenarios, the battery is sized by energy storage capacity. In profiles where peak loads are much higher than average loads and applications that require sharp frequency response and black-out starts, the battery requires large power capacity and is sized accordingly (Bowen et al., 2019; ADB, 2018).

On the other hand, in mobility applications, large peaks of power are generally needed. For example, acceleration and braking procedures require high power bursts, and thus the energy should be discharged in few seconds. Furthermore, for some transport applications which involve heavy vehicles, such as HDV and boats, batteries require high power in order to start moving such heavy-weighing vehicles.

In addition, in mobility applications it is possible to distinguish a continuous and a peak power requirement, which differ mainly in the power output and the time in which this is needed. Continuous power density is a measure that should represent a continuous driving situation of an electric vehicle and thus a constant power requirement. While peak power density should be representative for sharp bursts of power needed to start the car, accelerating or breaking procedures.

CYCLE LIFE

The cycle lifetime can be defined in terms of number of cycles (Garcia, 2021) or in terms of energy (Wh) (EUCAR, 2019). In general it indicates the number of charging and discharging cycles after which the battery reach the end of life, i.e when the State of Health (SoH) drops below the 80% (Garcia, 2021). Therefore, in terms of energy, it will be defined as the sum of

the energy exchanged during charging and discharging processes until the end of life of the cell (EUCAR, 2019). Cycle lifetime is usually affected by the average SoC, the range of SoC, but it is particularly affected by the Depth of Discharge (DoD) during the operation of the battery. In Figure 26 it is shown the relationship between the possible number of cycles of a battery during its lifetime and the depth of discharge (Qadrdan et al., 2018).

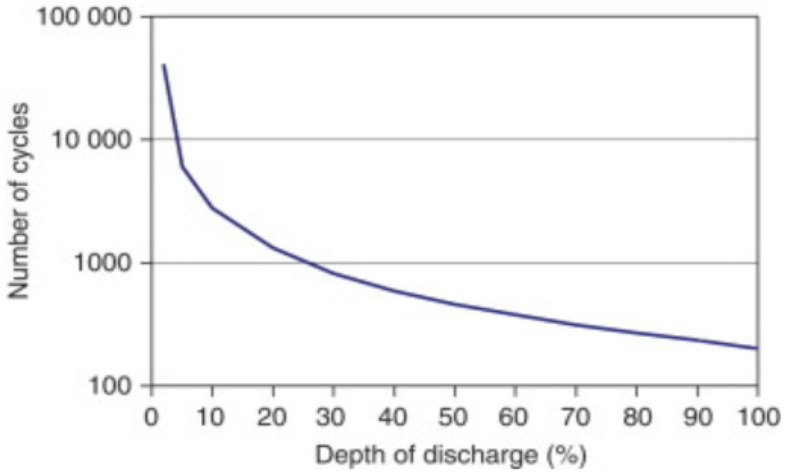

Figure 26: Number of possible cycles during the lifetime of a battery as a function of depth of discharge (Qadrdan et al., 2018).

As is also evident from the graph a battery that is discharged only by 20% of its capacity will have a greater cycle life than one that is discharged deeply by 80%. Cycle lifetime also depends on the temperature, in fact a battery operating at lower temperature will last more (Chaaban, 2018). On the other hand, low temperatures can activate other factors that degrades the battery. It is also quite clear why this parameter is important. In fact, having a large battery cycle lifetime increases the service life-time of the battery, which therefore results, for all the applications, in a longer wait before having to fix or substitute the battery, saving money and labour. In the transportation sector this will also lead to an increase of the possible driven kilometers before needing maintenance (EUCAR, 2019).

SELF-DISCHARGE

Self-discharge rate refers to how quick a battery is discharged without actually being connected to an external circuit (Bollini, 2022). It is a naturally occurring phenomenon that happens because the electrodes of a charged battery are thermodynamically unstable, and chemical reactions occur spontaneously which result in a loss of active material. However, this loss is not

permanent. This parameter is also commonly known as charge retention capacity (DNK, 2022). As a general rule, the lower the self-discharge rate, the higher the ability a battery has to retain its stored energy under specific conditions (Liu et al., 2022).

It is a complicated parameter to measure and quantify, but it is usually identified inside a cell as a voltage drop and represented to users as a percent charge loss per month.

The factors commonly affecting this parameter are the battery chemistry, SoC, moisture and temperature. Addressing operating conditions, it is important to know that the capacity of a battery decays faster under high SoC conditions. This is why some Li-ion batteries may have self-discharge rates of up to 10%/month when the SoC is above 80%, while 0.5%/month or less when SoC is between 30-80%. When it comes to temperature, it is the most significant factor to consider for this parameter. Self-discharge is intensified at high temperatures due to increased side reactions and SEI deterioration. In fact, one can expect the self-discharge rate to double for every 10 ºC rise, as shown in Figure 27. At extreme low temperatures, self-discharge rate will also be higher (DNK, 2022).

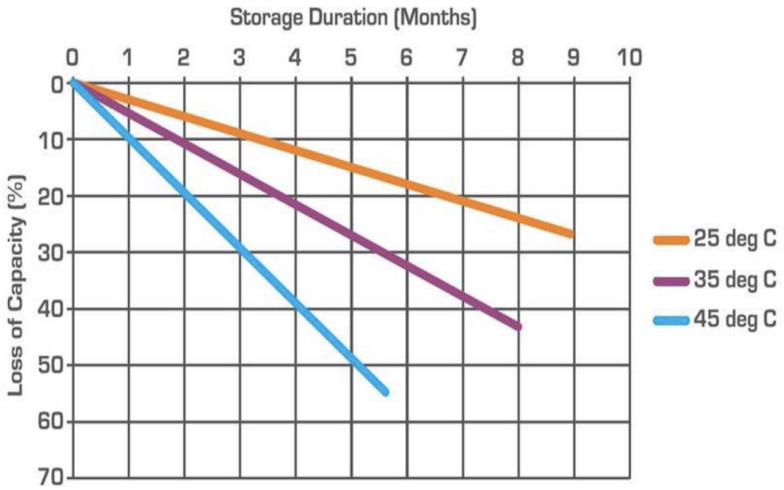

Figure 27: Temperature effect on self-discharge rate (Ansari, 2022).

The effect self-discharge has on the battery is a loss in SoC, which leads to a reduction in the OCV of the battery and thus less usable energy for its given application (Bollini, 2022). This is why self-discharge rate is an important parameter to consider when selecting a battery for an application and it is often overlooked. Depending on the application, this parameter can be of less or greater importance. It is also important to take into account the plausible temperature and moisture conditions found in the respective application.

In stationary applications, batteries are energy storage technologies and, as their purpose implies, they have to store energy for short and long periods of time. The self-discharge rate negatively affects the energy capacity of a battery (Bollini, 2022). We believe this leads to reduced back-up times for storage applications, causing the battery to not perform as it should (i.e. not peak-shaving enough or not covering the intended energy demand and thus recurring to fossil fuels). Additionally, this parameter should gain importance in cases where a battery is a primary energy source and thus its failure would lead to a black-out; in long-term energy storage applications; and in applications with large load variations which could lead to long storage times.

For transport modes, this parameter is also important especially because one of the main issues with current EVs is their driving range. A high self-discharge rate implies a lower energy capacity and thus a reduction in the driving range of the vehicle. This is especially the case for HDV which are usually commercial trucks that when not used are kept in the warehouse until required again; or that may have long routes and might be parked for an undefined period of time at their destination. On the contrary, there are other applications where it is more uncommon to leave the vehicle unused for long periods of time. For instance, private vehicles are generally used on a weekly basis. Furthermore, it is easier to plan your charges and minimize energy loss from self-discharge.

CHARGE-RATE

Charge and discharge rates are the speeds at which a battery is fully charged or discharged. The rate is dependent on the amount of current used, where higher speeds are obtained with higher currents. High charge and discharge rates are critical for fast charging and high power delivery, respectively (Tian et al., 2019). These rates are represented by the rating current nC, the current at which a cell is fully charged or discharged in $1/n$ hours.

The main issue with charging and discharging rates is that they are both limited. Above a certain threshold value, R_T, the cells become thermally unstable, leading to temperature increase which causes capacity fade and accelerated ageing (Tian et al., 2019). If R_T is maintained for some time, it can also permanently degrade the battery and there could be high risks of explosion (Ahmadi and Torabi, 2019).

The optimal and maximum charging and discharging rate depends on the battery chemistry and can vary quite a lot, including within the LIBs family. The factors influencing these rates are the electronic transport coefficient in the electrodes; the solid-state diffusion of ions in the active materials and the chemical reactions occurring inside the cell. For example, several studies have shown that charging rates above 1C significantly affect NMC battery's lifespan, with a 23% degradation after 300 cycles charging at 1.5C. On the contrary, LFP lifespan is not significantly affected by charging rates, obtaining very similar degradation at 4C (17%) compared to 1C (15%) after 4000 cycles (Mothilal Bhagavathy et al., 2021).

Charging time is one of the main challenges of secondary batteries. This parameter gains importance in battery applications that require more energy than the available energy in one cycle, and that need this energy as soon as possible to continue providing its services. Such is the case for most applications, mainly portable and transport (Ahmadi and Torabi, 2019). Given the scope of this project, we will focus mainly on transport and stationary applications.

Charging rate is especially important in transport modes. The charging time of conventional ICE vehicles is in the order of 5 minutes. However it can take about 3-4 hours to fully charge the batteries used in EVs with standard charges (Ahmadi and Torabi, 2019). In order for batteries to actually substitute conventional fossil fuel vehicles in the transport sector, they must at least have reasonable charging times (in the order of minutes) to become a competitive and attractive alternative for users. This is something that battery manufacturers are focusing on improving and results have started to appear with high power charging (up to 350 kW) which can fully charge the vehicle in less than 1 hour (Mothilal Bhagavathy et al., 2021). However, the battery's cyclic life is dramatically reduced in these cases, as observed in Figure 28.

Nevertheless, if there is a good thermal management system, temperature could be controlled and this degradation could be minimized as ageing is accelerated due to temperature increase.

For stationary applications, this parameter is not as important since the main limitation of energy storage is availability of excess renewable energy and big capacity to store as much energy as possible (Ahmadi and Torabi, 2019).

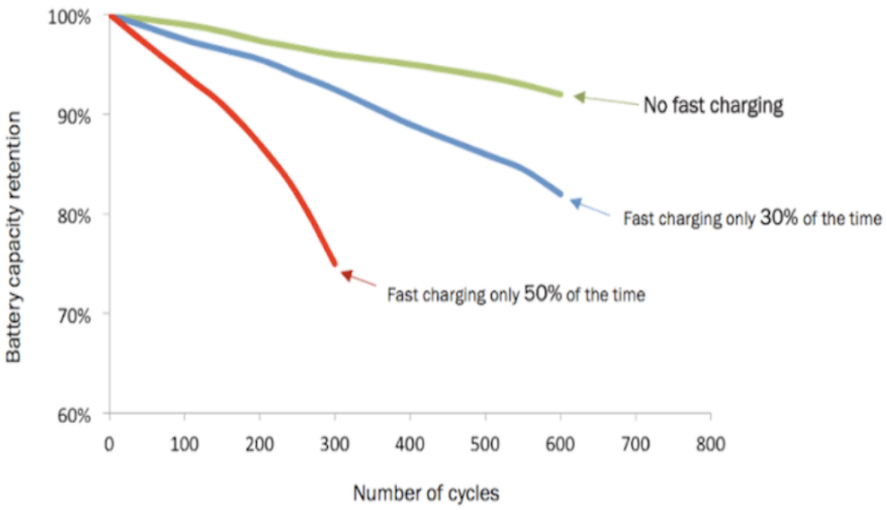

Figure 28: Effect of fast charging on battery cycle life (Evvanex, 2020).

RESISTANCE/IMPEDANCE

The impedance of a battery is a measure of its internal resistance, that is, the opposition to current flow through the battery. It is measured as a voltage drop when the battery is connected to a current; and it is highly dependent on the duration of the applied current and SoC of the battery (Barai et al., 2019).

The initial impedance of a battery depends on chemical properties and mechanical design of the battery pack (Hämmerle, 2017). It is a fixed and know value estimated by the manufacturer. However, impedance increases with use as it is a function of cell ageing, thus impedance evolution over lifetime of a battery is actually what interests battery manufacturers and users (Meddings et al., 2020).

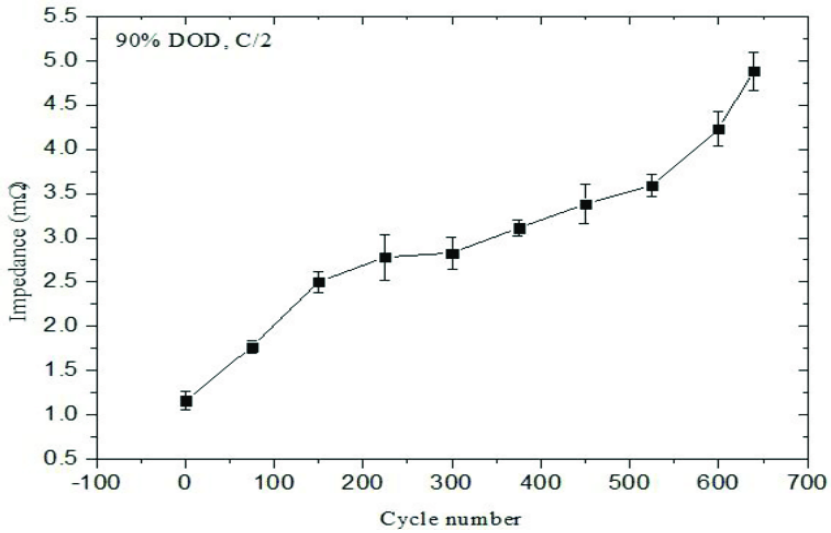

Figure 29: Ageing effect of impedance in a battery at C/2 discharge current (Zhang et al., 2014).

Resistance within a battery pack is very important as it has a direct effect on the operating voltage of the battery, efficiency, capacity and power capability (Hämmerle, 2017). All these aforementioned are key parameters when selecting a battery for a certain application. High levels of impedance indicate increasing weakness within a battery, which leads to stored energy being lost or converted to heat instead of useful current when operating the battery (Barai et al., 2019). Therefore, this translates into declining battery capacity, lower round-trip efficiency of energy discharged and lower operating voltage, which directly affects the power capability of the battery. Except for very few specific high resistance applications, generally the lower the impedance of a battery, the better and longer a battery can perform up to its initial standards.

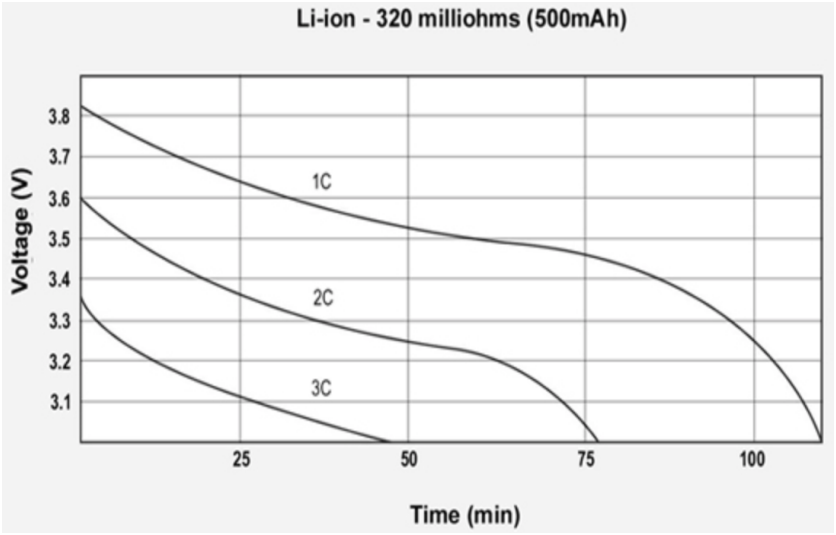

Figure 30: Capacity of Li-ion battery with internal resistance of 320 mOhm, at different discharge currents (Battery University, 2021).

Impedance correlation curves specific to the conditions found in a certain application, such as the one shown for mobile phones in Figure 30, can be obtained. These curves aggregated simulate the timeline of your systems battery performance. This allows for an estimated prediction of when a battery is most likely going to fail or when it will fail to deliver the necessary characteristics, in terms of energy and power, required for its application. In other words, a company can validate the suitability of a battery for its intended application through impedance testing. Furthermore, it is possible to correlate impedance with temperature rise inside a cell. Therefore, battery manufacturers can use this correlation to properly design the heating/cooling system of a battery pack (Secure Power, 2023).

EFFICIENCY

Charging and discharging processes are not ideal and some energy is lost during both processes. As a result, a battery does not deliver the same amount of energy that was used to charge it. This is known as the Charging Efficiency or Coulombic Efficiency (CE), and it can be determined by calculating the difference between the energy used for charging and the energy delivered by the battery in one cycle, as shown in equation 9 (Ahmadi and Torabi, 2019).

$$\text{Efficiency } (\%) = \frac{\text{Energy}_{\text{out}} \text{ (Wh)}}{\text{Energy}_{\text{in}} \text{ (Wh)}} \cdot 100 \tag{9}$$

CE is important as it is used to compute SoC and corrects the imbalance between charges stored and released. It can also be estimated through the SoC or OCV, meaning there are several methods that could be done to measure this parameter (Emeric, 2019). The higher the charging efficiency, the less energy required to charge the same battery. This results in potentially less fossil fuel consumption and more monetary savings. Therefore, for all applications it is preferred to have a high charging efficiency. The charging efficiencies of most Li-ion batteries are already quite high, above 90%, meaning that there is little room for improvement in this sense (Ahmadi and Torabi, 2019). Nevertheless, it is still important to check this parameter and compare between alternative options when selecting a battery.

4 Growing Applications for Batteries

In the following chapter, a research on the state-of-the-art and market growth analysis of four growing applications for batteries is presented. These applications were chosen based on current demands from AVL MTC clients. The goal of this chapter is to predict the potential market expansion of batteries in these applications to determine the two most interesting applications for AVL MTC in terms of new opportunities, products, and clients the company is likely to encounter in the near-future. The two more promising applications will then be studied in further depth in the next chapter to optimize the different battery testing done and required by both applications.

4.1 Electric vehicles

4.1.1 State-of-the-art

The big technology of Electric Vehicle (EV) can be divided into many sub-groups, including: battery-electric-vehicle (BEV), hybrid-electric-vehicle (HEV), plug-in-hybrid-electric-vehicle (PHEV), Fuel cell electric-vehicle (FCEV). In BEV the total electricity is provided by a rechargeable battery charged from an external energy source, such as the grid, by using a charging plug. On the other hand, HEV are usually made up of two or more sources of energy and power, so that if the primary source runs out, a second source, acting as a back-up system, kicks in, allowing the vehicle to continue operating. The energy sources used can be flywheel, battery or regenerative braking, while the power sources can be battery bank, fuel cell (FC), Ultra-capacitor (UC), or Internal combustion engine (ICE). An example are PHEVs, which can run both on gasoline and electricity supplied by battery usually charged by an ordinary plug or by a regenerative braking system (Verma et al., 2021). With regard to the battery technologies mainly used in EVs, the performance parameters to be taken into account are energy density, cycle life and, of course, cost. Today, lithium-ion batteries for EVs are either nickel-based (NMC and NCA) or Lithium-Iron-Phosphate (LFP) (IEA, 2022c), as it is shown in Figure 31.

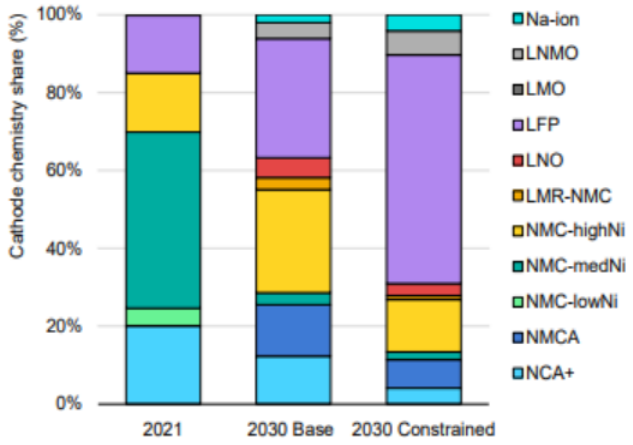

Figure 31: Light-duty vehicle battery chemistry projections according to IEA scenarios (IEA, 2022c).

NMC and NCA, mainly used for EVs, have a higher energy density, but also a higher cost due to high raw material prices for nickel and cobalt. On the other hand, LFPs have a lower energy density but a lower cost. In addition, it presents also the best cycle life compared to other technologies, for this reason it is used for both light and heavy vehicles. Among the various emerging technologies, particularly for mid-range vehicles, are Lithium Nickel Manganese Oxides (LNMOs), which have lower energy density and cost than LFPs; the latter due to the large presence of manganese, which reduces the cost of materials and commodity exposure. However, this technology is still underdeveloped and therefore will not be seen until the next few years. Another technology that could appear on the markets by 2023 is Na-ion batteries. These batteries will be the first technology able to compete with Li-ion batteries performance but without containing Lithium. This is beneficial since it will reduce the battery dependency on Lithium and the current issues associated to Lithium scarcity (IEA, 2022c).

4.1.2 Market estimation

The market for EVs has been growing strongly in recent years. As shown in Figure 33, around 6.6 million EVs were sold in 2021, more than doubled compared with 2020, to reach a total of 16.5 million EVs on the world's roads. Among the various technologies, BEVs accounted for most of the increase, with about 70% (IEA, 2021).

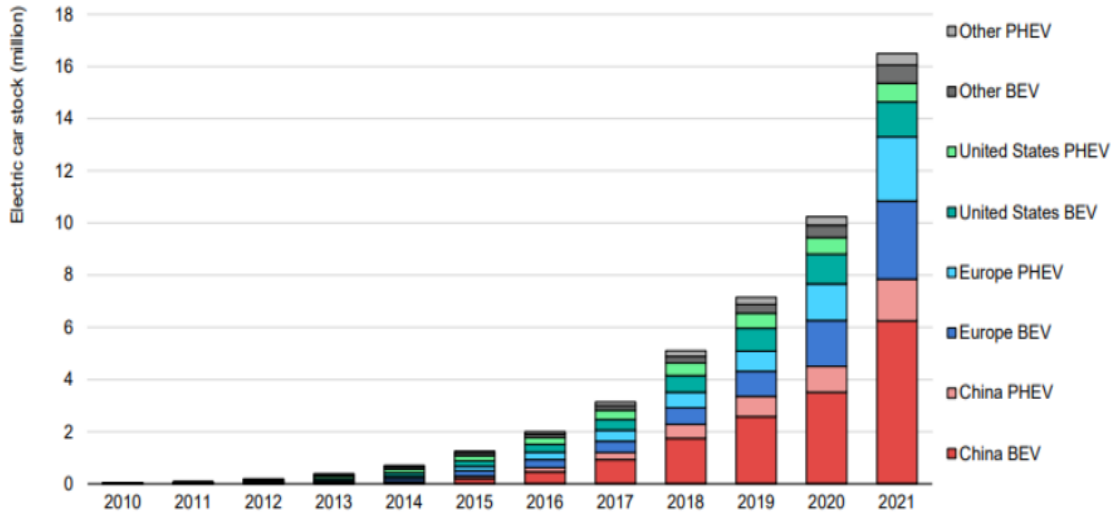

Figure 32: Electric car registrations in selected countries/regions, 2016-2021 (IEA, 2022c).

The countries with the largest sales are China and Europe, as it is shown in Figure 32, where they accounted for 85% of the world's total electric vehicle sales in 2021, followed by the United States (10%) where, again, EVs are becoming increasingly popular. Especially in Europe, electric car sales continued to increase in 2021 by more than 65% year-on-year to 2.3 million, after the boom of 2020.

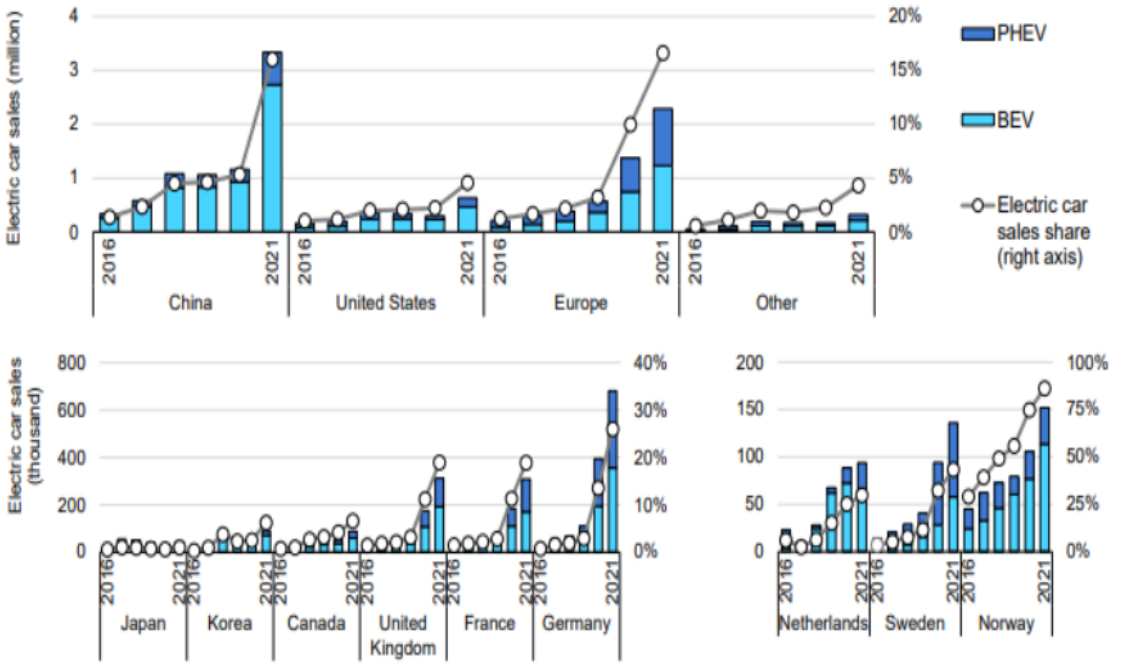

Figure 33: Global electric car stock 2010-2021 (IEA, 2021).

The countries with the highest market share for electric vehicle sales in 2021 in Europe were

Norway (86%), Iceland (72%), Sweden (43%) and the Netherlands (30%), followed by France (19%), Italy (9%) and Spain (8%) (IEA, 2021).

4.2 Heavy Duty Vehicles (HDV)

4.2.1 State-of-the-art

A vehicle is considered heavy-duty when it has a Gross Vehicle Weight (GVW) greater than 3.5 tons (3,500 kg). GVW is the declared permissible weight of the vehicle and the load it's supposed to carry. HDV can be further classified into class N1, N2 and N3 depending on their GVW, as seen in Figure 34 (European Commission, 2014). In 2017 in Europe, over 90% of road freight transport was carried out by class N3. More specifically, around 86% of road freight transport in Europe was done by commercial Heavy-duty truck (HDT) with a GVW over 30,000 kg (Cameron, 2019). Therefore, to facilitate the research in this thesis, electric heavy-duty truck (eHDT) will be the main focus of this section.

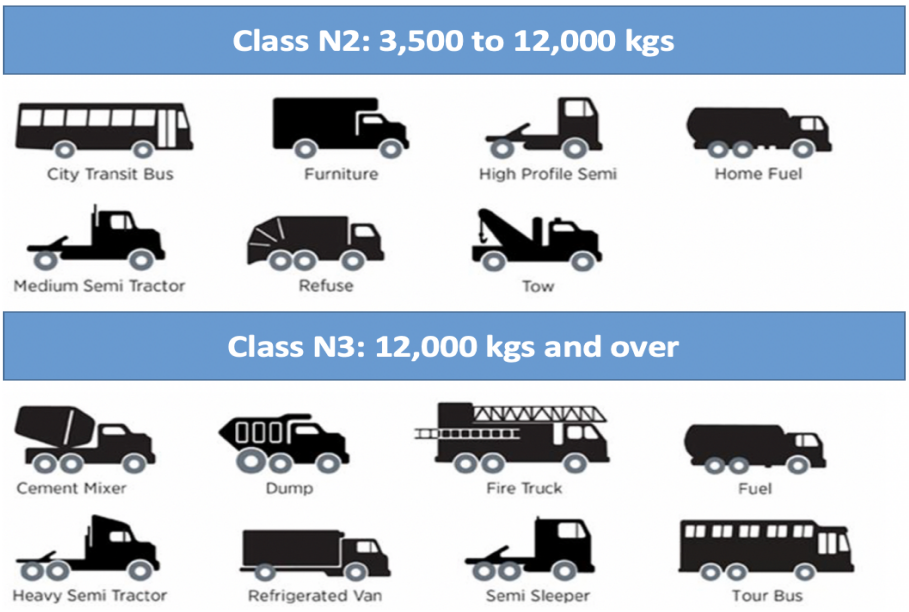

Figure 34: Classification of Heavy-duty-vehicles (HDVs) (Cunanan et al., 2021).

In terms of battery technologies, for HDT the most important performance parameters required to fulfill an applications intended purpose are energy, power, charging rate and cycle lifetime (Campillo et al., 2017).

At the moment, the average range of most eHDT is around 100-300 km on a single charging cycle. The range varies depending on the weight, battery chemistry and external ambient conditions. However, there are recent developments that can change this situation. For instance,

in the end of 2022, Tesla's semi-truck with a GVW of over 36,000 kg successfully drove for over 800 km on a single charge. Official details of the battery used are not made available yet but it is estimated that 9 Ni-based Li-ion modules were used adding up to almost 1 MWh of capacity (Cunanan et al., 2021).

The charging rate and time depend on the charger used and on the battery technology. Nowaday, eHDT can be charged with AC chargers of 50 kW or with DC chargers of up to 250 kW in stationary charging stations. For capacities as big as 1 MWh, these batteries would take 20h and 4h to fully charge, respectively. This charging time is an important bottleneck for eHDT, as conventional trucks take up to 15 minutes to fill up their 1,100 liters of tank. However, in 2017 Tesla announced that they were planning on building a network of "megachargers" that could deliver 1 MW of power and thus theoretically charge a 1MWh battery in 1 hour. Nevertheless, fast charging has proven to degrade batteries, reducing their overall lifetime (Cunanan et al., 2021).

The lifetime of a battery in most eHDT is between 1000-2000 deep cycles, corresponding to approximately 6 years. In order for eHDT to compete with conventional ICE trucks, the goal is to reach a lifetime of 10-15 years. In April of 2023, Swedish truck manufacturing company Scania, together with Swedish battery manufacturer Northvolt, announced a promising battery capable of powering trucks for 1.5 million km (approximately 15 years) (Cunanan et al., 2021).

All these recent developments show how quick this sector is developing and gives promising hopes for the near future of eHDT.

As discussed in Chapter 2.2.5 and Table 1, the most common battery used for HDV is lithium-ion due to its numerous advantages. Silicon based anodes are preferred due to their stability, good conductivity and fast charging capacity. For the cathode, at the moment, most HDV are nickel-based (NMC or NCA), and one of the most pressing questions for vehicle manufacturers is to continue with these batteries or switch to LFP batteries. Nickel-based cells offer 30% more energy density than LFP, whereas LFP have the benefit of being less expensive, using less cobalt (scarce and toxic material) and having a higher lifespan. Besides being more expensive, Nickel-based batteries enable higher payloads as they allow more weight to be carried in the truck, thus they are more cost-efficient (Engineering, 2022).

Ultimately, for lower end and mainly urban HDT, LFP will be the preferred chemistry since driving range is not the priority, while cost and durability is. While for loner range and high-volume trucks, Nickel-based chemistry's will be the primary option (IEA, 2022c).

4.2.2 Market estimation

Previously, the rapid growth in battery technology development in important companies was discussed. In Figure 35 the large growth of HDV is shown, mainly attributed to these vehicles having a key role in global supply chains (Cameron, 2019).

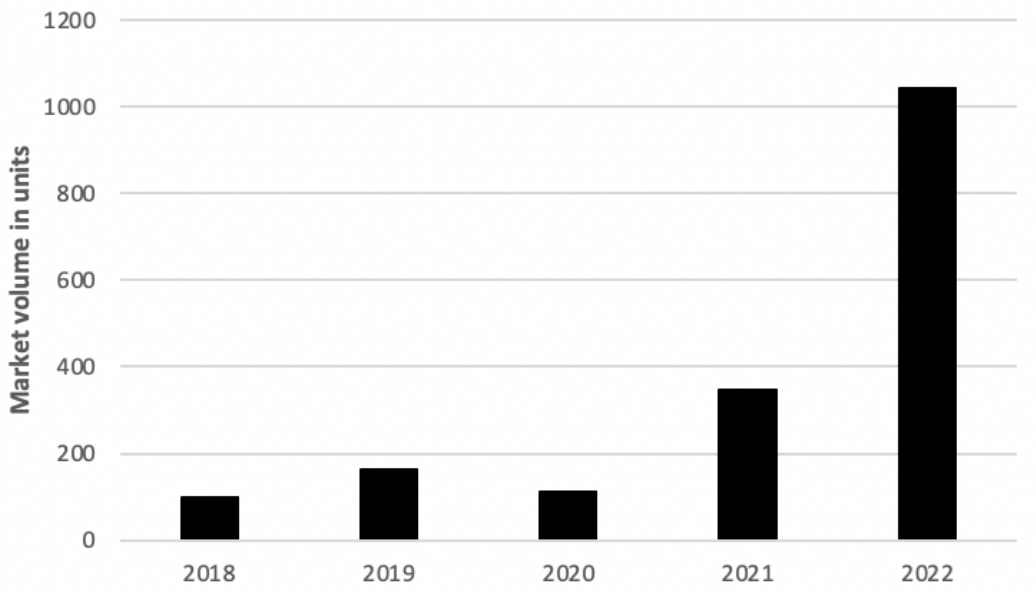

Figure 35: Electric heavy-duty truck market volume in Europe between 2018-2022 (Statista, 2021; Volvo Trucks, 2022; Sustainable Truck & Van, 2023).

The rate of growth of road freight transport in Europe has been constantly increasing every year since 2013, with the exception of 2020, most likely due to Covid-19 pandemic. In 2021, road freight transport grew by 6.5% (IEA, 2022c) in Europe. As observed in Figure 35, the rate of growth of eHDT in Europe has been around 200% for the last 2 years after Covid-19 and it is expected to maintain this rate for several years in order to comply with EU emission legislation's (Statista, 2021; Sustainable Truck & Van, 2023).

In 2021, the global eHDT stock was 66,000 units. Based on electrification targets worldwide and NZE pledges, the global electric truck fleet is expected to expand to 3 million in 2030. This would still only represent 2.8% of current total truck stock (IEA, 2022c).

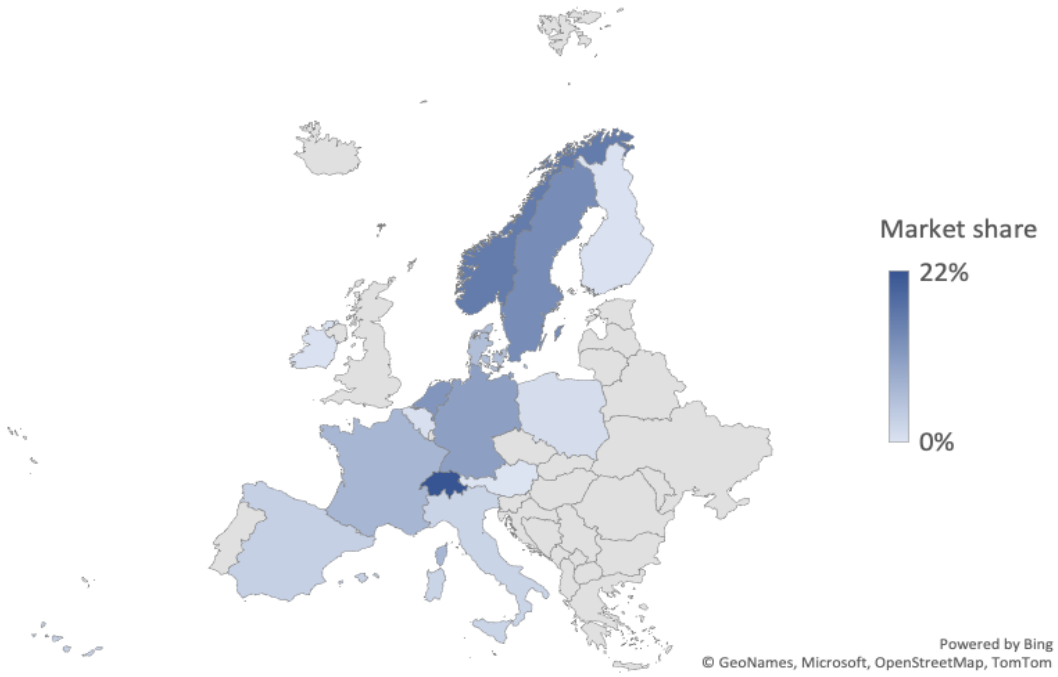

Figure 36: Electric heavy-duty truck registration share in 2021, Europe (Volvo Trucks, 2022).

In fact, as shown in Figure 36, in 2021 Sweden and Scandinavia led the total market volume of registered eHDT in the EU, with 14% and 36% of the total share of trucks, respectively (Volvo Trucks, 2022).

4.3 Maritime batteries

4.3.1 State-of-the-art

In recent years, batteries have started to become more widespread in the marine sector both as a propulsion system and for other auxiliary systems. To date, most of the batteries are used for hybrid propulsion, while 24% are used for plug-in hybrid and 18% are pure electric (Safety4Sea, 2019). In general, however, batteries are not preferred in this type of transport due to their high cost, safety issues and the large onboard volume required by large-capacity battery systems (Kaur et al., 2022). For the maritime systems, it is in fact important to choose a battery technology with properties that can provide an optimum combination of safety, life, performance and a reasonable cost (DNV, 2016). To date, the most widely used technologies are lead-acid and Ni-Cd, but in recent years Li-ion batteries are becoming increasingly popular due to their high energy density (of Shipping, 2019). The most popular technology used today in this sector are the lithium batteries NMCs. They are reasonably safe and present high specific energy. However, this technology presents problems with thermal stability and contains cobalt, which

is currently an expensive raw material, not widely available and with ethical issues regarding its exploited supply chain in Africa. In addition, all batteries in which lithium is present use flammable organic electrolytes, and NMC, in particular, has a high risk of thermal runaway occurring, where the cell temperature increases rapidly and leads to fires that are very difficult to extinguish. A good alternative already used in ships, could be found in LFPs, which would increase safety and solve the raw material problem, but at the same time have a specific energy about 65% of that of NMCs. In addition, the price of LFPs should also fall below that of NMCs in the coming years due to their widespread use (Verma and Kumar, 2021). Another technology that could be adopted in the coming years is Lithium Sulfur (Li-S), due to its higher energy density, lighter weight, and reduced cost due to highly abundant sulfur material (Kaur et al., 2022), which, however, presents problems with regard to cycle life. (Verma and Kumar, 2021)

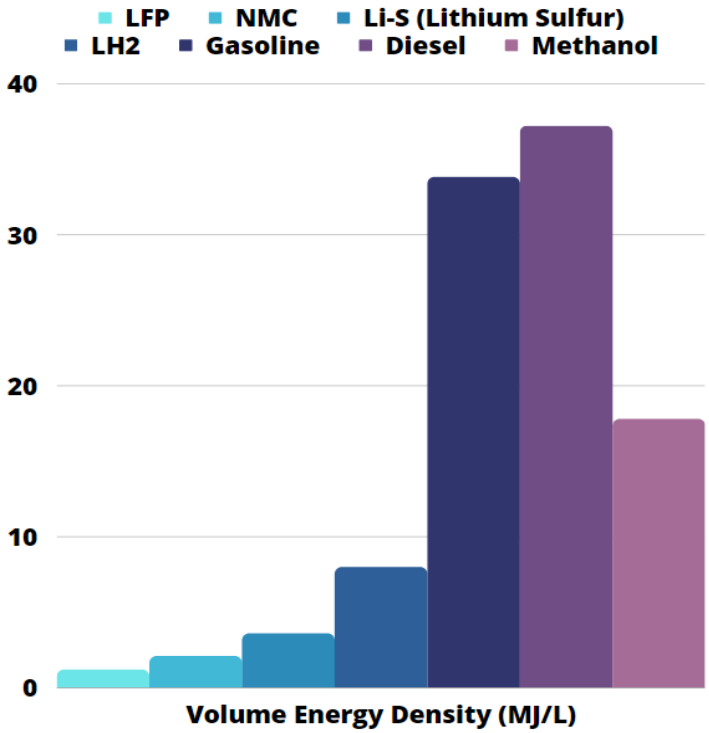

Figure 37: Comparison of volumetric energy densities between different battery technologies and conventional fuels (Epec Engineered Technologies, n.d) (Hydrogen and Office, n.d).

According to Figure 37, batteries may be considered to be used as the energy source of the auxiliary system of boats but not as their main power source. They have in fact a much lower volumetric energy density than the fuels used today, and, considering the high energy requirements of ships, these technologies would require a high volumetric space, thus reducing the available capacity on board, which, especially for the maritime sector, is a key condition.

Today, batteries are mainly used for onboard ferries, tugs and other small or specialised vessels or as an auxiliary system to the main propulsion system (Veritas, 2021). Instead, hydrogen fuel cell are a more promising and viable alternative for the marine sector as they have a higher volumetric density than batteries and are more reliable in terms of higher lifespan and energy quality (Elammas, 2023).

4.3.2 Market estimation

The Marine Battery Market size is projected to grow from USD 374 Million in 2021 to USD 1,897 Million by 2030, at a CAGR of 19.8% from 2021 to 2030 (Research and Markets, 2021). In 2019 there were 160 ships operating with batteries in the world and 104 were under construction (Safety4Sea, 2019).

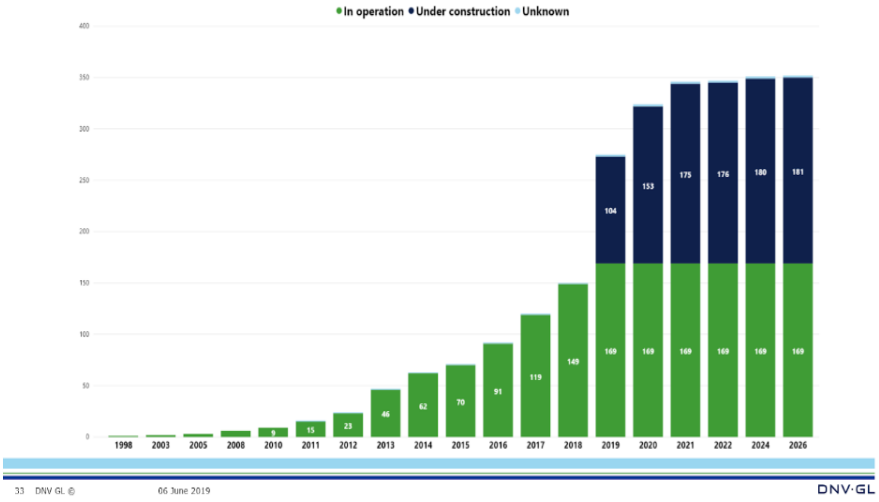

Figure 38: Overview of ships running on batteries, 1998-2026 (Safety4Sea, 2019).

According to Figure 38, there has not been a large increase in the number of boats operating with batteries. Among the different countries Norway is the leader in batteries use with 142 ships. The rest of Europe follows with 85, and then America with 24. Asia has to present 7 ships and Oceania 6 (Safety4Sea, 2019).

4.4 Stationary

4.4.1 State-of-the-art

The application of Li-ion batteries for stationary Energy Storage Systems (ESSs) has gotten a lot of attention because of its potential to increase the grid's penetration levels of renewable energy sources while also improving electricity reliability and quality. Two main categories can be differentiated in stationary applications: energy-focused applications, which involve, for instance, peak shaving; and power-focused applications, which involve frequency regulation and power quality. Energy applications require the system to be charged or discharged for long periods of time (several hours). On the other hand, power applications require short discharge periods, quick recharge times, and multiple cycles per day. Based on these applications, there are several Li-ion chemistry's that are suitable for different stationary applications (Stan et al., 2014).

Applications		Li-ion battery chemistries						
		LCO	LMO	LNO	NCA	NMC	LFP	LTO
Stationary	Grid frequency regulation			✓		✓	✓	✓
	Forecast accuracy improvement				✓	✓	✓	
	Power gradient reduction	✓	✓	✓	✓	✓	✓	✓
Back-up	UPS			✓	✓	✓		

Figure 39: Suitability of Li-ion chemistry's for stationary applications (Stan et al., 2014).

At the moment, more energy-dense chemistry's, such as NCA and NMC, have a larger market share in stationary applications due to space limitations in residential energy storage systems. These applications were the first to implement batteries as ESS. However, with the up-scaling of ESS, cost and lifespan have gained importance, making LFP batteries the preferred choice for grid-scale storage (IEA, 2022a).

In fact, according to a report by Wood Mackenzie, LFP batteries are predicted to surpass NMC as the leading stationary storage chemistry by 2030, with over 30% of the market share (Gupta, 2020).

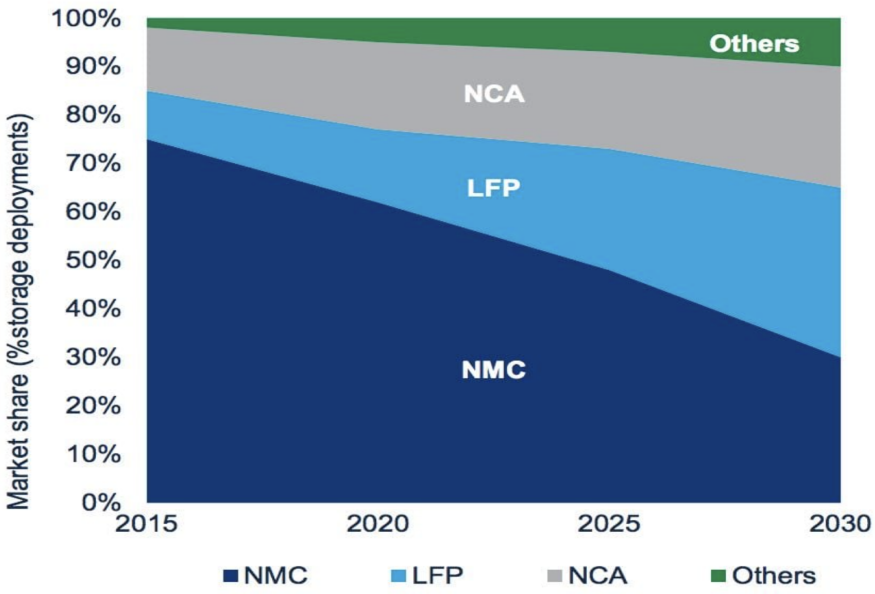

Figure 40: ESS battery chemistry market share forecast (Gupta, 2020).

Flow batteries are seen as a promising technology for stationary storage because of their extended lifespan and scalability. In 2022, the world's largest vanadium redox flow battery was installed in China, with a capacity of 100 MW and a storage volume of 400 MWh. Another potential source of energy storage are repurposed EV batteries, which can maintain up to 80% of their usable capacity. With increasing applicability of batteries in EVs, there is going to be a large supply of retired batteries. However, significant technological and regulatory challenges must be overcome to make second-life batteries a viable option, including the high cost of refurbishment (IEA, 2022a).

4.4.2 Market estimation

As of 2021, pumped-storage hydropower is still the most widely ESS used for grid-scale energy, with an installed capacity of around 160 GW. Nevertheless, grid-scale batteries are rapidly gaining popularity and are projected to account for the majority of storage growth worldwide. In these applications, batteries are mainly used for sub-hourly, hourly, and daily balancing. By the end of 2021, the total installed capacity of grid-scale battery storage was close to 16 GW. The majority of this capacity was added over the past five years, with more than 7 GW being added in 2021. In Figure 41, the evolution of battery storage solutions in the last years is shown where the United States, China, and Europe are leading the market with a gigawatt-scale capacity (IEA, 2022a).

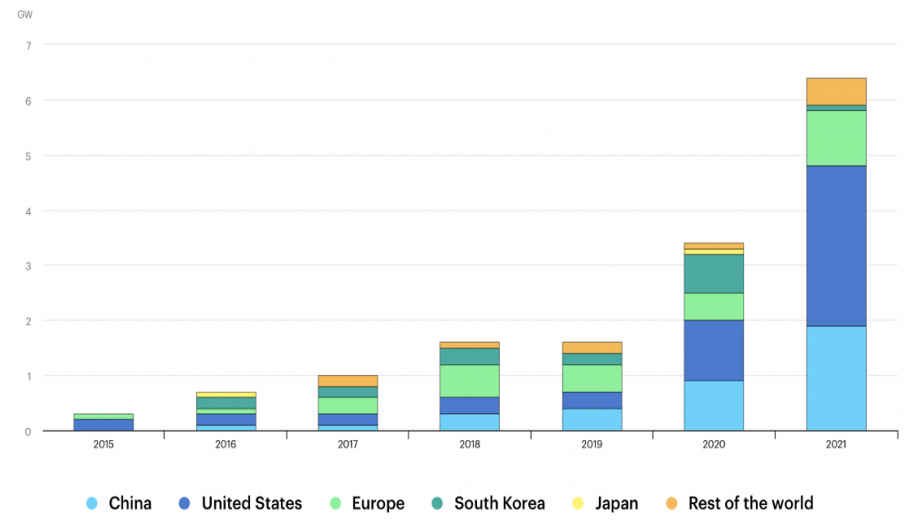

Figure 41: Evolution of installed capacity of battery ESS in the world (IEA, 2022a).

Total investment in battery energy storage exceeded USD 10 billion in 2021, with grid-scale deployment accounting for more than 70% of the total spending. This market is significantly dominated by lithium-ion batteries, which represented over 90% of the batteries used in 2020 and 2021 (IEA, 2022a).

In order to address the intermittency of wind and solar PV generation, an exponential increase ESS is crucial. In particular, following the Net Zero Scenario, grid-scale battery storage needs to drastically increase its capacity to 680 GW by 2030, as depicted in Figure 42. That is a 44-fold increase from 2021 level and it means that on average, annual additions have to be more than 80 GW per year (IEA, 2022a).

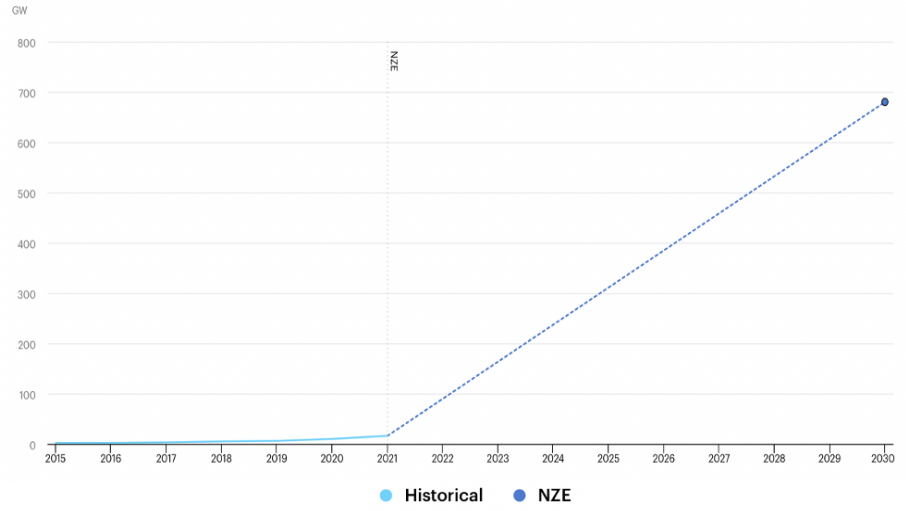

Figure 42: Installed grid-scale battery storage capacity in the Net Zero Scenario, 2015-2030 (IEA, 2022a).

4.5 Conclusions

The aim of this chapter was to determine which of the selected applications were more interesting to focus our testing methodology on, in order to cover a larger market share for future impact of this study.

Based on the analysis performed, HDV and stationary batteries for ESS were selected as the most promising options to pursue with the battery testing analysis and optimization. Electric HDV are growing in volume at a rate of 200% every year in Europe, with Scandinavia and Sweden leading the total volume of registered electric heavy-duty trucks (eHDTs) with 36% of total registered trucks in Europe. Furthermore, Sweden has more than one manufacturer investing heavily to be in the lead of the European production of eHDT.

Energy Storage batteries are growing at the fastest pace of storage growth worldwide to comply with NZE targets. In 2022, they reached a total investment of around 20 billion US dollars in the world. Additionally, Europes' first gigafactory for production of Li-ion batteries was recently established in Skellefteå in the north of Sweden.

On the other hand, light duty vehicles, such as private-owned electric cars, are well established in the market and there is a wide variety of studies and public information in Europe. Therefore there isn't much room for improvement in the battery testing done for these type of vehicles. The opposite is the case for the maritime sector, which has reached a technological bottleneck with batteries not providing sufficient energy and power to satisfy the needs. In addition, most studies suggest that there will not be a large increase in the number of operating electric boats in the near-future, as hydrogen fuel cells are a more promising solution for this application at the moment.

5 Heavy Duty Vehicles

5.1 Existing standards

In this chapter, we select specific performance parameters from the set of criteria discussed in Chapter 3, which are crucial in evaluating a battery's suitability for use in HDV. These chosen parameters will be further examined in the context of the conducted testing. The scope was limited to 2 performance parameters, which were chosen based on their relevance for the intended application: Capacity and Durability.

In summary: capacity represents the driving range of the EV; while durability refers to the lifespan, in number of cycles and number of days, of the battery under testing. These two parameters represent the main bottlenecks for the electrification of EVs.

The most relevant national and international standards have been considered for this study. That includes renown international organizations like the Society of Automotive Engineers (SAE), International Standardization Organization (ISO) and the International Electrotechnical Commission (IEC); and national organizations such as the Standardization Administration of China (SAC), Indian Standards (IS) for the automotive industry and United States Department of Energy (US-DoE) standards. There are several performance testing procedures published in these different standards that explicitly address batteries in EV applications. Most standards are based on previous standards and influenced by research articles, although sometimes can become outdated.

Due to the vast variety of applications and tests, these standards are mainly general for all EV applications, independent of the size or capability of the device being tested. In this way, reference quantities are used in the tests, such as W/kg, "cut-off voltage" or currents based on c-rates, which make it possible to scale the tests up or down depending on the case. This is possible because the majority of batteries used in this sector are Li-based batteries and share similar characteristics and behaviors. However, some distinctions are made in the testing depending on the system level (cell, module or pack) and on the intended application: high energy or high power applications.

Regarding the system level, cells are the fundamental units, each with specific voltage and capacity, often combined to meet desired energy needs. Modules assemble several cells, offering structural support and balancing systems, while battery packs integrate multiple modules,

forming complete energy storage systems. Most tests are aimed at full battery packs as they correspond to real devices ready to be used in an EV. Nonetheless, there are some existing standards, like the IEC, that have been made with special focus on individual cells for battery manufacturers developing new cell chemistry's.

As for the second distinction, high power applications require short bursts of high current rates during charging and discharging; while high energy applications require longer and continuous flow of currents at lower rates. Generally, the latter group corresponds to applications in which the battery is the only source of energy for propulsion and therefore must hold a large amount of energy. In the case of eHDT, they are categorized as a high energy application as they are intended to have an extensive driving range. However, due to their heavy weight (>15000 kg), acceleration and braking procedures will require large but short bursts of power, thus a combination of both test procedures should be considered for these vehicles.

The tests found in current standards with respect to the selected performance parameters are shown in Table 3 (ISO, 2018; IEC, 2018; SAE, 2008; SAC, 2006; U.S.DoE, 2015; IS, 2018).

Table 3: Existing standards of performance parameters for EVs.

Organizations	**ISO**	**IEC**	**SAE**	**SAC**	**US-DoE**	**IS**
Standard	**12405:2018**	**62660:2018**	**J1798:2008**	**743:2006**	**34184:2015**	**16893:2018**
Level	**System/module**	**Cell**	**Module**	**-**	**-**	**-**
Capacity	X	X	X	X	X	X
Durability	X	X	X		X	X

5.1.1 Capacity

Capacity represents the amount of electrical energy, measured in ampere hours (Ah), that can be extracted from a battery given specific conditions. Capacity testing is usually the first test done as it defines the effective capacity of the battery. This value can then be used as a reference to identify degradation (capacity loss) caused by subsequent tests. The result of the capacity test is used to verify the energy content ensured by the battery manufacturer and assess the suitability of the battery for the application.

Battery capacity is mostly evaluated in standards and scientific literature (Zhang et al., 2011; Kassem et al., 2012) using Constant Current (CC) cycling; even though it has been proven by researchers that using Constant Current and Voltage (CCCV) method for charging/discharging

a battery takes more advantage of the batteries available energy (Liu et al., 2019). Constant current cycling involves a series of charging and discharging steps at constant temperature and constant current, until the manufacturers cut-off voltage limits have been reached (usually V_{max}=4.2V when charging and V_{min}=2.7V when discharging for LIBs (Ruiz, 2018). Once fully charged, the battery is maintained for 1 hour in an open-circuit condition to allow it to reach electrochemical equilibrium before the discharging step is carried out.

Ideally, to ensure a proper and realistic representation of real-life scenarios, charging and discharging C-rates should align with those usually found in its specific application to obtain reliable results. On average, the battery of a light-duty EV discharges approximately after 3 hours, corresponding to a C/3 rate. This is considering a typical 60 kWh battery pack used in EVs. Similarly, most available charging stations now-a-day (level-2) can provide power at a voltage of 240V and a current of 30 to 50A, fully charging a 60 kWh battery in 3 hours, equivalent to C/3 rate for charging (Ruiz, 2018). Therefore, the standard value of constant current is defined to C/3 in all standards and used as a reference for battery packs. Nevertheless, different conditions must also be taken into account, thus some standards consider other C-rates to be performed for capacity determination. For instance, SAE-J1798 requires capacity testing at 1C rate (1 hour discharge), whereas SAC requires capacity testing at 1.5C rate.

In the case of ISO-12405, IEC-62660 and IS-16893, these standards distinguish between high energy and high power applications. For example, if the application demands lower power but high energy, the CC cycling may be set to 1C, 2C or even the maximum permitted C-rate (ISO-12405) defined by the supplier. If the application requires high power, the test is carried out at 1C rate (IEC-62660 and IS-16893) or 10C rate (ISO-12405).

Varying the C-rates is essential as it has been shown that capacity can drop by more than 5% when using higher discharging currents (Figure 19). This is mainly due to the increase in voltage drop with increasing rate, which causes the discharge cut-off voltage (V_{min}) to be reached earlier.

Currently, SAE-J1798 is the only standard that requires an additional dynamic capacity test, trying to simulate urban driving conditions for EVs. In this standard, a power profile with a duration of 360 seconds is repeatedly applied to the Device Under Testing (DUT) until it is fully discharged. This test also considers regenerative power (charging from breaking). This procedure is taken from the U.S. Advanced Battery Consortium (USABC) Dynamic Stress Test (DST), a simplified version of the Federal Urban Driving Schedule (FUDS) (U.S.DoE, 1996).

Table 4: Capacity test conditions found in the different standards.

Standard	ISO 12405:2018	IEC 62660:2018	SAE J1798:2008	SAC 743:2006	US-DoE 34184:2015	IS 16893:2018
Charging Current (A)	C/3	Manufacturer Specifications	Manufacturer Specifications	C/3	-	-
Discharge Current (A)	C/3 1C 2C Max C-rate	C/3	C/3 C/2 1C	C/3 1.5C	C/3	C/3
Temperature (ºC)	-18 -10 0 25 40	0 25 45	-20 0 20 45	-20 20 55	30	0 25 45
Additional testing	10C discharge for high-power applications	1C discharge for high-power applications	Dynamic Capacity Testing at 25ºC	-	-	1C discharge for high-power applications

ISO-12405 and IEC-62660 also demand a dynamic discharge test, but in this case, to evaluate the durability of the battery. In these standards, the New European Driving Cycle (NEDC) profile is used. These three synthetic driving cycles used for battery testing are shown in Figure 43. It is important to note that for this type of testing a power scaling is required relative to a percentage of the rated maximum power. The USABC situates current technology advancements at a maximum power of 400 W/kg, but this may vary depending on the manufacturer (Baure and Dubarry, 2019).

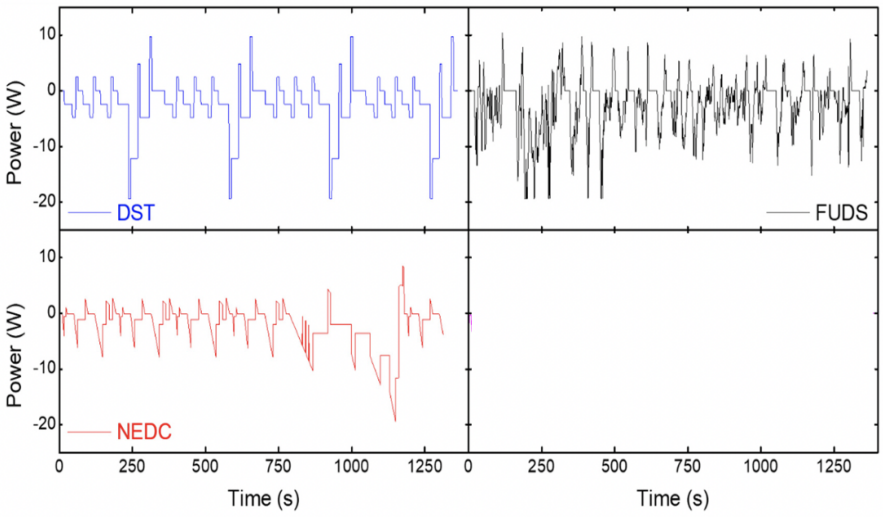

Figure 43: Synthetic power profiles of DST, FUDS and NEDC used for battery testing (Baure and Dubarry, 2019).

Cell capacity is affected by ambient temperature. As observed in Figure 20, capacity drops around 40% when temperature decreases from 23ºC to -20ºC and increases by around 5% when

temperature increases from 23^{o}C to 40^{o}C. Therefore, testing temperatures is also a requirement in different standards, which have temperatures ranging from -20^{o}C to 55^{o}C, as indicated in Table 4. This notable range in temperatures is used because during long periods of parking when the thermal management system of the battery pack is inactive, batteries may be exposed to a broad temperature range depending on their location. For this purpose, standards require that batteries are left for 30 min in a temperature chamber to reach thermal equilibrium prior testing.

5.1.2 Durability

Battery lifespan, referred to as durability in testing standards, is one of the main bottlenecks of the electrification of EVs due to the battery's limited cycle-life and high cost of replacement. This parameter can be expressed in terms of number of discharge cycles and/or number of calendar life years before the battery requires replacement due to failure or insufficiency to perform up to its requirements (when the battery loses 80% of its rated capacity (U.S.DoE, 1996)).

The US-DoE and the EU have set ambitious battery life targets for 2030, aiming for a battery lifespan of 2000-3000 cycles and 10-15 calendar life years (Eurobat E-mobility, 2015). In order to verify that these targets can be reached, a series of tests have been designed to represent the aging of batteries during predefined operating conditions in order to avoid waiting for the entire lifespan of the battery (i.e. 10 years) to pass. Initial battery performance degrades over its lifetime due to electrochemical aging (usage-related) and calendar aging (time). Therefore performance parameters such as capacity and internal resistance are also periodically measured in these aging methods to obtain the variation of performance as a function of the number of cycles or time. Degradation, as observed in Chapter 2, is affected by temperature, load currents, voltage levels (SoC), mechanical stress (time) and moisture. Two different tests are generally defined in standards to represent both aging mechanisms:

1. **Calendar Aging:** The calendar aging test assesses the losses of functional performance parameters as a result of prolonged periods of inactivity (when the vehicle is not being used). The battery is subjected to different temperatures and SoC for a defined period of time. In order to avoid the long periods of time needed to test calendar aging (10-15 years), performance deterioration from inactivity is estimated by extrapolating it from a temperature-dependent correlation model (i.e. Arrhenius model (Aoki and Okuyama, 2015)) which accelerates the aging and results in a shorter test time and costs. This model can be seen below in Figure 44.

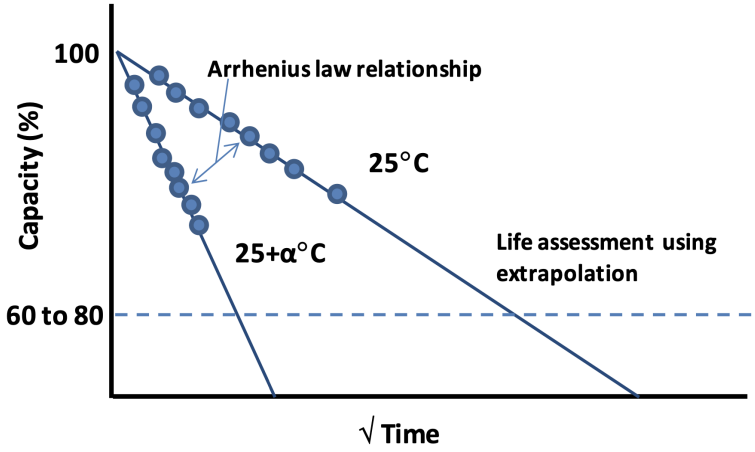

Figure 44: Arrhenius temperature-dependent model for extrapolating life prediction in Calendar Aging tests (Aoki and Okuyama, 2015).

All standards require calendar aging to be conducted at elevated temperatures (40-45 ºC), always maintaining a safety margin (∼15 ºC) above the manufacturer's specified maximum temperature to prevent the risk of thermal runaway.

Additionally, different standards vary in the State of Charge (SoC) used. US-DoE and IS specify 50% SoC, while ISO and both IEC and SAE recommend testing a more stressful and more common SoC of 80% and 100%, respectively. Higher SoC conditions lead to increased stress on the battery's active materials, which can degrade the battery's performance faster over time.

Similarly to capacity testing, both ISO-12405 and IEC-62660 distinguish specific testing conditions for high-power applications and for high-energy applications. As previously stated, we consider HDV to be both high-energy and high-power intensive, therefore both types of testing are taken into account for this application.

Furthermore, IEC standards require a longer testing period (126 days) compared to the other standards which are only tested for a maximum of 28-30 days.

Finally all standards end the test by recharging the DUT and fully discharging it again at standard C/3 rate to measure performance degradation (i.e. capacity fade). Storage tests related to calendar aging tests found in standards are compared in Table 5.

Table 5: Calendar aging test conditions found in the different standards.

Standard	ISO-12405		IEC-62660		SAE	US-DoE	IS
	High-Energy	**High Power**	**High Energy**	**High Power**	**J1798:2008**	**34184:2015**	**16893:2018**
Pre-conditioning Testing	Standard Cycle at C/3	Standard Cycle at 1C	-	-	Standard Cycle at C/3	Standard Cycle at C/3	Standard Cycle at C/3
SoC (%)	100	80	100	50	100	100	50
Temperature (ºC)	25 40	25 40	45	45	25 45	Specified by Manufacturer	45
Resting Period (Days)	1 2 7 30	1 7 30	126	126	2 14 30	30	28

2. **Cycle life aging:** The cycle life aging test assesses the losses of functional performance parameters as a result of electrochemical cycling (when the vehicle is being used). The battery is subjected to different temperatures, current rates and upper and lower cut-off voltages. In addition, similarly to capacity testing, repeated driving cycle tests are also used to represent real driving conditions to get a better estimate of the actual number of cycles that can be reached by the battery. The testing can be divided into 4 main categories and is summarized for each standard in Table 6:

   - The functional parameters used to determine the *initial performance* of the battery. These are first selected and then tested under certain conditions.
   - The specified charge/discharge cycles that will be conducted on the battery.
   - The periodic assessment of performance (using the same parameters and testing procedure as the *initial performance*.
   - Termination criteria for ending the test and reporting of functional parameter variation to determine capacity fade and power fade.

   All standards stress the importance of time and temperature in the aging of a battery and include these factors in their testing procedure. IEC and ISO standards differentiate testing conditions for high-power and high-energy applications. For instance, when determining the capacity, high-energy applications require CC cycling at C/3, whereas high-power applications demand a stronger rate (1C). In terms of SoC swing, both standards require that batteries intended for high-power applications shall perform their cycle life test between 30% and 80%. Additionally, ISO-62660 demands high-energy batteries to also test several SoCs, in this case ranging from 20-80%. Regarding the cycling mode,

high-energy batteries are tested using power-control profiles, while high-power batteries call for current-control profiles, as described in Table 6. In the case of HDV, they should be tested for both types of profiles.

In terms of initial performance, for SAE and IS its characterized through capacity, dynamic capacity and peak power testing. These performance parameters and their periodic evaluation (every 28 days) are similar to those in IEC-62660, with the only exception of IEC measuring pulse power rather than peak power. In the case of the US-DoE standards, they follow the U.S. Advanced Battery Consortium (USABC) Baseline Life Cycle Test Procedure (U.S.DoE, 1996) by performing a DST and considering capacity, pulse and peak power as performance parameters.

The testing temperature is a factor that varies among most standards. In IEC-62660, periodic performance tests are carried out at 25^{o}C for both high-power and energy batteries, while the cycling test is conducted at 45^{o}C. Conversely, ISO-12405 has dissimilar conditions for the two types of batteries. For high-power vehicles, all tests are performed at 25^{o}C; whereas for high-energy vehicles, periodic performance evaluation takes place at 25^{o}C cycling is conducted at both 25^{o}C and -10^{o}C. The rationale behind testing high-energy batteries at freezing temperatures is to verify that they can perform at extreme temperatures without extreme degradation, especially given that these batteries are intended to be the only power mechanism in vehicles. Therefore they need to be reliable enough to compete with ICE engines in cost effectiveness. SAE standards, on the other hand, perform all tests at 25^{o}C; while the US-DoE gives more importance to the manufacturer's specifications and if not specified, advises to use 30^{o}C for all tests. Lastly, Indian Standards (IS) suggests using 25^{o}C for the periodic performance testing and 45^{o}C for cycling test. It can be noticed how the different standards try to assimilate the more common temperature conditions found in their area of application.

Ultimately, all standards suggest terminating the cycling test when performance values of the battery do not fulfill the minimum requirements of their intended application. More specifically, all standards except ISO define this as performance values dropping below 80% of their initial values. Additionally, ISO, IEC and IS suggest a more precautious terminating criteria by concluding the test in case cell temperature or any reference parameter surpasses a certain limit imposed by the manufacturer. Moreover, US-DoE, IEC and IS also include a maximum number of cycling repetitions, defining a cyclability target in order to reduce unnecessary testing.

Table 6: Cycle life test conditions found in the different standards.

Standard		Initial Performance	Charge/Discharge Cycles	Periodic Performance	Termination Criteria
ISO	**High Energy**	1. T=25°C 2. Standard cycle[1] (C/3) 3. Repeat for -10°C and then 25°C	1. T=25°C 2. SoC swing: 20-80% 3. Dynamic discharge profile A[2] 4. Dynamic discharge profile B[3] 5.Repeat for 28 days	1. After 28 days repeat *Initial Performance* tests and pulse power test at 25°C 2. Every 8 weeks repeat *Initial Performance* tests and pulse power test at -10°C	Terminate if: 1. Any limits set by the manufacturer are reached 2. Power and capacity requirements are not fulfilled
	High Power	1. T=25°C 2. Standard cycle[1] (1C) 3. Standard Discharge to 80%	1. T=25°C 2. SoC swing: 30-80% 3. Dynamic discharge-rich profile[4] 4. Dynamic charge-rich profile[5] 5. Repeat for 22h, rest for 2h	1. Every 7 days perform power test 2. Every 14 days perform capacity test (at 1C)	Terminate if: 1. Any limits set by the manufacturer are reached 2. Power and capacity requirements are not fulfilled
IEC	**High Energy**	1. Capacity test at 25°C and 1C 2. Dynamic Capacity[6] test at 25°C and 45°C 3. Pulse power test at 25°C and 50% SoC, 10s pulses of 5C	1. T=45°C 2. Standard cycle[1] (C/3) 3. Dynamic discharge profile A[2] until 50% SoC at 45°C 4. Rest time of <4 h between steps 5. Dynamic discharge profile B[3] at 45°C 6. Dynamic discharge profile A[2] until 80% SoC at 45°C 7. Repeat for 28 days	1. After 28 days repeat tests done in *Initial Performance*	Terminate if: 1. The entire process is repeated 6 times or, 2. Any performance parameter is <80% of initial value 3. Cell temperature surpasses limit set by manufacturer
	High Power	1. Capacity test at 25°C and 1C 2. Power test at 25°C and 50% SoC, 10s pulses of 10C	1. T=45°C 2. SoC swing: 30-80% 3. Dynamic discharge-rich profile[4] A 4. Dynamic charge-rich profile[5] 5. Repeat for 22h, rest for 2h	1. Every 7 days perform power test 2. Every 14 days perform capacity test	Terminate if: 1. The entire process is repeated 6 times or, 2. Any performance parameter is <80% of initial value
SAE		1. T=25°C 2. Capacity test (C/3) 3. Dynamic capacity test[6] 4. Peak power test	1. T=25°C 2. Dynamic capacity test[6] until 20 SoC 3. Fully recharge 4. Rest time between each step 1-2h (using cooling if needed) 5.Repeat for 28 days	1. After 28 days repeat tests done in *Initial Performance*	Terminate if: 1. Capacity is <80% of initial value 2. Peak power capability is <80% of its rated value at 20% SoC
US-DoE		1. T= Defined by manufacturer 2. Capacity test (C/3) 3. Low current pulse power test 4. Peak power test	1. T=30°C 2. Fully charge DUT to Vmax 3. Scaled dynamic stress test at recommended T by supplier 4. Rest time between each step 15 min 5. Return T=30°C to the battery 6. Repeat all steps once per day	1. Repeat tests done in *Initial Performance* every 30 days	Terminate if: 1. Cyclability target are attained or, 2. Capacity or peak power drops <80%
IS		1. T=25°C 2. Capacity test (C/3) 3. Dynamic capacity test[6] 4. Peak power test	1. T=45°C 2. Standard cycle (C/3) 3. Dynamic discharge profile A[2] until 50% SoC at 45°C 4. Rest time of <4 h between steps 5. Repeat for 28 days	1. After 28 days repeat tests done in *Initial Performance*	Terminate if: 1. The entire process is repeated 6 times or, 2. Any performance parameter is <80% of initial value 3. Cell temperature surpasses limit set by manufacturer

[1]Standard Cycle: Standard discharge (CC), rest for 30 min or thermal equilibrium, standard charge (CC), rest for 30 min

[2]Profile A is a segment from NEDC profile with a short burst of power which simulates accelerating conditions.

[3]Profile B is a segment from NEDC profile with a long burst of power which simulates hill climbing conditions.

[4]Discharge-rich profile is a segment from NEDC profile with an overall net discharge over the battery after the test.

[5]Charge-rich profile is a segment from NEDC profile with an overall net charge over the battery after the test.

[6]Dynamic Capacity: Full discharge by simplified NEDC power profile A.

5.2 Gaps between real-life conditions and tests in standards

5.2.1 Capacity

Capacity test is performed in standards with a matrix of different temperatures (i.e. -20, -10, 0, 25, 40, 55) and constant discharge currents (i.e. C/3, 1C, 2C, 10C), simulating different speeds and climatic conditions, respectively. Capacity, C_i, is calculated according to equation 10, where t represents the time taken for the charging or discharging process, and SoC is the ratio of remaining available capacity over the nominal capacity (C_n) of the battery at the beginning (t_0) and end of process (t). The SoC can be calculated through several methods, with the main one used being the integral method where the SoC at a specific time, t, is estimated through the accumulation of current as shown in equation 11.

$$C_i = \frac{\int_{t_0}^{t} I dt}{SoC_t - SoC_{t_0}} \tag{10}$$

$$SoC_t = SoC_{t_0} - \frac{\int_{t_0}^{t} I dt}{C_n} \tag{11}$$

C_i is used to estimate the driving range of the EV and it is measured in Ampere hours, which means it actually represents the electrical range of a battery. However, driving range is more closely related to energy consumption, thus battery capacity in Watt-hours would be more practical to accurately estimate the driving range of an EV (Liu et al., 2014). This term is denominated as State of Energy (SoE) and represents the ratio of remaining energy with respect to the battery´s nominal energy. Similarly to SoC, SoE at a specific time is calculated as shown in equation 12, with the difference of integrating power (W) and using nominal energy instead of capacity as compared to equation 11.

$$SoE_t = SoE_{t_0} - \frac{\int_{t_0}^{t} P dt}{E_n} = SoE_{t_0} - \frac{\int_{t_0}^{t} U \cdot I dt}{E_n} \tag{12}$$

Until now there have been several discrepancies in the range claimed by OEMs of existing EVs (Birrell et al., 2014). This is due to several reasons, some of which will be discussed in this thesis. A potential reason that could be having a negative impact on range estimation is the use of SoC, instead of SoE, in battery testing. Unlike SoC, SoE directly translates into driving range; but compared to SoC, the research on SoE is much less and the procedure to estimate SoE and remaining driving range from this parameter needs to be further developed.

Capacity testing in standards is done using a CC discharge strategy for capacity estimation. This procedure is suitable in applications where the power demand of the battery is more stable and/or follows predictable patterns. Such is the case of laptops or Uninterruptible power supplies (UPS), which have a relatively constant power demand during operation. However, this is not the case of EVs in general, where the battery is discharged at variable power loads throughout its operation. These loads rapidly change in intensity, which means that sampling frequency is important to collect as much accurate data as possible. Furthermore, regenerative braking allows for intermittent charging during high discharge periods. Therefore, intermittent charging/discharging using real-life duty cycles that reflect the vehicles ordinary activity can provide a much more accurate estimation of the vehicles capacity and driving range.

As mentioned previously, only SAE standard demand a sort of dynamic duty cycle test for capacity estimation, while ISO and IEC demand it for lifetime approximation. The duty cycles used in these standards are shown in Figure 43. Nevertheless, all these profiles are synthetic and therefore limited in providing real driving behaviours. One of the few studies that compared these synthetic duty cycles with an actual driving cycle concluded that the synthetic profiles underestimated the driving range of EVs as they did not take into account sufficient regenerative braking, average discharge currents and traffic/resting periods (Birrell et al., 2014). Furthermore, these synthetic driving profiles target passenger vehicles in an urban driving environment, thus they are not suitable to represent the driving cycles of heavy-duty vehicles. For an accurate capacity estimation, the factors lacking in current driving cycle testing must be considered through the elaboration of a holistic driving cycle.

As analysed in Chapter 2.4, there are several degradation factors which affect the performance of batteries both momentarily and permanently. For instance, at a specific cycle: a higher discharge rate decreases the battery capacity (Figure 19); and if repeated periodically, it can permanently reduce the nominal capacity of the battery. For these reasons, most electronic devices are **de-rated**. This means that at certain critical points, the devices reduce their electrical, thermal and/or mechanical stress (Sun et al., 2018). In the case of EVs, this de-rating is mostly seen in discharge currents. Close to the battery's end of discharge, the maximum discharge current is reduced in order to avoid degradation and also to take advantage of remaining energy left in the battery. In this way, from Figure 19 it can be determined that if the battery is de-rated from 2C to 0.2C, it will allow around 10% more energy to be discharged. When driving, this de-rating is illustrated by limiting the top speed of the vehicle, but allowing it to drive for

10% more of its entire range. Constant Current (CC) capacity testing done in standards does not consider de-rating and thus possibly underestimates the battery´s capacity. A procedure that allows de-rating to be considered while performing capacity testing will be proposed in this thesis.

There is a big gap in current testing standards when it comes to estimating battery capacity in EVs (including HDVs) and potentially other battery applications (i.e. Energy storage). The following issues have been identified in the standards and will be addressed in Chapter 7:

1. Use of SoC to estimate capacity, instead of SoE which is in energy units and directly translates into driving range.
2. Dynamic capacity testing is rarely implemented and it is done with general synthetic duty cycles that lack real-driving behaviours and don't adjust to every EV category.
3. De-rating is not considered in current standards and could significantly affect the results of capacity testing.

5.2.2 Durability

Durability testing is divided in two tests that represent different aging mechanisms occurring in a battery. Calendar aging is estimated through short-term test extrapolations and/or accelerated aging test methods. During the latter, degradation factors are stressed to accelerate the aging and deterioration of the battery, obtaining the end-of-life of the battery in 6-7 months. However, extrapolating battery lifetime under normal usage from accelerated aging methods may not be very accurate. A comparison of both is necessary to validate this testing procedure. Furthermore, several models have been made that try to represent both cycling and calendar aging of a battery with the following inputs: Temperature, SoC, Discharge Current and DoD (Gewald et al., 2020). However, the analysis of these models is out of the scope of this thesis as we will only focus on actual battery testing. These models served as valuable information that led to identifying some of the missing gaps in current lifetime testing done in standards.

In terms of cycle-life aging, like capacity, synthetic dynamic profiles are repeatedly used on the battery until specific termination criteria is met. As with capacity, the synthetic driving profiles fail to represent real-world usage conditions, thus the cycle lifetime of a battery is usually

estimated with a significant degree of uncertainty. The situation is worse for HDV applications which don't have an official representative driving cycle. Therefore, cyclability testing of HDV battery's is non-existent in the standards. This issue will try to be addressed in this thesis through developing a methodology that converts a real life HDV duty-cycle into a suitable cycle-test. This methodology shall be limited by the availability of a power dispatch curve of a battery. With this information, different duty cycles of the same application are possible depending on the geographic region, ambient temperature or driving mode of the vehicle.

While analyzing the cycle-life test conditions specified in the standards and the accelerated ageing models in (Gewald et al., 2020), an important observation was made that was commonly repeated in all standards. All studies have the same charge-discharge cycles constantly repeated throughout the entire cycle-life test. This means that the SoC of the battery ranges throughout the same values for the entire test, assuming an ideal constant use of the battery throughout its lifetime. However, the reality is different from this as it is very rare that a HDV is used in the same way, with the same conditions and following the same routes throughout its entire lifespan. There is actually a random distribution of SoC_{start} and SoC_{end} when using a vehicle, as shown in figure 45.

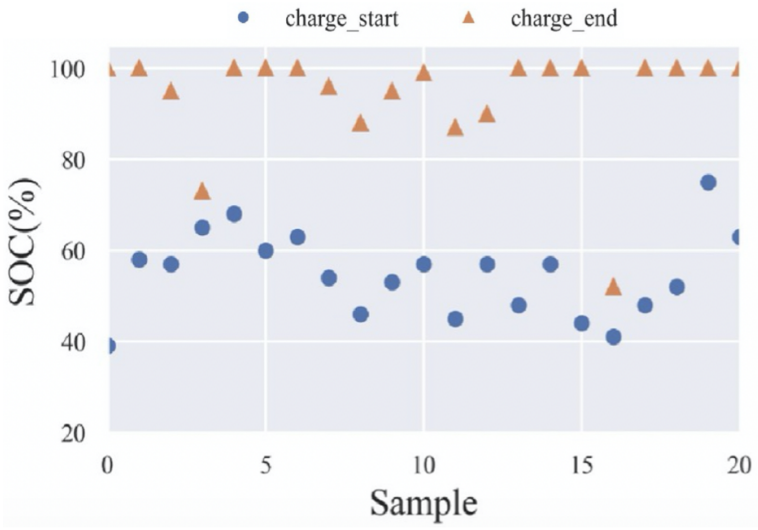

Figure 45: Small sample out of 707 EVs showing the random distribution of initial and final SoC when charging (Liu et al., 2023).

None of the evaluated standards actually tests the effect of charging and discharging at dissimilar ; but based on our previous analysis in Chapter 2, it is highly probably that there could be some degradation due to mechanical stress caused by different operating loads, voltages and

temperatures while charging.

Similarly, no test procedures exist that evaluate charging and discharging a battery at different temperatures; something that is constantly occurring in real life. For instance, when an EV is parked for some time and left in open-air conditions, since the thermal management system of the battery is shut-down due to the vehicle not operating, the temperature of the battery tends to approximate to that of the ambient conditions (which may vary depending on the season and geographic location). Temperature is an essential factor when it comes to battery degradation and it has been shown how it can significantly reduce the lifespan of a battery (Ma et al., 2018; Momidi, 2019; Miao et al., 2019).

It is important to assess these gaps in order to determine their impact on the lifetime of a battery. In this way, new suggestions can be made to current testing procedures in the standards to improve their representation of real-life conditions of batteries in EVs.

6 Stationary Energy Storage Systems

6.1 Existing standards

Battery cell performance testing is well developed for use in personal devices and EVs, however, for stationary applications, existing standards and requirements are not yet fully developed. The complexity in assessing the performance of Battery Energy Storage Systems (BESSs) results from their diverse applications. Testing one system's efficiency in a particular application doesn't guarantee the same efficiency in another due to the wide variety of uses. These applications are mostly connected to the power grid, presenting a significant challenge: finding a balance between the grid's requirements and the cells' performance demands. Moreover, the connections within these applications are intricate, uncertain, and continuously evolving. Additionally, grid service requirements constantly change as power system operators adapt their practices to integrate energy storage. To address these complexities and uncertainties, various approaches to cell performance testing are needed to clarify the requirements for cell storage performance. (Rosewater and Schoenwald, 2020)

Nowadays battery standards and requirements are studied and developed all over the world. In the USA for example the Pacific Northwest National Laboratory ((PNNL)) and Sandia National Laboratories, sponsored by DOE OE ES, have carried out multiple researches to develop ESS performance protocols for various grid services, especially regarding batteries. The parameters taken into account to be tested were, for example, round-trip efficiency, ramp rate for active and reactive power, stored energy capacity at various percent of rated power, energy capacity stability and standby energy loss. In addition, eight duty cycles were also taken into account, including: Peak Shaving, Frequency Regulation, Islanded Micro-grid, PV Smoothing, Volt/Var Support, Renewables (Solar) Firming, Power Quality and Frequency Control. Together with them the Institute of Electrical and Electronics Engineers ((IEEE)) developed some protocols similar to other found in other countries (Vartanian et al., 2021).

In Europe, the EU sets standards through the three officially recognized European Standardization Organizations: the European Committee for Standardization, the European Committee for Electrotechnical Standardization and the European Telecommunications Standards Institute. They create standards that are identified by 'EN' and so far they all resemble the standards from the International Electrotechnical Commission (IEC) and International Standardization Organization (ISO). In the past years these two institutes have been developing standards for storage systems, with the ISO focusing more on EV and environmental management while the

IEC focusing more on stationary applications (Blair et al., 2021).

Regarding tests, it is important to define whether the tests are performed at the cell or battery module level, as there may be big differences between the two modes. It is therefore important to point out that in the standards mentioned below, tests for BESS are always carried out at the system/module level. Particularly in IEC 61427-2:2015, only a specific number of cells can be taken into account according to the test performed.

The general characterization information, including test conditions and limits of applicability of an energy storage, are described in the IEEE 1679-2010, which allows also for valid comparisons.

Instead, the IEC 62620-2014 describes general testing procedures about batteries used for industrial application, including storage. It contains discharge performance tests at different rates and different temperatures, the high discharge rate permissible current test, the internal resistance measurement test, the charge retention test, the endurance in storage at different temperature and SOC test (calendar life) but the endurance cycling capacity test is not specific to electricity storage applications (a generic cycle from industrial application with full charge and discharge at constant rates) (Doetsch et al., 2015).

Some general requirements and test procedures are also described in the IEC 62932-2-1:2020, mainly the determination of energy at constant power, maximum deliverable input and output power, energy efficiency at constant power level and cycle life testing (IEC, 2020).

Finally, in the IEC 62933-2, an almost complete list of unit parameters and testing methods for ESS system are described. In the first part, a description of four different duty cycles: frequency regulation, fluctuation reduction, voltage regulation, peak shaving/shifting and back-up power, and their relative tests can be found. Subsequently, test methods for the following unit parameters are also described: actual energy capacity, input and output power rating, round trip energy efficiency, expected service life, system response, auxiliary power consumption, self-discharge of EES systems, voltage range and frequency range (Doetsch et al., 2015).

6.2 Test procedures

Some test procedures found in the standards differ from the general test done for other battery application. This is because, while some remain the same, new performance parameters, as it showed in Figure 46, can characterize a BESSs.

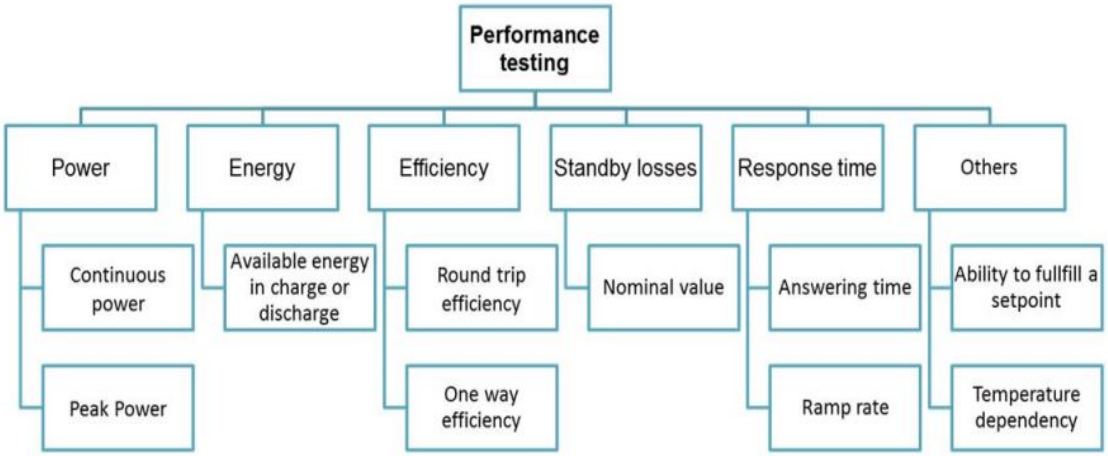

Figure 46: Performance parameters for stationary application testing. (Doetsch et al., 2015)

In particular, among these, the parameters more recurrent in standards and more predisposed to develop are going to be analyzed: energy, including the round trip efficiency, and response time. In addition, the use of duty cycles for performance tests will also be analyzed.

6.2.1 Actual Energy Capacity Test

The Actual Energy Capacity Test is mentioned in the standards IEC 62933-2-1:2017, IEC 62932-2-1:2020 and IEC 61427-2:2015. Instead, in the IEC 62620:2014 there are only some guidelines for charging and discharging procedures in case electrical tests are carried out. In stationary applications, it is in fact important to determine the charging capacity and the discharge capacity of the system in order to understand how much energy can it store and release. In addition it can be noticed from these standards that most of the tests are done without varying the usual conditions such as temperature or the charging rates, but are usually executed at ambient temperature and with different power rates, since that's usually what varies in different applications of BESSs. In most of these tests, the battery system is first discharged to its minimum energy level and then charged to its full available energy level at rated input power, always according with the system specifications and operating instructions. Then the system should be discharged again to its minimum available energy level, always following the systems specification and operation indications (including the needed resting times between charge and discharge). The output power, output time and energy consumption of the auxiliary subsystem shall be measured and recorded during discharge. The actual energy capacity is calculated in the IEC 62933 as follows (IEC, 2020):

$$E_o = \sum_{i=1}^{n} P_{O_i} \times \Delta t - E_{aux_o} \tag{13}$$

where

E_o	is the calculated total output energy at the point of connection (POC) (Wh);
$\sum_{i=1}^{n} P_{O_i}$	is the active output power at time i, measured at the POC (W);
Δt	is the sampling time of the measurement (h);
E_{aux_o}	is the energy consumption of the auxiliary subsystem measured at the auxiliary POC during the output operation (Wh);
n	is the discharge time (h).

Any change in the state of charge or state of health of the test unit; change in power consumption of the auxiliary sub-system; or the use of different discharge rates, temperatures or end-of-discharge parameters will result in different results. For this reason, any energy statement has to be accompanied by the declaration of the conditions operative during its determination. By running this test for a minimum number of cycles n of 2, it is also possible to estimate Round-trip efficiency, i.e the energy output divided by the energy input throughout a complete charging and discharging cycle, considering the rated input and output power. It can be evaluated according to the following formulation (IEC, 2020):

$$\eta_{rt} = \frac{E_o - E_{aux_o}}{E_i - E_{aux_i}} \tag{14}$$

where

E_o	is the total output energy measured at the (primary) POC considering energy losses including conversion loss and energy used for the auxiliary subsystem,
E_i	is the total output energy measured at the (primary) POC considering energy losses including conversion loss and energy used for the auxiliary subsystem is the total input energy measured at the (primary) POC,
E_{aux_o}	is the energy consumption of the auxiliary subsystem measured at the auxiliary POC during output operation,
E_{aux_i}	is the energy consumption of the auxiliary subsystem measured at the auxiliary POC during the input operation.

6.2.2 Response Time

The response time of a BESS is defined as the time between when the set point is received from the BESS (T_0), which is in stand-by mode, or when the grid parameter changes in a way to trigger the system response, and the instant in which the power increases by 2 percent from that required T_3, as showed in Figure 47 (IEC, 2020). This parameter is very important if the BESS is used in ancillary grid services but its value is usually not given or only the response time of the storage component is calculated (Doetsch et al., 2015).

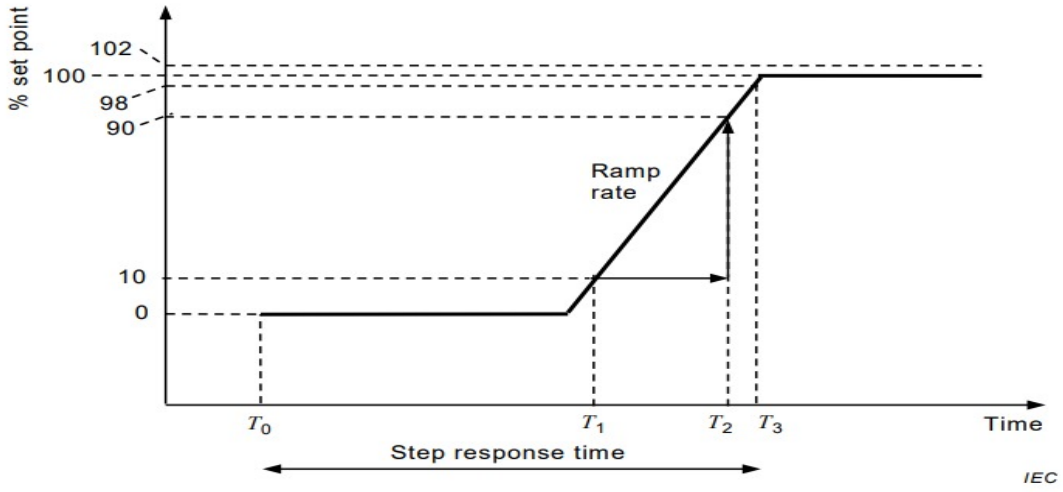

Figure 47: Example of Response Time and Ramp Rate of a BESS (IEC, 2020).

From the graph, we can also see how the response time can be divided in two different time steps:

- **Answering time or Communication Latency**, as defined in the literature and not in the standards, is the time step between T_0 and T_1, indicating the intervening time between sending the order and the moment when the power starts to increase/decrease (Doetsch et al., 2015).

- **Ramp time**, is the time step between T_1 and T_3 which defines the speed the system can ramp up or decrease the power from the moment the power is sent until it reaches the requested power. In particular T_1 represent the instant where the active power becomes higher than 2% of the set point value while T_3 is the time when the active power gets higher than 98% of the set point value (IEC, 2020). According to the standard IEC 62933-2-1:2017 it can be defined by the following equation:

$$RR = \frac{P(T_2) - P(T_1)}{T_2 - T_1}(W/s) \tag{15}$$

In particular, if the system has a rated value of reactive power, then the ramp rate shall be also tested at:

– rated input/output reactive power,

– rated input/output apparent power (with different ratios of active/reactive powers),

– other set points with reduced power respect to the rated one.

In Figure 48 an example of a System Response Test is shown. This test is mentioned in the IEC 62933-2-1:2017. In a first step, not shown in the diagram, the battery is brought to 50% of its state of available energy, and then charged and discharged several times according to predefined steps. These test shall be repeated more than two times (IEC, 2020).

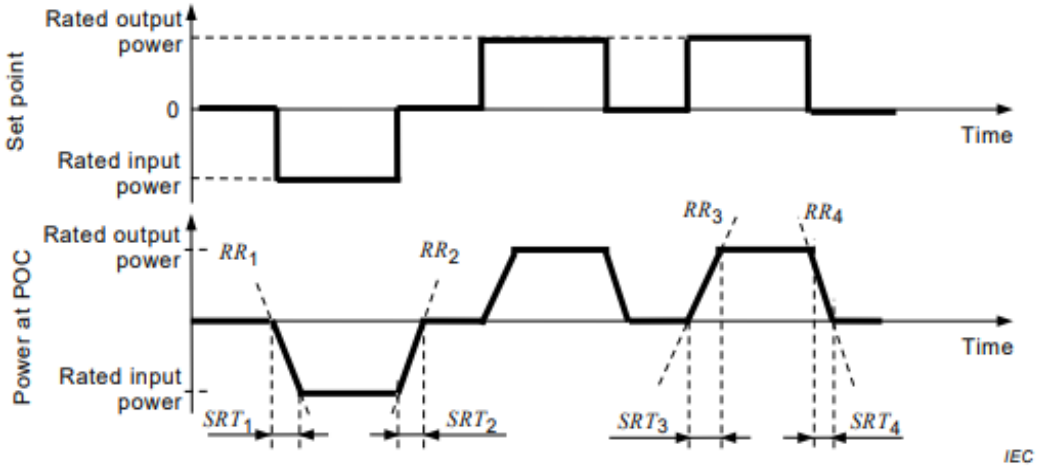

Figure 48: Response time test procedure (IEC, 2020).

6.2.3 Duty Cycles

The use of duty cycles for testing aims to assess performance capabilities of a battery for a given application but it can also be used to evaluate the degradation process of the battery (Rosewater and Schoenwald, 2020). In particular in this thesis, for simplicity, the performance tests will be the only focus. Duty cycle testing are assembled by using a common set of standardized measurement criteria and test procedures (Rosewater and Schoenwald, 2020). However, there is a notable absence of testing profiles specifically designed for stationary grid-connected storage systems within the existing system and requirement frameworks. When testing EVs, as mentioned in Chapter 5, this is accomplished by establishing performance targets and scaling the tests to the minimum number of cells that would meet the targets (Rosewater and Schoenwald, 2020). In the case of Energy Storage Systems (ESSs), the process is more complex due to the diverse range of applications and the absence of a universally applicable minimum performance metric. Therefore, it is essential to gather data on various applications based on specific criteria such as power rate, charge/discharge duration, and the number of cycles (Doetsch et al., 2015). An example is given in the standard IEC 61427-2:2015, where the tests are defined for 4 typical application profiles: Peak-power shaving, Load following, Frequency regulation and PV energy

time shift (IEC, 2015). However, several papers define many more examples of duty cycles that could therefore be integrated into the standards in order to have more accurate and application-specific tests to be studied, such as Wind Firming, Islanded Microgrid, Volt/Var Support, Power Quality and Frequency Control (Conover et al., 2014).

In IEC 62933-2-1:2017, the various types of applications are divided into three main classes:

1. **Class A**: short-duration applications that require the ESS to input/output the required power over a duty cycle for a short period of time (for example, the ESS is charged and discharged in less than 1 h). This class includes frequency regulation, fluctuation reduction and voltage regulation applications.

2. **Class B**: long-duration applications that require the ESS to input/output the required power over a duty cycle for a long period of time (for example, the ESS system is charged and discharged in more than 1 h). This class includes peak shaving/shifting applications.

3. **Class C**: ESSs that are used to supply AC power to electric power grids in emergency case, without relying on an external power source. This class includes back-up power applications.

It is important to note however, that one single ESS system can be used in different applications from different classes.

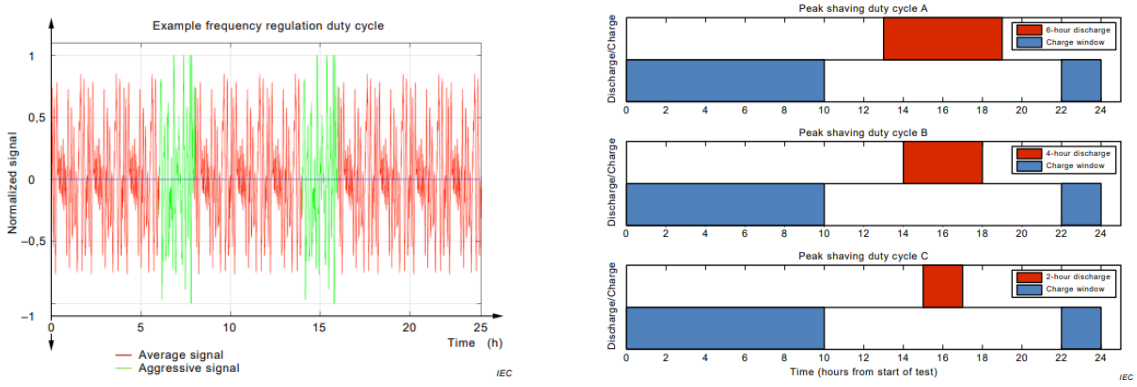

(a) (b)

Figure 49: Examples of duty cycles representing (a) frequency regulation and (b) peak shaving (IEC, 2020).

The type of tests done with these classes, according to the standards, are: Duty cycle round-trip efficiency test, fluctuation reduction test and black start output voltage (IEC, 2020). In Table 7 it is shown which test can be performed for each application class.

Table 7: Performance tests for different applications according to the standard IEC 62933-2-1:2017

Performance Test	Class A	Class B	Class C
Duty Cycle roundtrip efficiency	X	X	
Fluctuation reduction	X		
Black start output voltage			X

In IEC 61427-2:2015, the test performed with duty cycles is to measure endurance, with the intention to determine the suitability of the battery design to accept and deliver energy under certain conditions that represent in a simplified manner the duty the battery will be expected to perform in its application. In other words, the battery will be charged and discharged according to the typical actions it will perform during its operation and at the power levels that will be required by the application. In Figure 50, it is shown a typical example of a daily peak-power shaving service test routine profile (IEC, 2015).

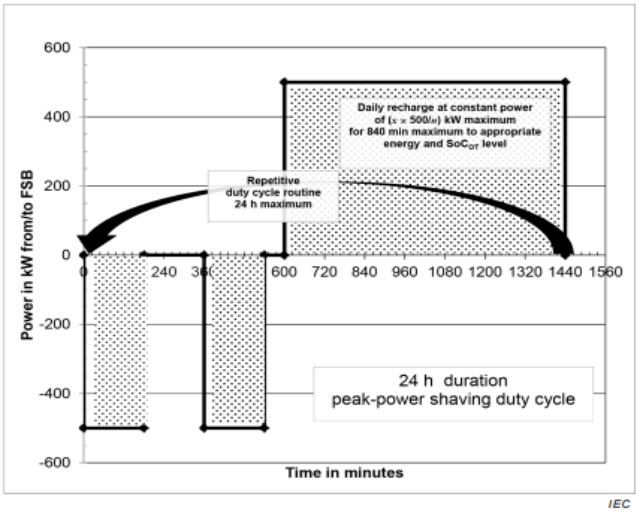

Figure 50: Daily peak-power shaving service test routine profile (IEC, 2015).

6.3 Gaps between real-life conditions and tests in standards

6.3.1 Energy capacity test

As already mentioned, for battery used in energy storage applications is very important to have knowledge regarding the energy the system can store and deliver under different condition and, therefore, the actual energy capacity test is very important. A first shortcoming that can be

identified in the standards, similar to what occurs in HDV, is the lack in defining of the energy level, just mentioned. A graphic explanation can be seen in Figure 51. With the introduction of this parameter we would be able to have a better knowledge of the energy that could be charged or discharged at different power rates from a given SoE.

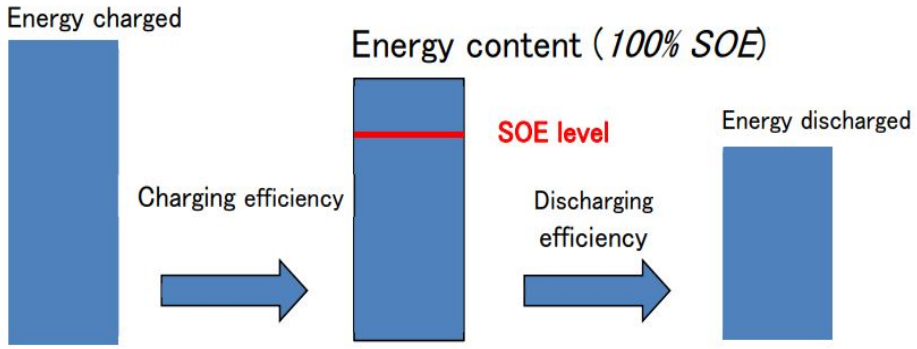

Figure 51: Explication of the SoE indicator.

To be able to use this indicator, it is necessary first to perform a series of measurements at different charge and discharge powers to obtain a mapping of available energy regarding required powers and eventually temperature. In standards and protocols the indications regarding the boundary conditions of the test are never given or recommended for temperature or neither power rates. Regarding the temperature, the explanation could be related to the fact that the BMS of the BESS is capable of maintaining an ideal temperature at all times and therefore does not affect the available capacity. Thus this will not be further looked into.

The following procedure, not present in the standards, gives general guidelines for carrying out the energy capacity test, taking into consideration all the factors mentioned so far. In particular, this method should be considered both for charging and discharging. Indeed, both charge and discharge are of interest in order to know how much energy could be injected into or consumed from the ESS.

The steps to follow would be:

1. standard charge following the charge process of the manufacturer until 100% SoE.
2. Discharge at the nominal power and record the discharged energy (E_{Pn}).
3. Definition of the four constant power values for the testing showed in the table 8.

In particular the values would be defined according to the technology that limits that power,

that in the case of BESS can be either the Power Converter System (PCS) or either the Storage Unit (SU).

Table 8: Conditions marked for capacity test procedure of ESS.

Steps	Maximum power limited by PCS	Maximum power limited by SU
1	P_{max} PCS	P_{max} SU
2	$\frac{3}{4}P_{max}$ PCS	$\frac{3}{4}P_{max}$ SU
3	$\frac{1}{2}P_{max}$ PCS	$\frac{1}{2}P_{max}$ SU
4	$\frac{1}{4}P_{max}$ PCS	$\frac{1}{4}P_{max}$ SU

Finally, in Figure 52 it is shown an example of the results achievable with the following procedure. As seen from the graph, by reducing the nominal discharge power the BESS will require more time to reach 0% of the SoE

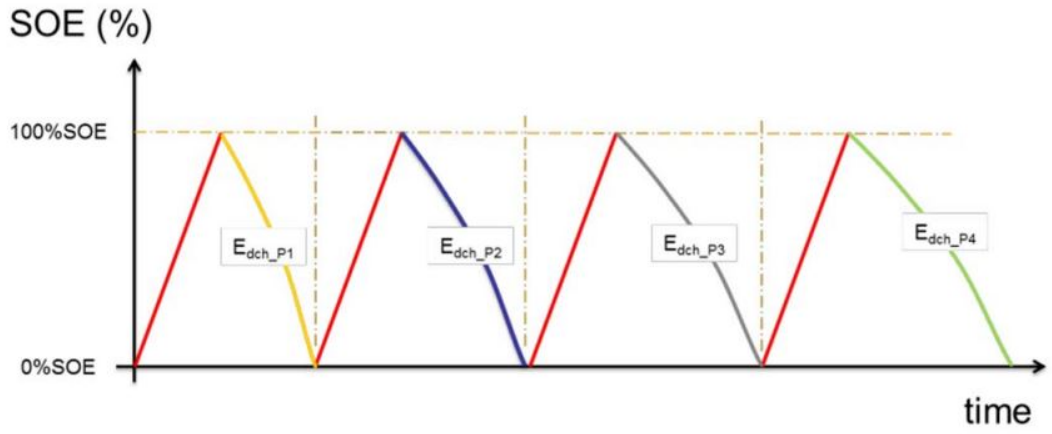

Figure 52: Example of an available energy capacity test taking into account the SoE.

6.3.2 Duty Cycles

The applications of BESS are many and, given recent developments in this technology, may increase and become even more differentiated in the coming years. That's why it's necessary to find a way to be able to develop your own duty cycle based on the specific application and battery conditions. In fact, current studies in renewable grid applications show the lack of a systematic approach to characterize grid-specific duty cycles. For example, the solution found in the standards is to group the various modes of operation into subgroups that have similar characteristics, thus reducing the accuracy and precision of the tests. Sandia National Laboratory

has implemented a testing protocol to assess the performance of ESSs using duty cycles obtained for various grid applications but they don't describe accurately all the factors that could occur in reality. For PV smoothing, ESS duty cycles were generated directly from existing PV generation profiles, without identification of characteristic duty cycles. For frequency regulation, duty cycling was analyzed via the Fourier transform, and "aggressive" and "average" days were extracted from the dispatch and used as characteristic duty cycles. It is therefore necessary to find a solution for the characterization of the grid-specific duty cycles.

In the literature, an efficient algorithm was developed to design duty cycles using a dispatch interval matrix to capture metrics in the ESS dispatch relevant to lithium-ion battery aging and performance. It implements unsupervised learning and dimensional reduction on this matrix to produce characteristic duty cycles of the dispatch. From these characteristic duty cycles, synthetic duty cycles are produced that are suitable for laboratory testing and fast simulation. This algorithm will be further explained and modified to be adaptable to all battery applications in Chapter 7.1.

In the following Figure 53 it is shown an example of the results obtained with the following algorithm when designing a peak shaving duty cycles, taken as an example from the literature (Moy et al., 2021).

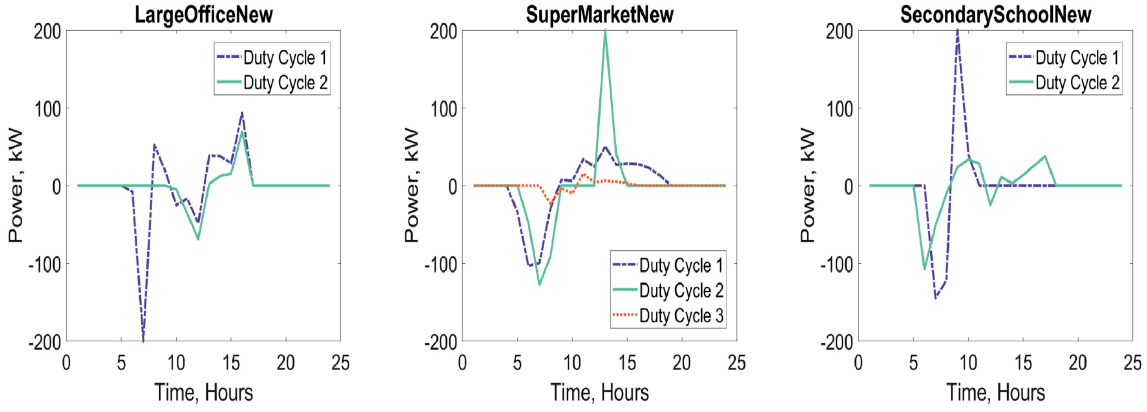

Figure 53: Example of a duty cycle evaluated with the algorithm (Moy et al., 2021).

7 Methodology to validate the gaps found in current standards

In the previous chapters, we conducted an analysis of the gaps present in two growing applications for batteries: Heavy-Duty Vehicles and Stationary Energy Storage Systems.

The methodology was as follows: initially, an extensive research was performed to identify the requirements and performance parameters specific to these applications. With the main performance parameters identified, we proceeded to review the existing testing standards for each application. It was discovered that the existing tests found in standards and used in the latest studies exhibited significant differences, indicating potential gaps that could be enhanced to better reflect real-life usage of these batteries. Surprisingly, despite the difference in nature of heavy-duty vehicles and stationary energy storage systems, their electrification bottlenecks were found to be quite similar due to the shared reliance on the same battery technology, Li-ion. Consequently, the gaps identified for both applications are interconnected and could be tackled collectively. In this chapter only the most interesting gaps were further discussed and these mainly affected capacity, duty cycles and cycle lifetime tests.

This chapter now proceeds with the development of a methodology to address these gaps. The methodology will be based on the foundation of both theoretical insights from the literature and practical test procedures, serving as essential components to understand, evaluate, and validate the identified gaps.

7.1 Duty cycle

In order to overcome one of the gaps in the standards, an algorithm to design and validate synthetic duty cycles that could be used for the various tests was developed and is described in the following chapter. In particular, the algorithm designs duty cycles in the context of power dispatch of Li-ion batteries in diverse applications by using clustering techniques and Principal Component Analysis (PCA) to identify characteristic duty cycles based on a dispatch interval matrix. The only input data required to make the algorithm work are: power dispatch, State of Energy (SoE), which can be obtained from the power dispatch data; and the ambient temperatures of the time period and location selected for the operation of the battery.

The algorithm is divided into four main sections that will be deepened in the following chapters. First, the dispatch interval matrix is obtained, representing twelve metrics related to the input data for each non-zero power dispatch interval. PCA is then applied to reduce the dimensions of the matrix, finding patterns and relationships within the data and representing them using a smaller set of variables called principal components. K-means clustering is performed on the PCA subspace matrix to identify clusters and determine the optimal number of clusters. This step results in the generation of cluster centroids, which represent characteristic duty cycles. Finally, the conversion into a testable duty cycle can be obtained, which can then be used for battery testing and validation of some main parameters, such as capacity and lifetime cyclability.

7.1.1 Input Data

In order for the algorithm to function, it requires of some essential input data regarding the system under testing. Such key information is: the power dispatch (kW), the nominal energy of the system (kWh), and the external temperature of the environment in which the system is located.

For the purpose of this thesis, we have developed a case study to validate our algorithm prior to applying to the battery module used for our dataset. The power dispatch data we have used has been provided to us by the Master thesis of our colleague Mariana Lopes: *Forecasting and Optimization Models for Integrated PV-ESS Systems*, which developed an algorithm to forecast battery production and optimise the battery load. Therefore, keep in mind that the data used in our case study may seem real but it is merely speculative, with the purpose of providing

information for our study.

For our case study, a BESS is chosen which is located close to a storage facility in KTH campus. This battery system is used for arbitrage purposes, to reduce and optimize the cost of electricity consumption of KTH students accommodations. A BESS used for energy arbitrate applications is responsible for storing energy when electricity prices are lower and offering it to the grid when prices rise. While the peak shaving aims to reduce peak energy demand and alleviate strain on the grid, arbitrage focuses on taking advantage of price differentials in energy markets to generate profits.

Power Dispatch

The power dispatch W(t) of a BESS represents its operation during a selected time period. It involves determining how much power the BESS should inject or absorb from the grid based on various factors such as grid conditions, demand response signals, energy market prices, and system operator commands. The power dispatch aims to optimize the BESS operation for maximum efficiency, grid stability, and economic benefits.

In the data-set of our case study, the power data is sampled in kW every 1h interval over one year; and the BESS has a rated energy capacity of $E_{nom} = 100$ kWh. In this data-set, positive values represent the power output of the battery (discharging) to the grid or to a load, while the negative values represent the power injected into the system (charging). In the following Figure 54, an example of the battery power dispatch for the first day is shown.

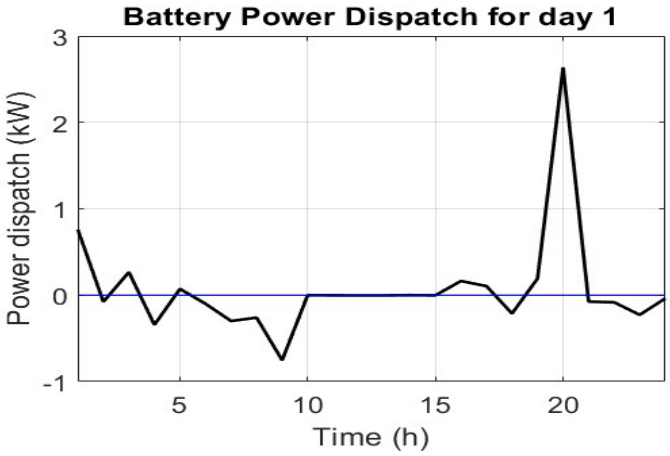

Figure 54: Power Dispatch of day 1

To get a broader perspective, below in Figure 55 is shown the operation of the BESS throughout an entire year of activity.

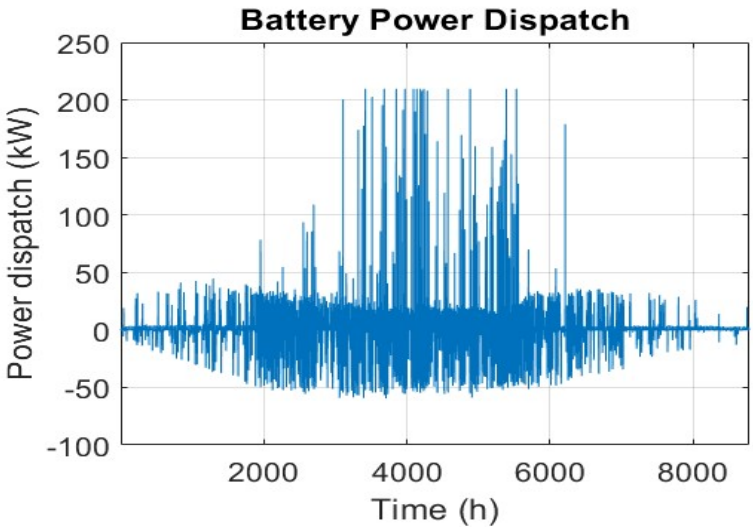

Figure 55: Total Power Dispatch of the BESS during the year

State of Energy (SoE)

The SoE is another data input that is required by the algorithm but that can be evaluated from the power dispatch. The SoE, as previously defined in Chapter 5.2.1, is the ratio of the battery residual energy under specific operating conditions i.e., varying load and temperature, over the total battery available energy (Ma et al., 2021). It can be evaluated through equation 12.

For our case study, the initial SoE is set as $SOE(0) = 0.5$ while the rated energy capacity of our system is $E_{nom} = 100kWh$. Given these parameters and the power dispatch of the system, the SoE of the battery operating in the entire year is shown below.

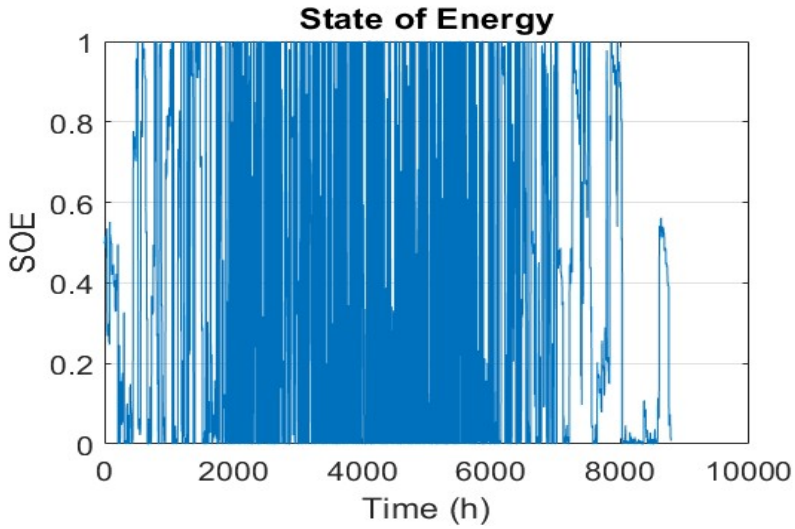

Figure 56: SoE of the BESS during the year.

Outdoor air temperature $T(t)$

Another input that must be recorded is the outdoor air temperature $T(t)$ registered in the location and time period selected. In particular, for this analysis, the weather data was collected from the POWER Data Access Viewer from NASA and the location selected is in Stockholm, inside the KTH campus as showed in Figure 57.

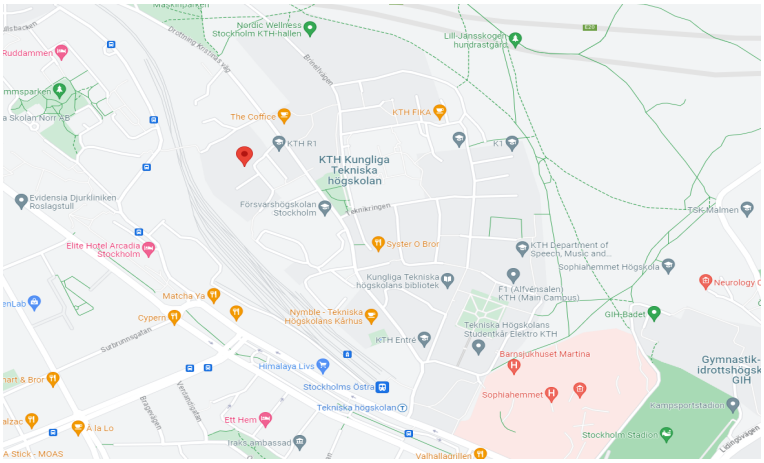

Figure 57: Selected location for the data set (59.350068, 18.067054).

The selected year, during which the BESS should operate, is 2021, and in that year outdoor temperatures at the selected location followed the trend shown in Figure 58. The data was obtained from the National Aeronautics and Space Administration (NASA) Langley Research Center (LaRC) Prediction of Worldwide Energy Resource (POWER) Project funded through the NASA Earth Science/Applied Science Program.

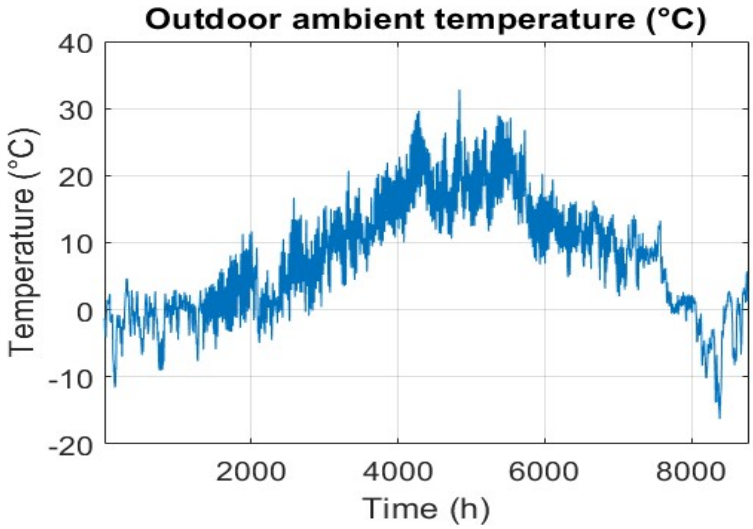

Figure 58: Outdoor temperature trend in the location selected in 2021.

7.1.2 Dispatch interval matrix

After describing and collecting all the input data, these are reorganised inside a dispatch interval matrix M.

To do so, first, the data set is grouped in intervals. Depending on the application, they can be organized into a one day interval in the case of peak shaving (since the power dispatch data is collected every hour); or in hour intervals as in the case of frequency regulation, since the data samples are collected every 2 seconds. Since our application is arbitrage the data will be organized in an interval of 24 hours.

Next, twelve metrics related to the power, SoE, and temperature are computed for each non-zero power dispatch interval. An example of these metrics for 1 random day is shown in Table 9. These metrics were chosen to address characteristics of the dispatch relevant to lithium-ion battery calendar and cycle aging by including the power and frequency contents of the dispatch, as well as the operating conditions (i.e. SoE and temperature) during dispatch.

Table 9: Interval metrics used in the algorithm with example extracted from the chosen dataset for one random day.

Number	Name	Example
1	Number of discharge events	16
2	Number of charge events	8
3	Peak discharge power (kW)	5,7
4	Peak charge power (kW)	19,1
5	Average discharge power (kW)	0,15
6	Average charge power (kW)	0,52
7	Average discharge SOE	0,44
8	Average charge SOE	0,51
9	Average discharge temperature (°C)	-2,4
10	Average charge temperature (°C)	-2,63
11	Peak discharging frequency (Hz)	1,74e-05
12	Peak charging frequency (Hz)	3,5e-05

From this table, metrics 1 and 2 represents the number of discharge/charge events, i.e when the ESS dispatch positively, in the case of discharge, or negatively, in the case of charge. Metrics 3 and 4 record the absolute maximum positive/negative power dispatch of the ESS during all

discharge/charge events, while metrics 5 and 6 represent the absolute average positive/negative power dispatch of the ESS during all discharge/charge events. Metrics 7 and 8 record the average SoE of the ESS during all discharge/charge events. Similarly, metrics 9 and 10 record the average outdoor air temperature of the ESS during all discharge/charge events. Finally, metrics 11 and 12 represents the Peak discharging/charging frequency. In order to evaluate these last two metrics, first, all the charge/discharge segments are collected, concatenated and then mean-centered. After, the Fast Fourier Transform (FFT) is used to evaluate the frequency required.

7.1.3 Methods

Principal Component Analysis (PCA)

Principal Component Analysis (PCA) is an ordering technique used to display patterns in a very diverse data-set, i.e display the relative positions of data points in fewer dimensions while retaining as much information as possible, and explore relationships between dependent variables (Syms, 2008). In this case study, it is used to reduce the dimension of the data set of interrelated variables. For this, orthogonal vectors representing new, uncorrelated variables, named as principal components, will be initially obtained. Given a data set of m observation with n variables in a matrix $X \in \mathbb{R}^{m \times n}$, PCA produces the principal components $v_1, v_2, ..v_n$ with corresponding singular values $\sigma_1, \sigma_2, ..\sigma_n$ sorted in ascending order. Subsequently, the dimension of X is reduced by projecting the matrix along a subset of its principal components with dimension $p < n$, resulting in $v_1, ..., v_p$. The optimal number of principal components p^* is determined using the retained variation F_p of X_p over its original variation X.

$$F_p = \frac{\sum_{i=1}^{p} \sigma_i}{\sum_{i=1}^{n} \sigma_j} \tag{16}$$

After finding F_p, the optimal number p^* will be defined as the minimum number of components needed to exceed a minimum threshold, that in our case was defined as $F_{min} = 0.9$ as recommended by the literature (Moy et al., 2021). Finally, the projection of X onto the optimal number of components p^*, P can be obtained.

$$P = X[v_1, ..., v_{p^*}], P \in \mathbb{R}^{m \times p^*} \tag{17}$$

The matrix found represents the optimal PCA subspace for X and will be used to evaluate

the k-means clustering in the following step of the algorithm (Moy et al., 2021).

K-means clustering

The k-means clustering is one of the most used technique for clustering (Sterling et al., 2017). Clustering is a common technique for statistical data analysis, which is used in many fields, including machine learning. It is the process of grouping similar objects into different groups, or more precisely, the partitioning of a data set into subset according to some defined distance measure (Ashour et al., 2019). Regarding the k-means clustering, it groups the m data points into K clusters and defines the center positions, named centroids, with a mean value of each cluster (Omran et al., 2007). In this case each individual is placed in the cluster closest to the cluster centroids according to the smallest Euclidean distance with the cluster centroid. An example of a clustering on a set of observations is shown in Figure 59.

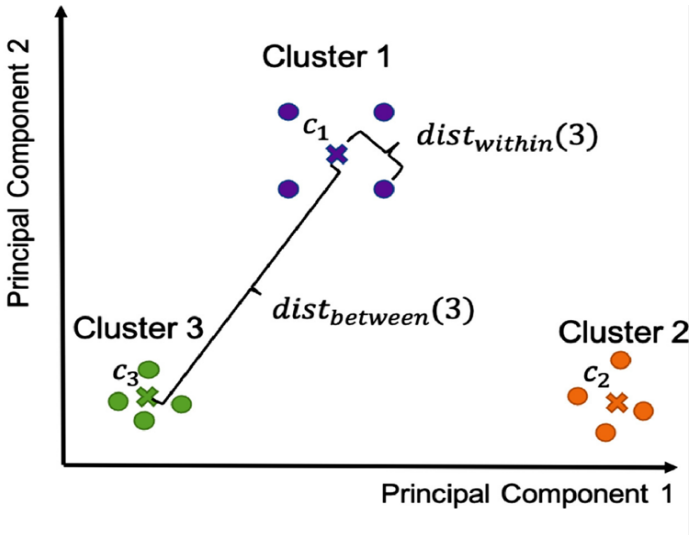

Figure 59: Example of clustering on observations in a PCA subspace of two principal components with k=3 (Moy et al., 2021).

Given k desired clusters and data-set of observation vectors $x_1, .., x_m$ k-means clustering determines k cluster centroids as a solution $\phi^* = [c_1, ..., c_k]^T$ that minimizes the cost function J:

$$J = \sum_{i=1}^{m} \min_{j=1,..,k} \|x_i - c_j\|^2 \tag{18}$$

In this technique the most important part is to find the optimal number of cluster N_c. The process consist in evaluating the distances between the centroids of each cluster, $dist_{between}$ and the distance between each individual of the cluster and their centroid, $dist_{within}$. In general, it must be ensured that $dist_{between} > dist_{within}$, otherwise several clusters could overlap and the

results would be indistinguishable. In particular the $dist_{within}$ will be defined as the maximum average distance between the cluster centroid c_j and all m_j of the cluster members:

$$dist_{within}(k) = max \left\{ \frac{1}{m_j} \sum_{x_i \in clusterj} \|x_i - c_j\|^2, j = 1, 2, .., k \right\} \tag{19}$$

Instead, the relative position between each cluster will be defined as the minimum pair-wise distance between each pair of cluster centroids:

$$dist_{between}(k) = min \left\{ \|c_a - c_b\|^2, a \in 1, .., k, b \in 1, .., k, a \neq b \right\} \tag{20}$$

In order to produce clusters distinct from each other, the optimal number of cluster N_c can be defined as the value of k which maximizes the difference between $dist_{within}$ and $dist_{between}$ (Moy et al., 2021).

$$N_c = argmax_k \left\{ dist_{between}(k) - dist_{within}(k) \right\}, k = 1, 2, .., k_{max} \tag{21}$$

7.2 Capacity

The current capacity testing required by internationally recognized standards for both EVs and stationary applications involves constant charge/discharge steps at various C-rates and temperatures. However, these tests fail to accurately represent actual battery usage and behavior in their respective applications. Firstly, constant current discharge rates do not capture the dynamic discharge profiles of batteries during real-world operation. Secondly, as batteries reach a low SoC, their load current is reduced to fully utilize the stored energy, thereby improving the efficiency and safety of the system.

Moreover, the SoC estimation derived from capacity tests, is used by end-users to determine available driving range (for EVs) or stored electrical energy (for BESS), which leads to inaccurate estimations. This is because SoC is not directly correlated to energy. Therefore, it is crucial to develop a modified test procedure that reports capacity in *Wh* instead of the conventional *Ah* used today, while incorporating current de-rating towards the end of the discharge. Finally, validating through an adaptable duty cycle generated from the model we described in Chapter 7.1), which uses power dispatch data from a real battery in operation.

7.2.1 State of Energy (SoE)

The BMS of a battery determines its SoC through a process known as Coulomb counting. This involves the continuous measurement of the current flowing through the battery over a specific time period. The current is then integrated to estimate the charge that has entered or exited the battery in relation to the initial stored charge. Nowadays, the SoC is used to determine the available driving range for EVs or the stored electrical energy for BESS. However, discrepancies have been noted in range estimations for existing EVs (Birrell et al., 2014).

The primary issue appears to be that the SoC represents capacity **Ah**, while the distance a vehicle can travel is proportional to energy in **Wh**, which is the State of Energy (SoE). The SoE can also be calculated through Coulomb counting, but the main difference is that power, rather than current, is integrated over time. This allows for the quantification of the battery's energy input and output, which can then be used to indicate the remaining energy.

By using power, both current and voltage variations of the battery are considered in calculating the energy flow, making it a more accurate and reliable indication of the actual available energy in the battery. This is because the voltage of a battery fluctuates during its discharge cycle, affecting the energy delivered, while capacity alone does not account for voltage fluctuations.

Other potential benefits of using SoE include a standardized and consistent metric for comparing different battery chemistry's used in the same or different applications. This is because different battery cells have varying voltages, which would now be a parameter considered.

Furthermore, the energy of a cell also takes into account losses in the battery which are otherwise not considered in SoC estimation. These losses are due to irreversible joule heating from Li-ion transport (internal resistance) and heat generation due to entropy change inside the cell, as shown in equation 22 (Uddin et al., 2014).

$$E_{loss} = \int_0^{t_{end}} \bar{i} \left[V - V_{oc} - T_{ref} \cdot \frac{\partial V_{oc}}{\partial T} \right] \partial t \tag{22}$$

Where $\bar{i}$ is average current, V_{oc} is the voltage at open circuit, V is the cells terminal voltage, T_{ref} is a reference temperature (usually 25ºC) and the differential term for electrochemical reactions under constant pressure is given by equation 23 (Uddin et al., 2014).

$$\frac{\partial V_{oc}}{\partial T} \cong \frac{\triangle S}{F} \tag{23}$$

However, this term is only significant at really low levels of SoC, where the ratio of entropy change to Faraday's constant can reach orders of around 10^{-4} (Uddin et al., 2014), thus it can be neglected considering that low levels of SoC are undesired for batteries.

Therefore, ion transport is the dominant term in equation 22 and E_{loss} can be further approximated to equation 24.

$$E_{loss} = \int_0^{Q_{max}} \left(\bar{i} \cdot R_{tot} \right) \partial Q \tag{24}$$

In this equation Q represents capacity in Ah and R_{tot} is total resistance. Since $\bar{i}$ is average current, it can be considered a constant. Therefore, by measuring voltage over current, the slope of the line equals the total resistance of the battery at each SoC (capacity levels). With the total resistance, it is possible to obtain the energy loss at any given current and consequently adjust the energy level of the battery by subtracting from it the energy loss.

$$E_{bat} = E'_{bat} - E_{loss} \tag{25}$$

In this way, by applying equation 12, one can obtain a much more complete parameter, the SoE, to accurately estimate available energy for usage in applications. In equation 12, the nominal energy can be calculated from the multiplication of the nominal capacity (Q_{nom}) and

nominal voltage (V_{nom}) specified by the manufacturer. The following steps shall be followed to estimate SoE while performing capacity testing.

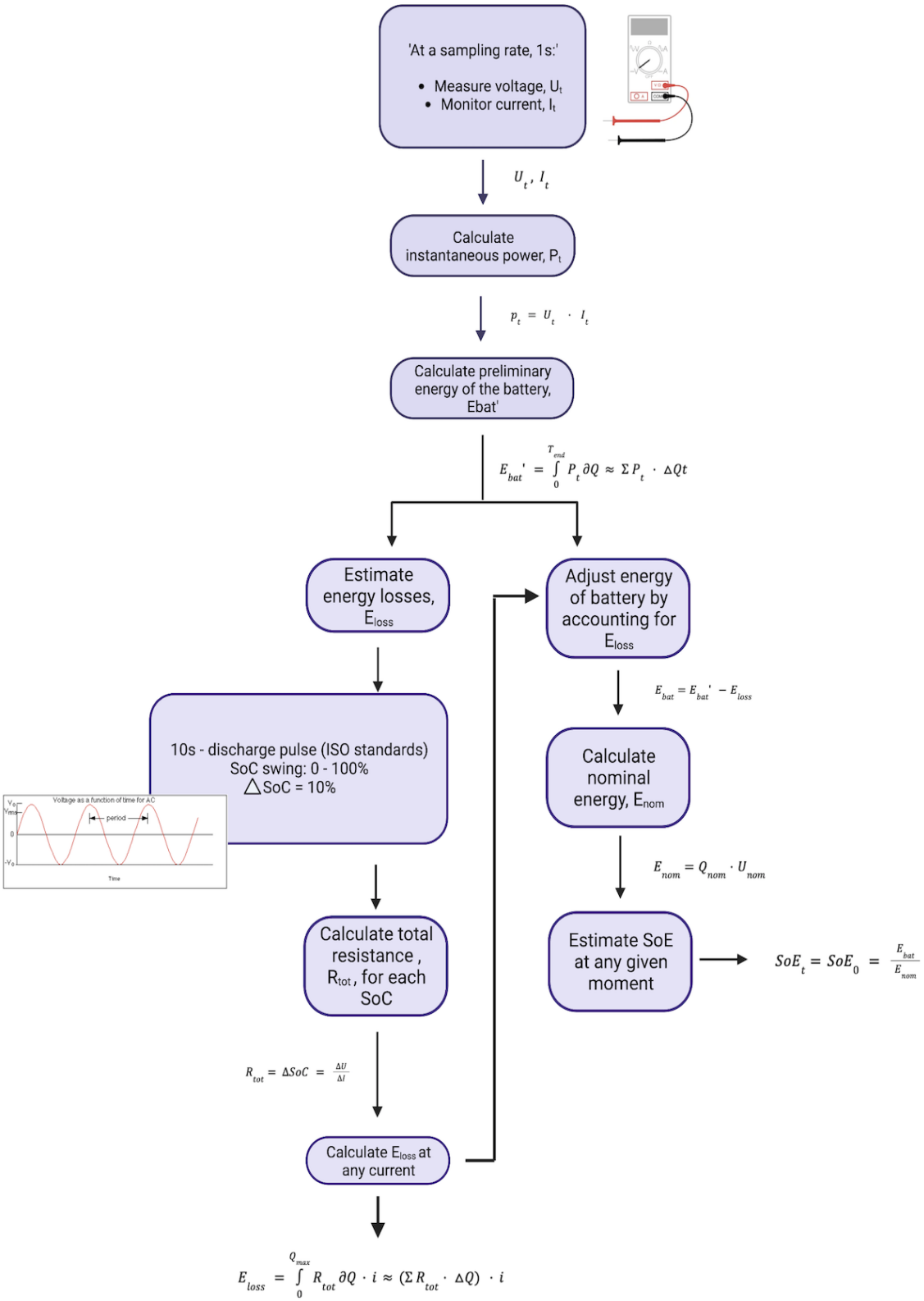

Figure 60: Modified capacity test procedure to verify de-rating of Li-ion batteries.

7.2.2 Current De-rating

Currently, as per industry standard, capacity tests have not taken into account the automatic de-rating imposed by the BMS, leading to inaccurate estimations of battery capacity at various c-rates. The BMS optimizes battery performance by limiting the discharge current when the battery's SoC is low, thereby using all of the available stored energy in the battery. According to Figure 19 and some studies (Lu et al., 2020), this method can increase a battery's energy content by approximately 5 to 15%. This extension in energy content allows the battery to prolong its use, either for transportation or storage systems. Additionally, the process of de-rating also serves to protect the battery from operating under conditions that could lead to degradation, such as deep DoD, under voltage or high temperatures.

The procedure in Figure 61 is designed to evaluate a battery's capacity, considering the de-rating imposed by the BMS. The impact of current de-rating will be assessed in relation to both capacity (Ah) and energy (Wh). To simulate a realistic de-rating scenario, it is assumed that the battery will operate normally until it reaches 20% SoC, at which point it will enter de-rating mode. This threshold was selected based on the common practice of the BMS implementing de-rating measures when the battery's SoC falls to a low level, typically between 20 and 30%.

The proposed test procedure shown consists of three stages. The first stage involves a pre-conditioning cycle, where the battery is acclimatized to a constant temperature. This is done to ensure that the temperature does not influence the results, allowing for a clear measurement of de-rating's effect on capacity and energy. Once the temperature is stabilized, a standard charge-discharge-charge cycle will be conducted following the ISO procedures for preconditioning batteries (ISO, 2018). That is, CCCV charge at C/3 rate until $\mathrm{Vmax}_{\text{cut-off}}$ or other specification given by the supplier; and CC discharge at 1C until $\mathrm{Vmin}_{\text{cut-off}}$.

The second stage commences the real testing, which involves discharging the battery from 100 to 20% SoC using high CC discharge rates. In the event that the end of discharge condition is reached before the completion of the second stage, the third stage will then begin regardless of the battery's SoC. This may occur at the highest discharge rates, where the cut-off voltage could be reached before the battery's SoC falls to 20%.

The third and final stage involves discharging the battery until it reaches the end of discharge conditions defined by the manufacturer. To represent the de-rating implemented by the BMS, a lower CC discharge rate of C/5 is used throughout the entire test as it is reasonable to assume

that an EV limited to 0.2C should be able to achieve and maintain appropriate speed limits, given the typical battery sizes found in current EVs.

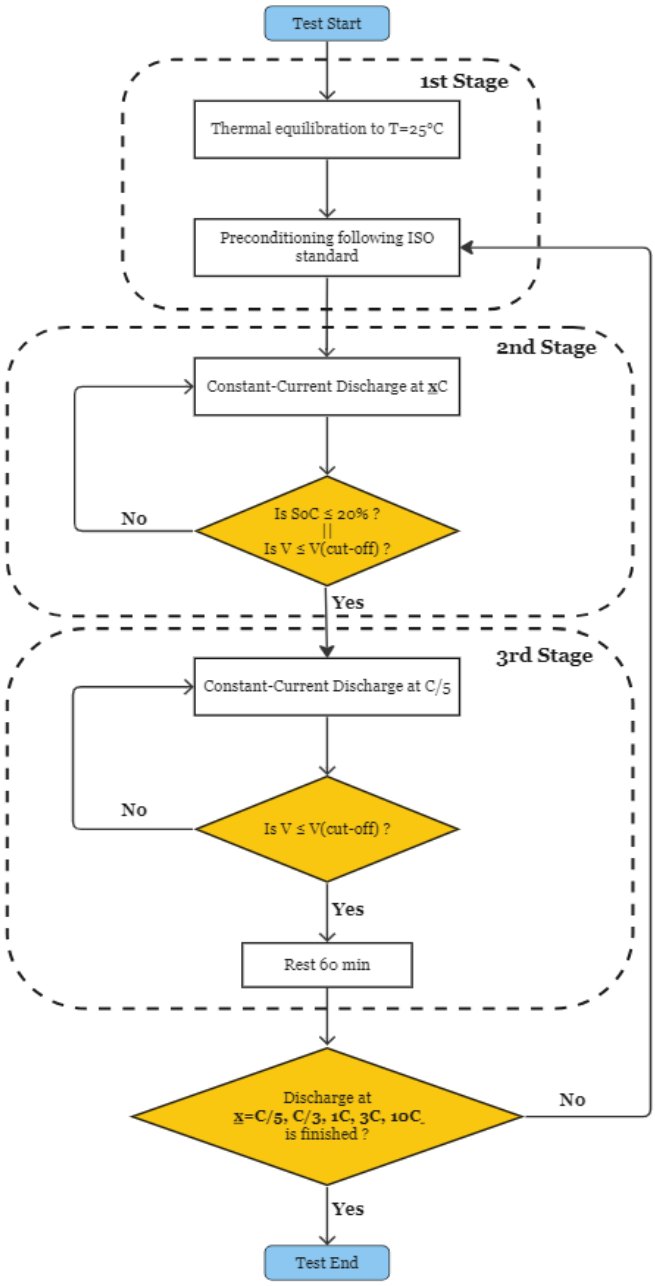

Figure 61: Modified capacity test procedure to verify de-rating of Li-ion batteries.

It is important to note that if performing a 10C discharge rate on the battery module is not safe or feasible given the experimental set-up, a 5C discharge rate will be used instead as the maximum. This change will not impact the purpose of the test. The objective remains to verify that, by de-rating, a battery discharging at high C-rates can use more capacity/energy compared to the typical capacity tests outlined in the standards.

7.3 Cycle Lifetime

The cycle lifetime of a battery is very hard to estimate. It is hard to anticipate and predict operating conditions around the battery and physical usage patterns of the battery. Nevertheless, throughout this study it has been possible to identify the most significant factors affecting the lifetime of a battery, being these: **Temperature**, **Average SoC**, **Change in SoC (ΔSoC)** and the **C-rate**.

Temperature, SoC, and C-rate are key factors impacting a battery's lifetime. Temperature influences kinetic processes and degradation mechanisms, while SoC affects stress and degradation during charging and discharging. The current lifetime testing does not consider all possible scenarios occurring in real-life battery applications. It would be good to consider dissimilar charging/discharging temperatures and distributed SoC levels to quantify their independent impact on the cyclability of the battery. Besides this, the rate of charge/discharge also plays a significant role in battery lifespan, making it better to include a dynamic personalized duty cycle to validate the suitability and predict the lifetime of a battery across different application scenarios.

7.3.1 Dissimilar Charging and Discharging Temperature

Temperature significantly affects a battery's lifetime by influencing its kinetic processes and accelerating degradation mechanisms (Chapter 2.4. This is why different temperatures are currently tested in standards: to verify the battery's safe operation in remote locations with extreme conditions. However, while the standards vary the temperature of their tests, they do so by conducting the entire test at a constant temperature and then repeating the same test at a different temperature. This means that the same temperature is used for both charging and discharging; thus disregarding the potential impact of dissimilar charging and discharging temperatures, which could lead to irreversible battery degradation. Therefore, it is essential to study this impact on the battery's lifetime cyclability and analyze the results to determine whether the testing should be incorporated into the standards, especially for applications where the battery is shut down or in standby mode for extended periods without an active auxiliary system.

The procedure to study the effect of dissimilar charging and discharging temperatures on the battery's cyclability is shown in Figure 62. This procedure can be split into three main phases: battery conditioning, reference performance and long-term cycling.

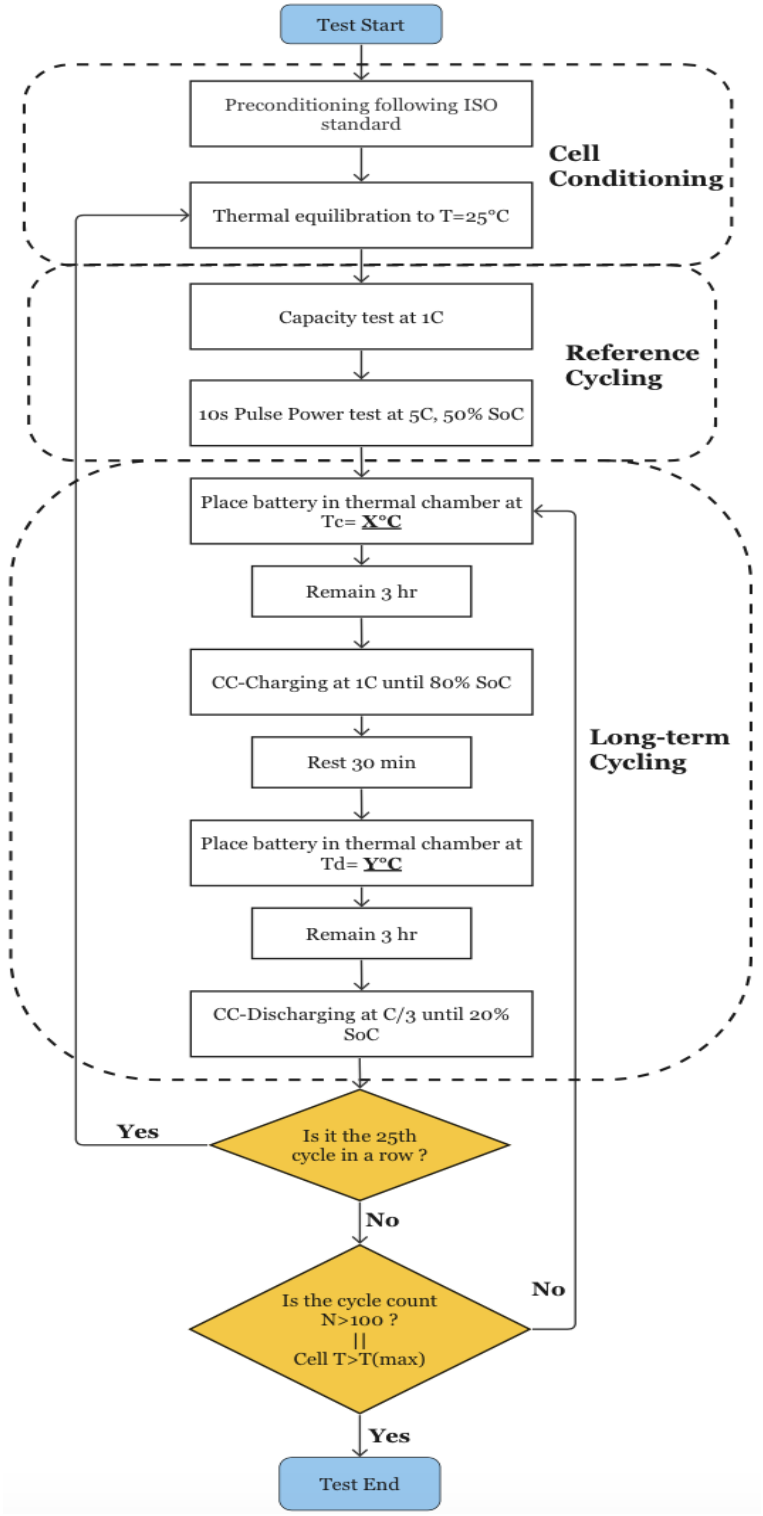

Figure 62: Lifetime cyclability test procedure to measure impact of dissimilar charging and discharging temperatures.

Prior to starting the *real test*, the battery shall be conditioned through a standard charge-discharge-charge cycle at 25 ºC following ISO standards: CCCV charge at C/3 rate until

$Vmax_{cut\text{-}off}$ or other specification given by the supplier; and CC discharge at 1C until $Vmin_{cut\text{-}off}$. This is done to ensure that the battery is operating normally and to equalize the conditions for all batteries tested.

The next phase consists of performing a reference capacity and power test to calculate the initial capacity and power which allows for the determination of the Capacity Retention (CR) and Power Retention (PR) of the battery. These parameters are used to assess irreversible degradation while providing comparable results across the different batteries tested. Reference performance tests shall periodically be done every 25 consecutive ageing cycles at the conditions indicated in Figure 62 and following ISO standard procedures.

$$CR(\%) = C_{nth} \cdot \frac{100}{C_{1st}} \tag{26}$$

$$PR(\%) = P_{nth} \cdot \frac{100}{P_{1st}} \tag{27}$$

The final phase consists of the actual long-term cycling tests performed at different charging/discharging temperatures. The first step is to place the battery in a temperature-controlled chamber at *Charging Temperature*, T_c, and let it heat/cool inside for 3 hours. This extensive waiting period is done to ensure superficial and interstitial thermal equilibrium of the battery. Then, the battery shall be charged with a CC of 1C until 80% SoC. This charging strategy is chosen over CCCV to avoid the long waiting time associated to the CV step. After resting for 30 minutes, the battery shall be introduced once again into the temperature chamber to heat/cool the battery to its *Discharging Temperature*, T_d. The battery shall remain 3 hours in the chamber to achieve thermal equilibrium and then it shall be discharged at a CC of C/3 until 20% SoC. A CC of C/3 is used as this represents the average discharge rate of a battery (Ruiz, 2018). The SoC swing of 20-80% is used throughout the test to optimize charging/discharging time and reduce stress on the battery without affecting the purpose of the test. This SoC swing is also going to be considered as 1 cycle for this test.

The charging and discharging temperatures to be tested are -10, 20, 45 ^{o}C, representing low, average and high temperatures. All temperatures should be independently tested with each other, adding up to a total combination of 9 tests (9T) as shown in Table 10. The order of the tests shall follow the order indicated in Table 10. In the case where T_c=T_d, a 30 minute rest period between charge and discharge will substitute the acclimatization step.

Table 10: Temperature matrix combination for cyclability test to measure impact of dissimilar charging and discharging temperatures.

Discharging Temperature (Td)	**Charging Temperature (Tc)**		
X=	-10 ºC	20 ºC	45 ºC
Y=			
-10 ºC	T1	T4	T7
20 ºC	T2	T5	T8
45 ºC	T3	T6	T9

7.3.2 State of Charge (SoC)

The **SoC** also influences a battery's lifetime through both its average SoC, which affects the overall stress on the battery, and the ΔSoC during charging and discharging, which affects degradation mechanisms. Currently, battery lifetime testing is conducted with a SoC swing of 20 to 80%. This means the test is scaled up in such a way that the battery is charged to 80% and discharged to 20% throughout all the test. This results in an average SoC of 50% and a ΔSoC=60%. However, this testing approach assumes a battery that consistently operates between this range of SoC. This is not always true in real-world battery applications (Figure 45), potentially leading to overestimation or underestimation of battery cyclability.

To test the impact of both different average SoC and distributed SoC level will have, the procedure in Figure 65 has been designed. This design is based on the procedure shown in Figure 62 used in the previous chapter. It contains the same first two stages: cell conditioning and reference cycling; and differs slightly in the long-term cycling stage.

In this occasion, the external temperature will be maintained constant at 25 ºC throughout the entire duration of the individual test and across the entire set of tests conducted to solely measure the impact of SoC. Also, a C-rate of 1C is going to be used for all the charge and discharge processes. Higher rates were also considered to reduce the testing time, but after some research, it was concluded that it is recommended to use a low to moderate C-rate (C/3) as it lowers the stress on the battery and enhances accuracy of the results. But to speed up the testing, 1C was also considered to be acceptable in term of these factors.

To simulate real-life usage, the battery shall be initially discharged to $SoC_{initial}$, then charged up to SoC_{final}, and this repeated until test termination conditions.

The ΔSoC is equivalent to Depth of Discharge (DoD). Three different DoD were chosen to

accurately represent the typical ΔSoC observed during battery operation: 10% (low operation), 50% (average operation) and 80% (high operation). The test evolution in terms of SoC can be seen in Figure 63.

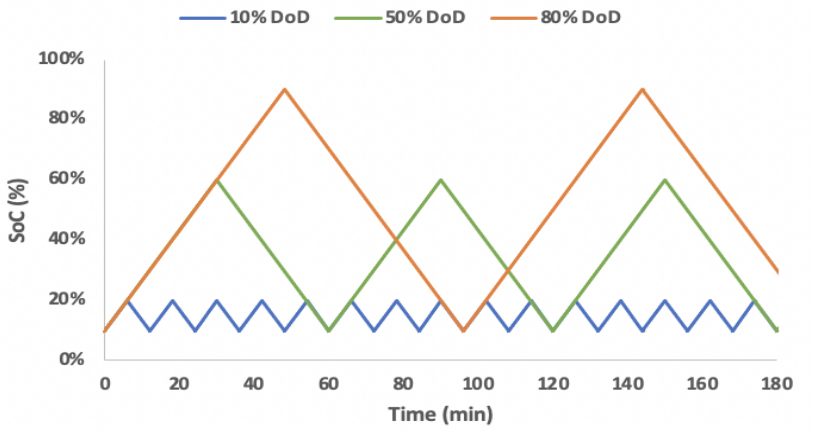

Figure 63: Test procedure flowchart of typical ΔSoC found in battery applications.

Similarly, to test the effect of different average SoC, three different averages evenly distributed throughout the SoC of the battery were selected to cover most possible scenarios: 20%, 50% and 80%. To obtain these averages, the battery shall be charged and discharged 10%, up and down respectively, around these values. The procedure flowchart looks something like the following.

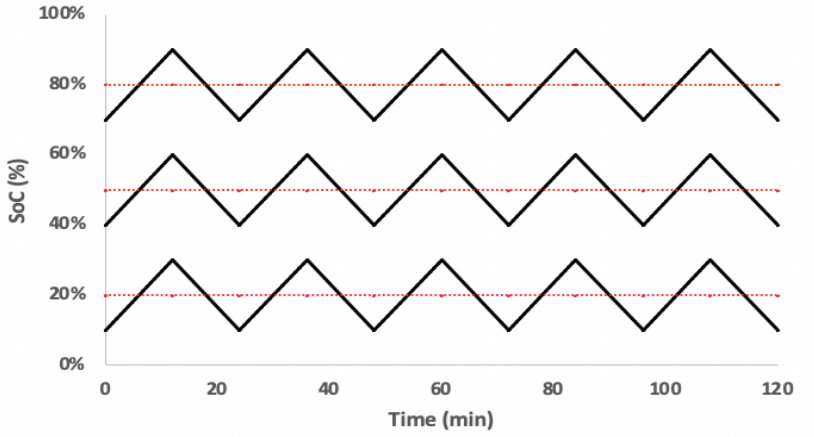

Figure 64: Test procedure flowchart of average SoC found in battery applications.

For all these tests, to accurately control the level of SoC, the OCV curve of the cell tested shall be used to adjust SoC levels with voltage values. In addition, to verify the accuracy of the method, Ah-counting shall also be done, where it is assumed that a percentage of SoC is equal to that same percentage of the nominal capacity. This is why Constant Current (CC) strategy shall be used for charging and discharging until the target voltage limit is reached.

Furthermore, in order to measure the effect of this tests, reference cycling shall be performed every 25 cycles until a total of 100 cycles have been performed. However, since the battery is not close to fully being charged nor discharged in these tests, it is complicated to measure when 1 cycle is complete. For this, it shall be considered that 1 cycle=Q_{nom} of the battery. Therefore, current over time shall be constantly monitored to account for the number of cycles.

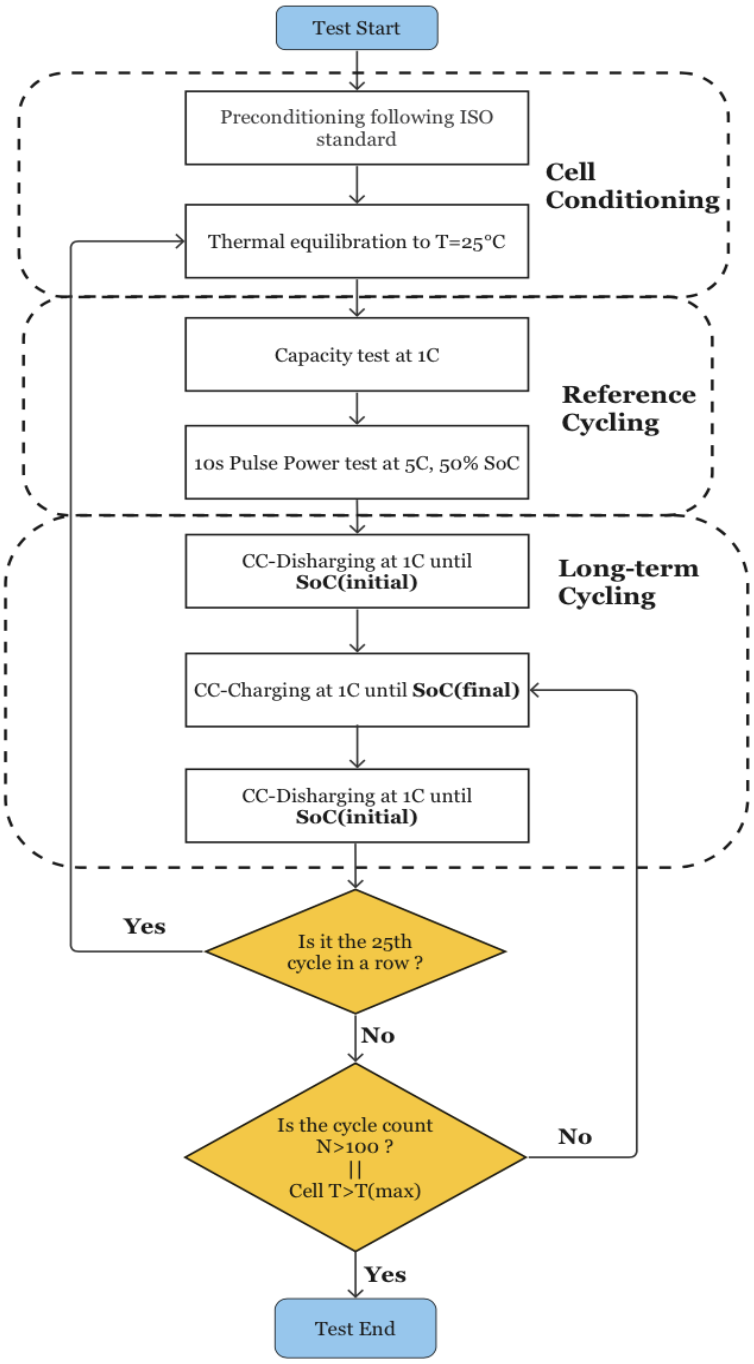

Figure 65: Lifetime cyclability test procedure to measure impact of State of Charge (SoC) across the battery.

8 Experimental Set-up

For the final stage of our project, the primary objective was to validate and verify some missing gaps that we had identified and analyzed from current battery testing standards. Initially, the plan involved conducting practical experimentation on a built battery module, implementing the modified testing procedures we had developed, obtaining our own experimental results, conducting thorough analysis, and drawing insightful conclusions from the findings. Unfortunately, due to delays in the delivery of the materials and time constraints, we were unable to carry out the practical experimentation in time. Nevertheless, we still proceeded to build the module with the company to gain knowledge and skills on the assembly of a battery, thus this chapter is for informational purposes only.

A new official project was started in AVL MTC for the development and assembly of 2 battery modules. The project was led by our supervisor, Filippa Bengtsson, and supported by us all the way.

The first step was to design the size and configuration of the battery. To ensure compliance with local and international regulations, the module built should not exceed 60 V for safety reason (Bengtsson et al., 2023). For this, the cells need to be chosen prior in order know their nominal voltage and design the module according to regulations. Cilindrical Lithium-Nickel-Cobalt-Aluminum (NCA) cells from Samsung were selected due to their well-known performance, price and availability in local markets. The parameter specifications of Samsung INR21700-40T3 cells are shown in Table 11 (Samsung, 2020).

Table 11: Cell specification and data sheet of Samsung INR21700-40T3 (Samsung, 2020).

Samsung INR21700-40T3		
Size (mm)	Diameter	21.22
	Height	70.30
Chemistry	Cathode	NCA
	Anode	Grafite+SCN
Nominal Capacity (Ah)		4.0
Nominal Voltage (V)		3.6
Charge	$V_{Cut\text{-}off}$	4.2
	$I_{Max\ continuous}$	6
Discharge	$V_{Cut\text{-}off}$	2.5
	$I_{Max\ continuous}$	50

Given the cells specifications, a maximum of 16 cells connected in series was chosen to keep the nominal voltage of the module (57.6V) below the delimited 60V. To simplify current requirements

and for safety reasons, only 1 string per module was selected as this would keep the capacity of the module only 4Ah. Although this capacity is small, since the battery chemistry is Li-ion, the results can be extrapolated for larger sizes, scaling up to the capacity needs of each application.

The cells were arranged in a line of 8 cells connected in series and repeating this same configuration with another line of 8 cells, as exemplified in Figure 66. By arranging the cells in lines, the module can be designed in a compact and efficient manner, using space effectively. This configuration also allows for easier management and control of the cells within the module.

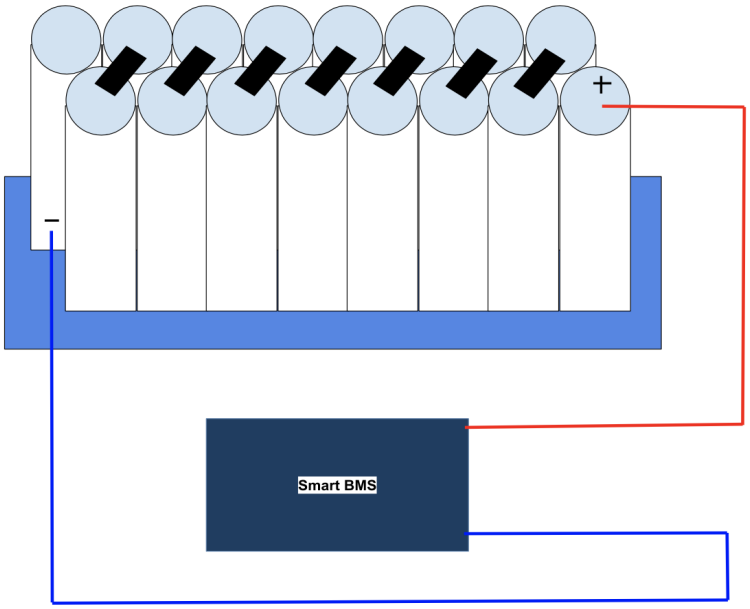

Figure 66: Simplified example of the selected configuration for our battery module.

The next step was to select the other materials needed to build a module. Table 12 indicates all the materials needed, the number of units per material and some comments. For the selection of the components, the maximum voltage and current had to be defined based on the test procedures designed in Chapter 7, to ensure all materials could resist these values. A maximum voltage of 60V and maximum current of 40A was determined to be the limit for all materials.

For all components, when possible, local suppliers were preferred due to the reliability and ease of transportation of the materials. However, some components were inevitably ordered from China, like the BMS. In fact, a smart programmable BMS with a common port connector was selected. This allows the cycler to charge and discharge the battery simultaneously, a feature needed in order to perform the duty cycle test. The BMS is also smart, meaning it can be monitored from a phone app via Bluetooth. 20 Thermocouples were also bought to verify that the parameter readings of the BMS were accurate throughout the module.

Table 12: List of components needed to build 2 battery modules.

Component	**Quantity**	**Comment**
Cells	32	
Busbars cell-cell	1	Pure Nickel strip
Bullet connectors	3	
Cell holder	1	1 to swap between both modules
Heat shrink	1	
Fuses	4	Amp rated: 50A 1 per module + 2 extras
BMS	2	Programmable (smart) Common port connector
Cooling Plate	-	In house blower
Thermocouples	20	Position strategically in locations of interest

For cooling, a thorough research of potential cooling methods were explored within our budget, such as air blowers, water-cooled plates used in computers and a copper block surrounding the module. Eventually, it was concluded that AVL MTC had sufficient equipment to control the battery in case of an explosion (i.e. with an emergency blast plate) and a blower in case the temperatures rose above 130^{o}C, which is the temperature at which the cells might leak according to their manufacturer (Samsung, 2020). Nevertheless, these events are really unlikely to happen given the nature of the experiments.

The black strips welded between cells shown in Figure 66 represent nickel strip bus-bars electrically connecting the cells together. Only 0.15 mm thick strips were available in the market, thus experiments were limited to 20-30A, as recommended by the supplier. This translates to having a maximum discharge rate of 5C rather than 10C.

As for the structure, a single interchangeable cell holder will be used to equally space-out the cells of the modules, making the battery more solid. Also, a Polyvinyl Chloride (PVC) heat shrink will be used for insulation and management purposes.

Finally, fuses will be used for safety reasons to interrupt any electrical current from passing in case it is above 40A.

9 Results and Discussions

Unfortunately, due to delays in the delivery of the materials and time constraints, we were unable to carry out the practical experimentation in time. As a result, we opted to validate our findings through alternative approaches that relied on theoretical and logical methods; such as using the necessary data and insights from several literature studies to analyse and draw conclusions relevant to our findings.

In the case of our duty cycle model, the duty cycles generated will be presented in this Chapter, showing the capability of our model to generate representative duty cycles for virtually any battery application in theory.

9.1 Duty Cycle Algorithm

Once developed the algorithm (Chapter 7.1), the following results were achieved. Starting from our dataset, PCA is first performed. After setting a threshold, to evaluate the principal number of components, of $F_{min} = 0.95$, it was found that this number is $p^* = 11$, as shown by Figure 67, starting from our initial metrics matrix X, which is then reduced according to Equation 17.

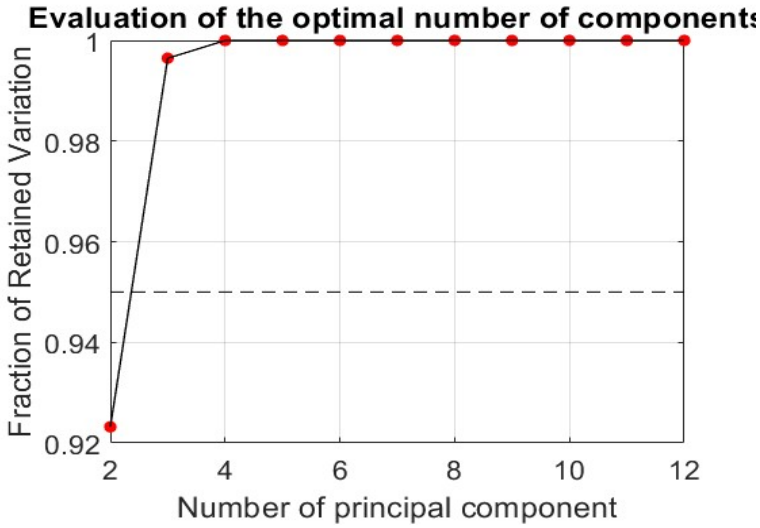

Figure 67: Graphical evaluation of the optimal number of principal component

The new matrix found P is now used as a subspace to perform the k-means method and obtain the clusters and their relative centroids. The results obtained are shown in Figure 68. The optimal number of cluster found is $N_c = 4$, starting from a maximum number of clusters $k_max = 10$. From this division, the $dist_{between_k} - dist_{within_k}$ is large and the clusters are tightly-packed and far apart from each other, thus allowing for accurate results. Another option

might have been to choose the optimal number of clusters based on our assumptions, but it was concluded to derive it from the algorithm via Matlab's *kmeans* function.

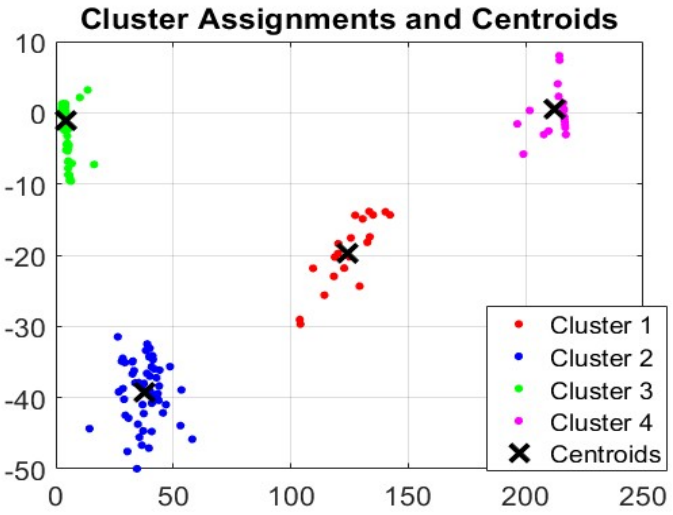

Figure 68: Clusters and their centroids obtained with k-means.

Finally, the representative intervals of the four cluster centroids obtained are the days April 21st, June 19th and 24th and October 24th, and the power dispatch of those days is shown in Figure 69, which are the characteristic duty cycles obtained.

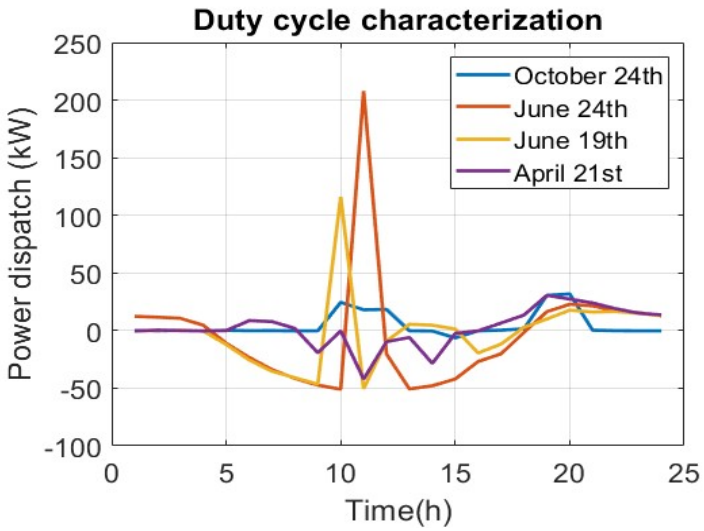

Figure 69: Characteristic duty cycles found from the cluster centroids.

The distinct duty cycles obtained agglomerate all the days of the year into their corresponding different scenario considering this specific BESS engaged in arbitrage.

Examining the results closely, Figure 70a reveals a typical day with a relatively low power dispatch activity in the BESS. Furthermore, the charging and discharging are well-balanced,

alternating between the hours of the day. This duty cycle will cause little battery degradation throughout the lifespan of the BESS and is therefore defined as **Best Case-scenario**. In the case of Figure 70d, this duty cycle also represents a day with a relatively low power dispatch activity in the BESS. However, the discharges are less distributed throughout the day, slightly degrading the BESS more than in the previous case. As a result, this duty cycle is a representation of an **Intermediate Case-scenario**. Moving onto Figure 70b, this duty cycle characterises a cluster of operational days of the battery where charge and discharge actions are well-balanced, except for a large discharging peak around 10am. This peak is much more intense than the peaks observed in the previous cases and if periodically repeated, would potentially affect the battery's performance in the long-term. This duty cycle represents an **Intense Case-scenario**. Finally, Figure 70c stands out due to a concentrated energy discharge peak during midday, nearly double that of the preceding duty cycle. This cycle represents the days of very high intensity, which could single-handedly degrade the BESS, thus represent the **Worst Case-scenario**.

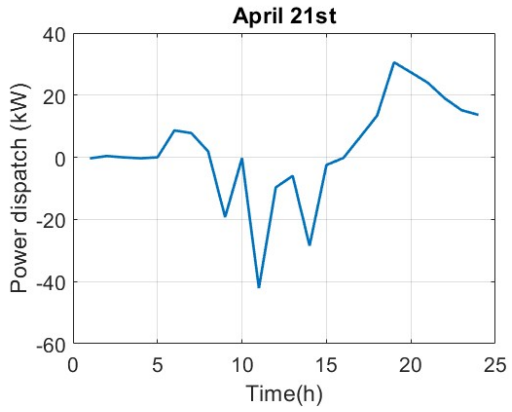

(a) April 21st

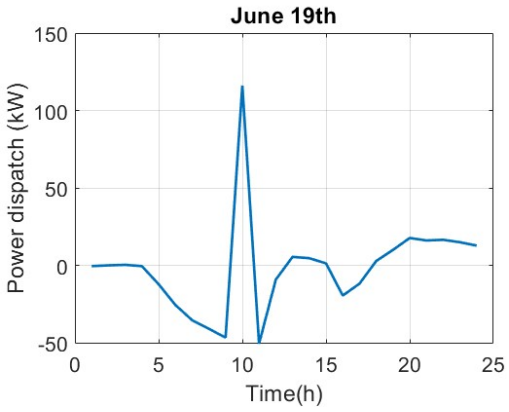

(b) June 19th

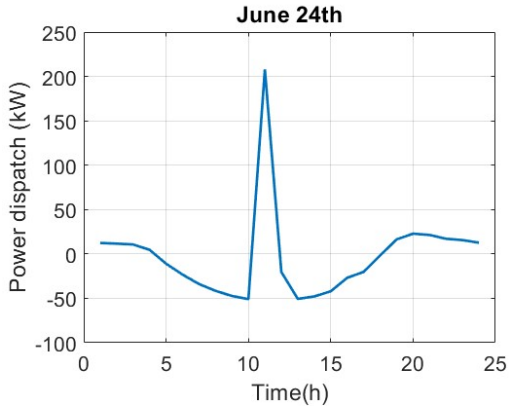

(c) June 24th

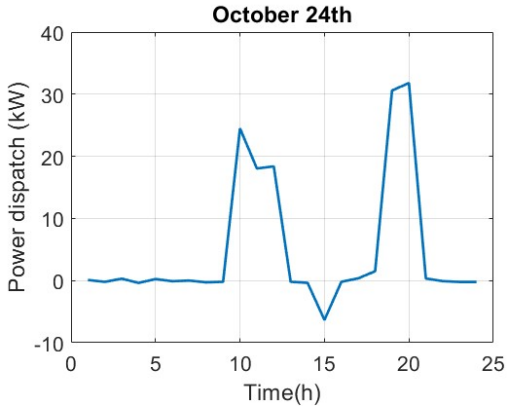

(d) October 24th

Figure 70: Four Characteristic Duty Cycles obtained representing characteristic days of BESS operation

The duty cycles can be used to estimate the capacity fade of the battery during its operation and have accurate information about the lifetime of the battery. To obtain this information, is important to derive the synthetic duty cycles, which can be implemented in a laboratory environment in reasonable time. In order to account for both the cycle aging and calendar aging processes, two different synthetic duty cycles are constructed (Moy et al., 2021). The first one, showed in Figure 71a, is obtained by concatenating all the characteristic duty cycles found. Alternatively, the zero-dispatch segments can be removed to form the cycle life synthetic duty cycle, as shown in Figure 71b. These synthetic duty cycles are a good representation of the yearly operation of the BESS and, thus, can be more easily tested in the laboratory instead of using the all power dispatch for 8760 hours.

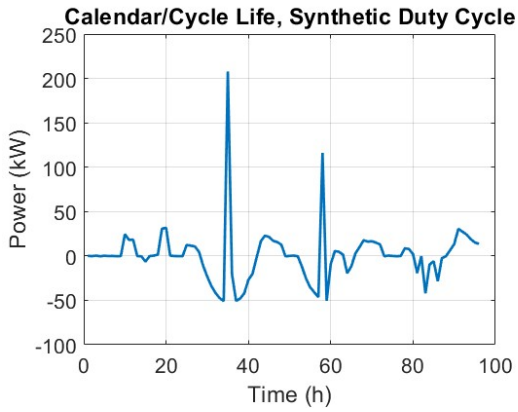

(a) Calendar/cycle life synthetic duty cycle.

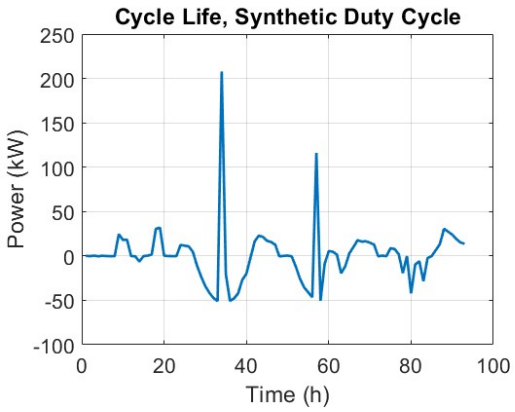

(b) Cycle life synthetic duty cycle

Figure 71: Calendar/cycle life synthetic duty cycle and (b) Cycle life synthetic duty cycle obtained for the arbitrage dataset.

9.2 Capacity

Although we were unable to test our battery module in time, we developed a unique approach to validate our capacity testing results. This involved combining insights from various research papers in the literature together with real data of the cells utilized to assemble the module.

For instance, the discharge capacity (measured in Ah) and temperature of the cell at different discharge rates is shown in Figure 72 and the end results are quantified in Table 13. This data was obtained through CC discharges at several rates until the $V_{cut\text{-}off}$ was reached, which for these cells is 2.5V (Samsung, 2020).

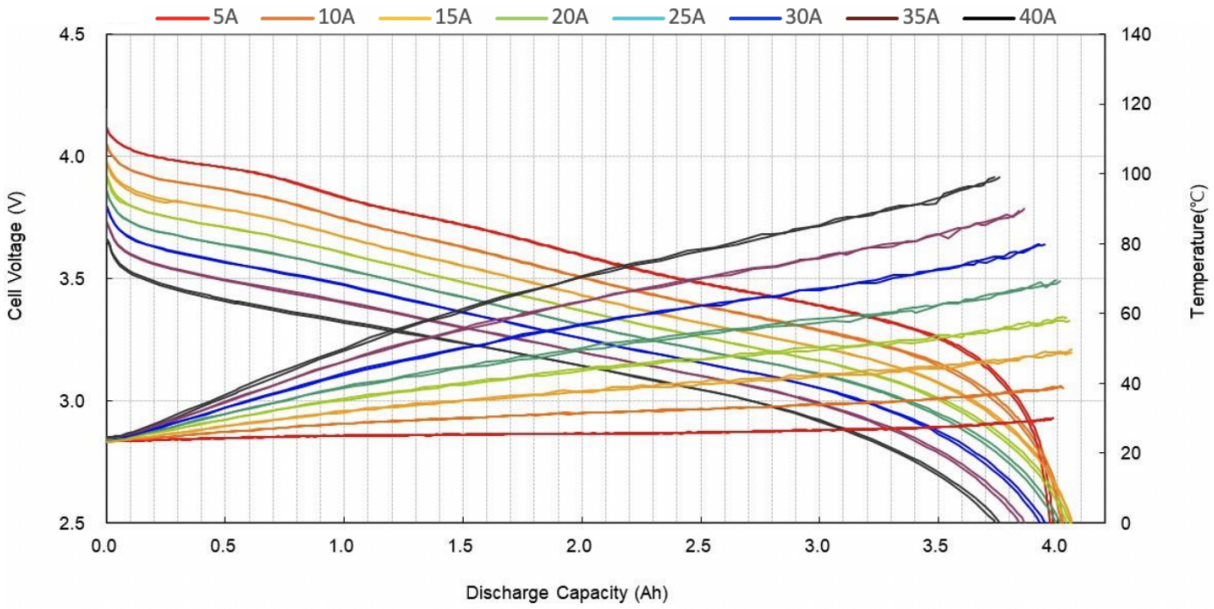

Figure 72: Discharge capacity and temperature of Samsung 40T3 cells at different CC discharge rates.

Table 13: Discharge capacity and temperature results of Samsung 40T3 cells at different CC discharge rates.

	Discharge Current							
	5A	10A	15A	20A	25A	30A	35A	40A
Capacity (Ah)	3.98	4.02	4.06	4.05	4.00	3.94	3.85	3.75
Temperature (ºC)	30.0	39.1	49.3	58.5	69.4	79.9	89.6	99.0

It is noticeable that at the start of the discharge, the cell voltage is lower at higher discharge rates. This is mainly due to a higher voltage drop due to higher current flowing through the resistance of the cell, according to Ohm's law.

$$V = I \cdot R \tag{28}$$

Furthermore, the highest capacity observed occurs at 15A ($\sim$ 4C) and from there it constantly decreases with increasing c-rate. This last behavior is expected and in accordance with the literature since the $V_{cut\text{-}off}$ is reached before at higher discharge rates. However, the initial trend surprisingly follows the opposite direction. This can be explained by looking at the cell's chemistry and its internal temperature. As mentioned in Chapter 2.2.4, NCA batteries can deliver high discharge currents without significant capacity loss and optimize performance at higher discharge rates compared to other chemistries. Also, at higher discharge rates, more heat is generated in the battery, and this increased temperature can improve the cell's electrochemical reactions, leading to higher apparent capacity.

To represent the de-rating proposed in Chapter 7.2.2, Figure 73 was made based on Doerffel and Abu Sharkh's study but using the capacity of the Samsung 40T3 cells used to build our module. This is why, once 3.2Ah are discharged (equivalent to 20% SoC left), the de-rating is applied. Nevertheless, this figure is just a representation of the supposed shape that would have been obtained in our battery testing, thus the numbers are mere estimations. As this study shows (Doerffel and Sharkh, 2006), when de-rating or applying a lower discharge rate at low SoC, a battery can recover some of its capacity that would otherwise be lost.

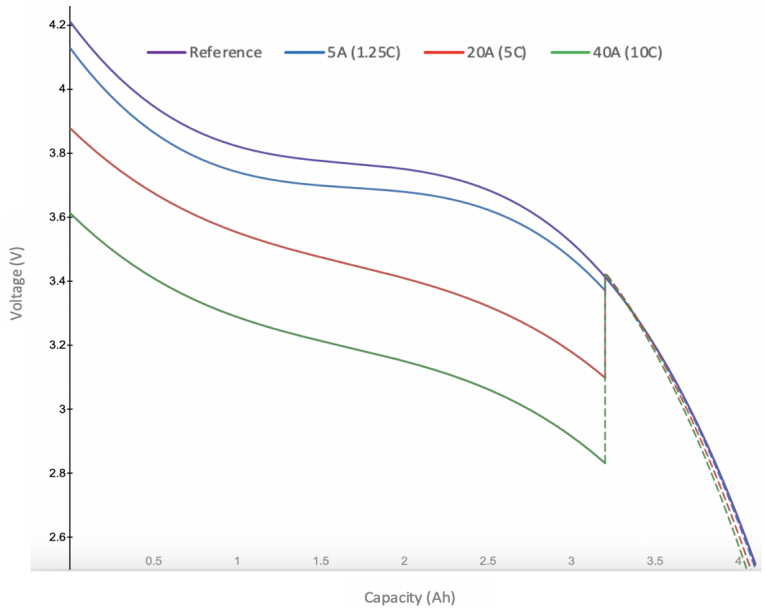

Figure 73: Graphical illustration of probable discharge capacity (Ah) of 4Ah battery module with second phase de-rating applied. Solid line indicates initial discharge rate employed; dotted lines indicate reference (C/5) de-rating.

In their experiment, when discharging a 65Ah Lead Acid battery (LAB) at 50A (10C), 34.6%

of capacity is initially lost when compared to the capacity obtained when discharging the same battery at 5A (1C). However, through de-rating from 50A to 5A, 95.1% of its initial capacity loss is recovered, whilst 4.9% is non-recoverable due to the high rate initially used. This means that 29.7% of capacity reduction can be recovered through de-rating (Doerffel and Sharkh, 2006).

In another experiment with a Li-ion battery, a similar result is obtained for a 20Ah LMO battery when de-rating from 5C to C/3, with the difference that in this occasion, all the capacity is recovered (Barai, 2015). This means that no matter which discharge rate is initially employed, capacity can be fully recovered and barely lost through de-rating.

Both these examples show the tremendous impact de-rating has on the capacity and cyclability of a battery and how important it should be to include it in testing standards to accurately represent battery behavior in real life applications.

Now, to analyse the difference between using SoC and SoE. The same test shall be considered but obtaining the total energy discharged instead of capacity, by following the procedure shown in Figure 60. In this way, Figure 74 can be obtained. Once again, it is important to note that while this figure uses real energy data from the cells we used to build our battery module, the curves obtained are just representations of what the test would most probably generate considering literature insights (Barai, 2015; Dong et al., 2015).

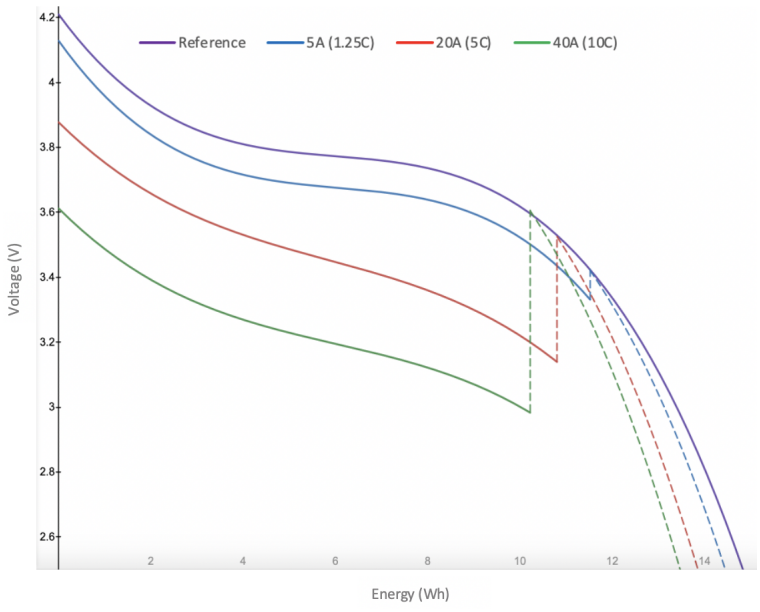

Figure 74: Graphical illustration of probable discharged energy (Wh) of 4Ah battery module with second phase de-rating applied. Solid line indicates initial discharge rate employed; dotted lines indicate reference (C/5) de-rating.

As analysed by Barai and Dong et al., while most capacity loss can be recovered, energy does not follow the same trend and some of it is non-recoverable regardless of de-rating or not. More specifically, through their experiments, 29% of capacity reduction with 5C CC test can be recovered through C/3 current de-rating, however, 7% of total energy is not recoverable.

The reason for this is that SoE considers both current and voltage. During higher discharge rates (currents), the battery experiences lower average voltages due to increased voltage drops, as illustrated in Figure 72. The increase in current is not sufficient to counteract the reduced voltage, thus slightly reducing the amount of extractable energy. Consequently, the energy loss during high discharge rates is not as pronounced as the capacity loss observed in both LAB and Li-ion battery; however, while this capacity is recoverable through de-rating, the energy is not.

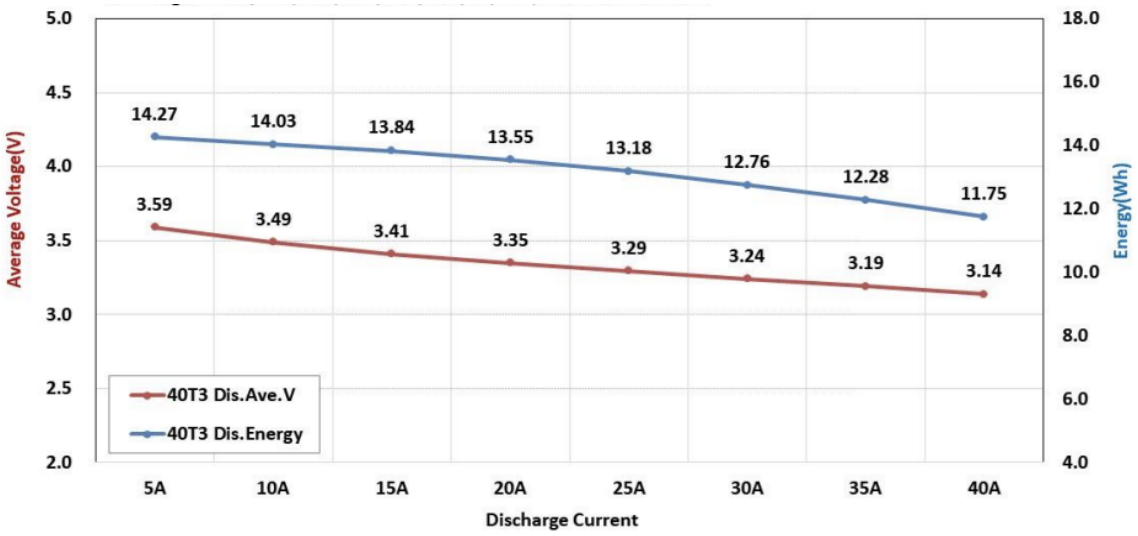

Figure 75: Energy discharged and average voltage of Samsung 40T3 cells at different CC discharge rates.

In this experiment the difference was around 7%, but this percentage could be potentially higher for larger batteries. This leads to a significant disparity between capacity (measured in Ah) and energy (measured in Wh). As the estimation of a battery's range for electric mobility or the operational duration of a BESS relies on energy, not capacity, the SoC inaccurately estimates these factors. Therefore, it is recommended that the BMS be adjusted to place greater emphasis on the SoE, which is a more comprehensive and suitable measure to estimate the remaining travel distance or operating time of an energy storage system.

As future work, it would be necessary to conduct the pending tests to confirm all the outlined hypotheses. Furthermore, it would be interesting to combine de-rating with the synthetic duty

cycle generated by our algorithm (Chapter 7.1), leading to a personalized dynamic capacity test. In this test, the battery would be evaluated with its intended duty cycle while adjusting to the following constraint:

- During the trans-course of the dynamic capacity test, if the battery's SoE drops below 20%, an automatic shift to a pre-defined de-rating discharge current would take place.
- If switched to charging, the de-rating would be deactivated, and the rates specified by the duty cycle would be utilized.

A de-rating of C/5 has been presented in this study but could potentially be adjusted as required based on battery use. If certain applications demand greater available power at all costs, the de-rating current would increase and adjust accordingly.

Additionally, the development of an algorithm indicating instances when the battery has entered de-rating mode would be beneficial. This would provide awareness to both the customer and supplier regarding occurrences and frequency of limitations on the battery's performance.

9.3 Cycle Lifetime

Cycle lifetime testing requires a lot of time and equipment, space availability to perform the tests and full-time dedication monitoring the cells. This was not feasible considering the full scope of the thesis. Still, this parameter caught our attention due to its importance in the sector. As a result, in Chapter 7.3 we designed 2 test procedures to be performed on dissimilar charging and discharging conditions as further research. This chapter will focus on gathering the most interesting findings that may push for the implementation and inclusion of these tests in future battery standards.

9.3.1 Dissimilar Charging and Discharging Temperature

When analyzing the effect of temperature during battery lifetime testing, it's essential to recall that periodic reference cycling tests are carried out at room temperature, regardless of the test temperature. This is done to distinguish between reversible and irreversible degradation.

There are temperatures that decrease the performance of the battery due to decelerated electrochemical processes. However, this drop in performance doesn't necessarily imply it is permanently lost, as some of it can be recovered with a change in temperature. For instance, at extremely low temperatures (<-20^{o}C), ionic conductivity is reduced and charge transfer resistance increases, slowing down the kinetic processes within the battery. But, as the temperature is raised, these processes accelerate and partially restore the performance.

On the other hand, there are temperatures that momentarily have less impact on battery performance, but can permanently damage the battery's components. This damage remains irreversible, independent of the temperature, thus reducing battery performance indefinitely. For example, at very high temperatures (>30^{o}C), side reactions are triggered inside the battery resulting in the partial rupture of the SEI and electrode decomposition. These impacts diminish the amount of energy carriers within the battery and reduce active sites, causing permanent power and capacity fade.

The capacity monitored throughout the entire lifetime test reflects both reversible and irreversible degradation, as the battery's performance is assessed at a specific test temperature. Since reference cycling is conducted at room temperature, the impact of cycling at extreme

temperatures is neglected. This eliminates reversible degradation from the results, leaving only the impact of irreversible degradation.

Ruiz et al. studied the effect of dissimilar charging and discharging temperatures on the long-term performance of an LFP battery. They performed a total of 10 temperature combinations, ranging from -20°C to 30°C (Ruiz et al., 2017). Although a limited number of tests were performed, they found the following trend: when cycling at the same Td, greater degradation was observed at higher Tc; while when cycling at the same Tc, greater degradation was observed at lower Td. However, these findings were only true for a pair of temperature combinations, and therefore remain inconclusive. More tests and research are needed to confirm these hypotheses.

9.3.2 State of Charge (SoC)

In one study, lifetime cycling tests were performed on a 26Ah Li-ion pouch battery and the effect of distinct average SoC on the cyclability was measured (Wikner, 2017). The results of the study have been slightly adapted to our test procedure in Chapter 7.3.2 and are plotted in Figure 76.

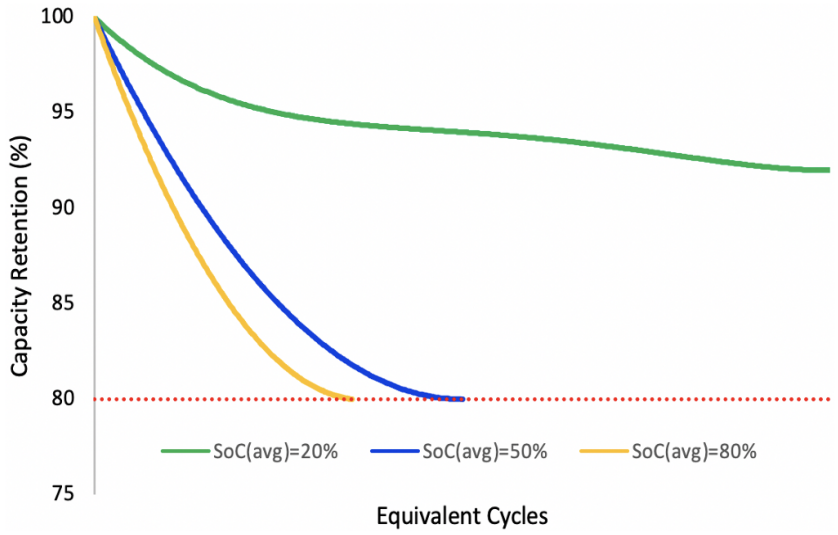

Figure 76: Graphic representation of the effect of different average SoC on the cycle lifetime of a battery.

There is a clear trend in the capacity retention of the battery with respect to the average SoC employed: the higher the average SoC, the more rapid aging can be observed. To specify, a battery with an average operational SoC of 20% retains more than 90% of its initial capacity after 8000 cycles; while the same battery, with the same energy consumption, but with an average

SoC of 80%, reaches end-of-life (<80% SoC) after a short 2800 cycles. The lower lifespan of the latter is thought to result from the higher ion concentration at the anode, leading to electrode cracking and SEI decomposition, as aforementioned in Chapter 2.4.

On another study, historical data from the battery packs of 707 operational EVs was analysed, including the charging starting and ending SoC (Liu et al., 2023). From these parameters it was possible to extrapolate the average SoC and it was concluded that, below an average SoC of 40% but above 10% was considered benign, with no significant degradation. This data represents real usage of the batteries, thus it validates the findings of the previous experiment.

Now, there appears to be an apparent contradiction at play: if batteries are consistently operated at a low State of Charge (SoC), the Battery Management System (BMS) may prioritize not fully charging the batteries, which can reduce their overall autonomy. Maintaining batteries at a low SoC and employing short discharge cycles does have a positive impact on battery longevity, but it doesn't fully address the practical requirements of the specific application.

The ideal solution in this scenario would involve the implementation of a smart BMS that adopts a hybrid approach. This means allowing the battery to occasionally undergo full charge and discharge cycles when necessary, but when possible regulating the charging or discharging of the battery. For example, in the case of recharging an EV, the smart BMS could assess whether the destination is within reach with just 40% of the battery's capacity or if there's a charging station on the way. It could then consult with the user, allowing them to make an informed decision to minimize the battery charge, stop at the next charging station, and thereby extend the overall battery lifespan.

On another note, ΔSoC also influences the lifetime cyclability of a battery (Chapter 7.3.2). Similarly as with the average SoC, Figure 77 was made based on Evelina Wikner's Depth of Discharge (DoD) experiments but adapted to the parameters indicated in our test procedure in Figure 65. It should be noted that the choice of average SoC is important and can impact the results as it is not the same to have an average SoC of 20% and 80%, even though both could have the same ΔSoC=10%. In our procedure, an average SoC=20% was selected, which is an optimal value to minimise electrode cracking and SEI decomposition. This is why the difference in cyclability observed is quite big. However, Evelina Wikner did also test the worst average SoC=90% with a 10% ΔSoC and it still doubled the lifetime of the 90% ΔSoC (Wikner, 2017).

This could be because larger ΔSoC leads to a bigger change in lithium ions intercalating in the electrodes, inducing higher mechanical stress on the battery.

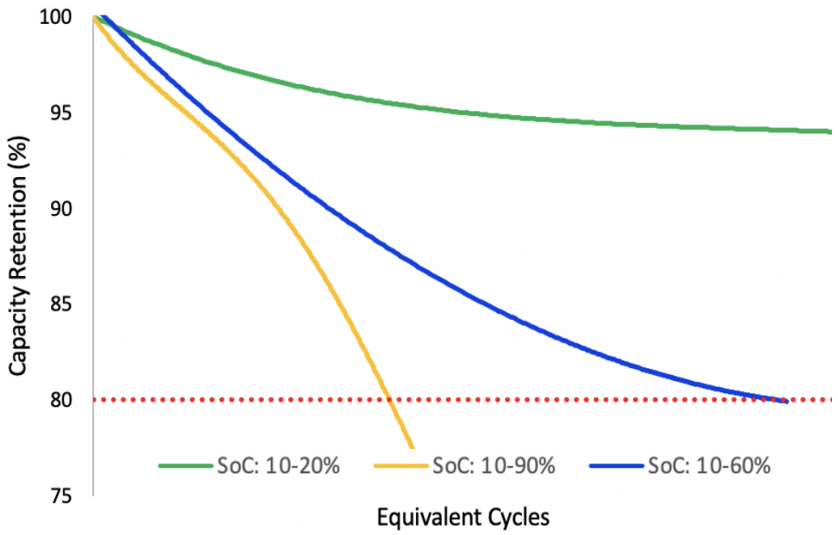

Figure 77: Graphic representation of the effect of the SoC charging-discharging width on the cycle lifetime of a battery.

From all these analyses, it becomes evident that frequent, brief charging cycles reduces degradation compared to rare and prolonged charges. Also, by maintaining the battery at a low SoC, between 10 and 40%, and preventing it from falling below 10%, degradation can be minimized.

10 Conclusions

Throughout the progression of this master's thesis, the primary objective has been the development of a versatile and enhanced battery testing methodology. This methodology aims to more accurately emulate real-world battery usage scenarios, particularly in emerging applications within the industrial and electric mobility sectors. This methodology has been built based on important testing gaps that were found on the most relevant international standards, such as ISO and IEC amongst others, which fail to reflect in some aspects the real operating conditions of batteries. In this way, AVL MTC can anticipate upcoming changes in battery testing and be more prepared in the subject to open the door to new potential customers in the industry.

The methodology started with comprehensive background research, understanding various battery technologies, particularly focusing on LIBs due to their wide use and versatile chemistry. The research identified three testing categories: performance, safety, and environmental. Obtaining an indication of AVL MTC's typical battery testing requests from customers led to the focus on performance testing, as it addressed the main bottlenecks in current battery technology. Performance parameters were then researched with the objective of understanding the nature of each parameter and their relation to real-life applications.

On a parallel note, four growing applications in the battery industry were selected due to potential business opportunities in the near-future. In this way, the market of batteries for Electric Vehicles (EVs), Heavy-duty-vehicles (HDVs), Maritime transports and Stationary applications were studied. The analysis led to selecting HDV and Stationary applications as the most promising areas as they are rapidly growing in Europe, especially in Sweden, where several local companies are expanding in both applications.

An extensive review was done on the existing testing standards for both applications. It was discovered that the existing tests found in standards and in the literature exhibited significant differences, indicating potential gaps that could be enhanced to better reflect real-life usage of these batteries. Despite the difference in nature between HDVs and Stationary applications, the gaps identified for both applications were interconnected and tackled collectively. To maintain an acceptable length for the scope of the thesis, only the most interesting gaps were further developed and these mainly affected duty cycles, capacity and cycle lifetime tests.

One gap identified the absence of suitable duty cycles that align with a battery's specific operation for a given application. To address this, an algorithm was developed that is able to design a specific duty cycle for the considered application by only using as input data the battery's power dispatch, SoE and the ambient temperatures, within the chosen time-frame and location. These duty cycles are created using machine learning techniques, including PCA and k-means to group battery operations throughout the year according to their similarity in power distribution. Ultimately, these duty cycles can be translated into dynamic stress tests that are feasible to conduct within a reasonable timeframe. In conclusion, a case study was introduced, demonstrating the effectiveness of our model in generating representative duty cycles for all battery applications.

The capacity tests indicated in all the standards involve Constant Current (CC) for discharging steps at different C-rates and temperatures. However, CC discharges do not capture the dynamic discharge profiles of batteries during real-life operation, mainly because of battery de-rating at low SoC. Moreover, capacity testing requires reporting capacity in Wh (SoE) instead of Ah (SoC) to accurately report driving range and/or remaining stored energy in the battery. Therefore a modified test procedure was designed that reports capacity in Wh instead of the conventional Ah used today, while incorporating current de-rating towards the end of the discharge.

Estimating battery cycle lifetime was found to be challenging due to uncertain operating conditions and usage patterns. Within thesis identified the factors which significantly affected the battery's lifespan to be: Temperature, average SoC, Change in SoC (DoD), and C-rate. Two test procedures were developed considering different charging/discharging temperatures and distributed SoC levels as boundary conditions of the tests. This is not addressed in the standards and covers the most common scenarios occurring in the distinct applications.

Neither capacity or lifetime testing could be conducted due to time constraints. Instead, they were validated through a combination of other research studies, which collectively helped support the proposed hypotheses. De-rating proved to recover a significant amount of capacity, but not in the same proportion as energy, distinguishing between SoC and SoE. As for the cyclability: frequent, brief charging cycles were shown to reduce degradation compared to rare and prolonged charges. Also, by maintaining the battery at a low SoC, between 10 and 40%, degradation can be minimized. Practical studies are still to be carried out to fully validate the hypotheses and arrive at a definitive conclusion.

Bibliography

Battery Design Ebook. DNK Power, 2022. URL https://www.dnkpower.com/myth-or-fact-lithium-ion-batteries-self-discharge/.

D. M. f. E. ACEA. Co2 emissions from car production in the eu, July 2022. URL https://www.acea.auto/figure/co2-emissions-from-car-production-in-eu/#:~:text=European%20car%20makers%20have%20reduced%20total%20CO2%20emissions,industrys%20efforts%20to%20reduce%20CO2%20emissions%20from%20production.

ADB. *Handbook ob battery energy storage system*. Asian Development Bank, ADB, December 2018.

P. Ahmadi and F. Torabi. *Simulation of battery systems: Fundamentals and applications*. Academic Press, 2019.

A. Aktas and Y. Kircicek. *Solar hybrid systems: Design and application*. Academic Press, 2021.

Y. Ansari. Why does a lead-acid battery self-discharge?, May 2022. URL https://www.payperwatt.com/post/why-does-a-lead-acid-battery-self-discharge.

Y. Aoki and A. Okuyama. Lithium-ion secondary battery accelerated testing. Technical report, Technology Development Department, ESPEC CORP, 2015.

D. S. Arar. The three major li-ion battery form factors: Cylindrical, prismatic, and pouch, 2020. URL https://www.allaboutcircuits.com/news/three-major-lithium-ion-battery-form-factors-cylindrical-prismatic-pouch/.

A. S. Ashour, Y. Guo, and A. R. Hawas. Neutrosophic hough transform for blood cells nuclei detection. In *Neutrosophic Set in Medical Image Analysis*, pages 207–227. Elsevier, 2019.

A. Barai. *Improvement of consistency, accuracy and interpretation of characterisation test techniques for Li-ion battery cells for automotive application*. PhD thesis, University of Warwick, 2015.

A. Barai, K. Uddin, M. Dubarry, L. Somerville, A. McGordon, P. Jennings, and I. Bloom. A comparison of methodologies for the non-invasive characterisation of commercial li-ion cells. *Progress in Energy and Combustion Science*, 72:1–31, 2019.

C. Battery University. How does rising internal resistance affect performance?, October 2021. URL https://batteryuniversity.com/article/bu-802a-how-does-rising-internal-resistance-affect-performance.

G. Baure and M. Dubarry. Synthetic vs. real driving cycles: A comparison of electric vehicle battery degradation. *Batteries*, 5(2):42, 2019.

B. C. G. BCG. Batteries for electric cars: Challenges, opportunities, and the outlook to 2020. *Boston Consulting Group*, page 12, 2020.

F. Bengtsson, O. Lundblad, R. Berners, E. Hjorth, B. E, C. Ciminieri, and F. J. Carreras, editors. *Project BatModule*, AVL Sweden, 2023. AVL.

M. Bini, D. Capsoni, S. Ferrari, E. Quartarone, and P. Mustarelli. Rechargeable lithium batteries: Key scientific and technological challenges. In *Rechargeable Lithium Batteries*, pages 1–17. Elsevier, 2015.

S. A. Birrell, A. McGordon, and P. A. Jennings. Defining the accuracy of real-world range estimations of an electric vehicle. In *17th International IEEE Conference on Intelligent Transportation Systems (ITSC)*, pages 2590–2595. IEEE, 2014.

R. Bisschop, O. Willstrand, F. Amon, and M. Rosenggren. *Fire safety of lithium-ion batteries in road vehicles*. 2019.

N. Blair, A. Schiek, A. Burrell, M. Keyser, A. Deadman, I. Ellerington, L. Govaerts, G. Mulder, P. Hendrick, T. Polfliet, et al. Global overview of energy storage performance test protocols. 2021.

R. Bollini. Understanding charge-discharge curves of li-ion cells. *EVreporter*, 2022.

T. Bowen, I. Chernyakhovskiy, and P. Denholm. *Grid-Scale Battery Storage: Grid integration toolkit*. National Renewable Energy Laboratory, NREL, September 2019.

S. Byun, J. Park, W. A. Appiah, J. Park, M.-H. Ryou, and Y. M. Lee. Effects of environmental humidity on self-discharging behaviour and electrochemical performance of lithium-ion batteries. *The Electrochemical Society*, 2(432), 2016.

D. Cameron. Batteries and the electrification of heavy-duty transportation. Master of science thesis, KTH Royal Institute of Technology, Stockholm, Sweden, 2019. URL https:

//kth.diva-portal.org/smash/record.jsf?pid=diva2%3A1350364&dswid=9628. School of Industrial Engineering and Management.

J. Campillo, E. Dahlquist, D. L. Danilov, N. Ghaviha, P. H. Notten, and N. Zimmerman. Battery technologies for transportation applications. *Technologies and applications for smart charging of electric and plug-in hybrid vehicles*, pages 151–206, 2017.

X. Cao. Important factors for the reliable and reproducible preparation of non-aqueous electrolyte solution for lithium batteries. *Communication Materials*, 4(10), 2023.

M. A. Chaaban. Interpreting battery parameters and specification sheets, 2018. URL https://www.e-education.psu.edu/ae868/node/896.

L. Cole. Northvolt 'will source directly from the miners' to ensure clean supply chain. *Euractiv*, November 2019. URL https://www.euractiv.com/section/energy-environment/news/northvolt-will-source-directly-from-the-miners-to-ensure-clean-supply-chain/.

D. R. Conover, A. J. Crawford, V. V. Viswanathan, S. Ferreira, and D. Schoenwald. Protocol for uniformly measuring and expressing the performance of energy storage systems. Technical report, Pacific Northwest National Lab.(PNNL), Richland, WA (United States), 2014.

C. Cunanan, M.-K. Tran, Y. Lee, S. Kwok, V. Leung, and M. Fowler. A review of heavy-duty vehicle powertrain technologies: Diesel engine vehicles, battery electric vehicles, and hydrogen fuel cell electric vehicles. *Clean Technologies*, 3(2):474–489, 2021.

E. T. C. Danfoss. Electrification is the future. April 2022. URL https://www.danfoss.com/en/about-danfoss/articles/cf/electrification-is-the-future/.

G. DNV. Dnv gl handbook for maritime and offshore battery systems. Technical report, Tech. Rep, 2016.

D. Doerffel and S. A. Sharkh. A critical review of using the peukert equation for determining the remaining capacity of lead-acid and lithium-ion batteries. *Journal of power sources*, 155 (2):395–400, 2006.

C. Doetsch, B. Droste-Franke, G. Mulder, Y. Scholz, and M. Perrin. Electric energy storage-future energy storage demand. *International Energy Agency: Paris, France*, 2015.

G. Dong, X. Zhang, C. Zhang, and Z. Chen. A method for state of energy estimation of lithium-ion batteries based on neural network model. *Energy*, 90:879–888, 2015.

J. Edge, S. O'Kane, R. Prosser, N. D. Kirkaldy, A. N. Patel, A. Hales, A. Ghosh, W. Ai, J. Chen, J. Yang, S. Li, M.-C. Pang, L. B. Diaz, A. Tomaszewka, M. W. Marzook, K. N. Radhakrishnan, H. Wang, Y. Patel, B. Wu, and G. J. Offer. Lithium ion battery degradation: what you need to know. *Physical Chemistry Chemical Physics*, 23:8200–8221, 2021.

T. Elammas. Hydrogen fuel cells for marine applications: Challenges and opportunities. *International Journal of Research in Advanced Engineering and Technology*, 9(1):38–43, 2023.

Electropedia. Battery chargers and charging methods, n.d. URL https://www.mpoweruk.com/chargers.htm.

B. Emeric. Key performance indicators for the monitoring of large-scale battery storage systems. Master of science thesis, KTH Royal Institute of Technology, Stockholm, Sweden, 2019. URL https://www.diva-portal.org/smash/get/diva2:1371050/FULLTEXT01.pdf. School of Industrial Engineering and Management.

E. Engineering. Challenge of batteries for heavy-duty evs, 2022. URL https://www.emobility-engineering.com/challenge-of-batteries-for-heavy-duty-evs/.

I. Epec Engineered Technologies. Lithium battery technologies, n.d. URL https://www.epectec.com/batteries/lithium-battery-technologies.html.

I. EUCAR. Battery requirements for future automotive applications. Technical report, European Council for Automotive R&D, July 2019.

I. Eurobat E-mobility. Battery rd roadmap 2030. battery technology for vehicle applications, 2015.

E. European Commission. Commission strategy for reducing heavy-duty vehicles' (hdvs) fuel consumption and co2 emissions, 2014.

I. European Commission. Paris agreement, February 2023. URL https://climate.ec.europa.eu/eu-action/international-action-climate-change/climate-negotiations/paris-agreement_en.

E. Evvanex. Electric vehicle charging batteries, February 2020. URL https://insideevs.com/features/396459/debunking-3-myths-ev-batteries-charging/.

C. Fear. Overdischarge and external short behavior of lithium-ion batteries, May 2017.

J. Fleischmann, M. Hanicke, E. Horetsky, D. Ibrahim, S. Jautelat, M. Linder, P. Schaufuss, L. Torscht, and A. van de Rijt. Battery 2030: Resilient, sustainable, and circular. pages 1–18, 2023. URL https://www.mckinsey.com/industries/automotive-and-assembly/our-insights/battery-2030-resilient-sustainable-and-circular#/.

J. L. Garcia. Electric power systems. In *Cubesat Handbook*, chapter 9, pages 185–197. Elsevier, 2021.

T. Gewald, A. Candussio, L. Wildfeuer, D. Lehmkuhl, A. Hahn, and M. Lienkamp. Accelerated aging characterization of lithium-ion cells: Using sensitivity analysis to identify the stress factors relevant to cyclic aging. *Batteries*, 6(1):6, 2020.

I. Grand View Research. Battery Market Size, Share Trends Analysis Report By Product (Lead Acid, Li-ion, Nickle Metal Hydride, Ni-Cd), By Application, By End-use, By Region, And Segment Forecasts, 2023 - 2030. Technical report, 2023. URL https://www.grandviewresearch.com/industry/power-generation-and-storage.

D. Gräf, J. Marschewski, L. Ibing, D. Huckebrink, M. Fiebrandt, G. Hanau, and V. Bertsch. What drives capacity degradation in utility-scale battery energy storage systems? the impact of operating strategy and temperature in different grid applications. Technical report, 2022.

M. Gupta. A new battery chemistry will lead the stationary energy storage market by 2030, 2020. URL https://www.greentechmedia.com/articles/read/lfp-will-overtake-nmc-for-stationary-storage.

Hydrogen and F. C. T. Office. Hydrogen storage, n.d. URL www.energy.gov/eere/fuelcells/hydrogen-storage.

F. Hämmerle. *HBattery Impedance Measurement*. Omicron Lab, 2017.

C. Iclodean, B. Varga, N. Burnete, D. Cimerdean, and B. Jurchiş. Comparison of different battery types for electric vehicles. In *IOP conference series: materials science and engineering*, volume 252, page 012058. IOP Publishing, 2017.

IEA. Grid-scale storage. Technical report, International Energy Agency (IEA), 2022a.

I. E. A. IEA. Global EV Outlook 2021. Technical report, 2021. URL https://www.iea.org/reports/global-ev-outlook-2021.

I. E. A. IEA. Co2 emissions in 2022, 2022b. URL https://iea.blob.core.windows.net/assets/3c8fa115-35c4-4474-b237-1b00424c8844/CO2Emissionsin2022.pdf.

I. E. A. IEA. Global supply chains of ev batteries. Technical report, 2022c. URL https://iea.blob.core.windows.net/assets/4eb8c252-76b1-4710-8f5e-867e751c8dda/GlobalSupplyChainsofEVBatteries.pdf.

I. E. A. IEA. World energy outlook 2022. Technical report, 2022d. URL https://iea.blob.core.windows.net/assets/830fe099-5530-48f2-a7c1-11f35d510983/WorldEnergyOutlook2022.pdf.

IEC. International electrotechnical commission, iec 61427-2 secondary cells and batteries for renewable energy storage – general requirements and methods of test – part 2: On-grid applications, 2015.

IEC. International electrotechnical commission, iec 62660-1 secondary lithium-ion cells for the propulsion of electric road vehicles - part 1: Performance testing, 2018.

IEC. International electrotechnical commission, iec 62932-2-1 flow battery energy systems for stationary applications – part 2-1: Performance general requirements and test methods, 2020.

IS. Indian standard, is 16893-2 secondary lithium - ion cells for the propulsion of electric road vehicles: Part 2 reliability and abuse testing, 2018.

ISO. International organization for standardization, iso 12405-4 electrically propelled road vehicles —test specification for lithium-ion traction battery packs and systems — part 4: Performance testing, 2018.

A. Jain. How rechargeable batteries, charging, and discharging cycles work, n.d. URL https://www.engineersgarage.com/how-rechargeable-batteries-charging-and-discharging-cycles-work/.

T. Joshi. *Capacity and power fade in Lithium-ion batteries*. Doctor of philosophy in the school of chemical biomolecular engineering, Georgia Institute of Technology, May 2016.

M. Kassem, J. Bernard, R. Revel, S. Pelissier, F. Duclaud, and C. Delacourt. Calendar aging of a graphite/lifepo4 cell. *Journal of Power Sources*, 208:296–305, 2012.

D. Kaur, M. Singh, and S. Singh. Lithium–sulfur batteries for marine applications. In *Lithium-Sulfur Batteries*, pages 549–577. Elsevier, 2022.

W. Kester and J. Buxton. Battery chargers, section 5. Technical report, 2015. URL https://www.analog.com/media/en/training-seminars/design-handbooks/Practical-Design-Techniques-Power-Thermal/Section5.pdf.

S. Laestander. Battery and degradation modeling of hybrid electric heavy-duty long hauler. Master of science thesis, KTH School of Industrial Engineering and Management, Stockholm, Sweden, 2017. Division of Heat and Power Technology.

A. Lajunen, P. Sainio, L. Laurila, and J. Tammi. Overview of powertrain electrification and future scenarios for non-road mobile machinery. *Energies*, 11:1184, 2018.

J. Lamb and C. J. Orendorff. Evaluation of mechanical abuse techniques in lithium ion batteries. *Journal of Power Sources*, 247:189–196, 2014.

A. Laumann, M. Bremholm, P. Hald, M. Holzapfel, K. T. Fehr, and B. B. Iversen. Rapid green continuous flow supercritical synthesis of high performance li4ti5o12 nanocrystals for li ion battery applications. *Journal of the Electrochemical Society*, 159(2):A166, 2011.

H. Liu, Z. Deng, Y. Yang, C. Lu, B. Li, C. Liu, and D. Cheng. Capacity evaluation and degradation analysis of lithium-ion battery packs for on-road electric vehicles. *Journal of Energy Storage*, 65:107270, 2023.

K. Liu, Q. Li, C. Peng, and Zhang. A brief review on key technologies in the battery management system of electric vehicles. *Frontiers of Mechanical Engineering*, pages 47–64, 2019.

X. Liu, J. Wu, C. Zhang, and Z. Chen. A method for state of energy estimation of lithium-ion batteries at dynamic currents and temperatures. *Journal of Power Sources*, 270:151–157, 2014.

Z. Liu, J. Xie, H. He, K. Wang, and W. Huang. Prediction method for battery self-discharge voltage drop based on pre-classifier. *Measurement*, 204:112065, 2022.

Z. Lu, Q. Zhang, Y. Yuan, and W. Tong. Optimal driving range for battery electric vehicles based on modeling users' driving and charging behavior. *Journal of Advanced Transportation*, 2020:1–10, 2020.

L. Ma, C. Hu, and F. Cheng. State of charge and state of energy estimation for lithium-ion batteries based on a long short-term memory neural network. *Journal of Energy Storage*, 37: 102440, 2021.

S. Ma, M. Jiang, P. Tao, C. Song, J. Wu, J. Wang, T. Deng, and W. Shang. Temperature effect and thermal impact in lithium-ion batteries: A review. *Progress in Natural Science: Materials International*, 28(6):653–666, 2018.

H. Maleki and J. N. Howard. Effects of overdischarge on performance and thermal stability of a li-ion cell. *Journal of power sources*, 160(2):1395–1402, 2006.

J. Marsh. Comparing lithium-ion battery chemistries, 2019. URL https://news.energysage.com/comparing-lithium-ion-battery-chemistries/.

N. Meddings, M. Heinrich, F. Overney, J.-S. Lee, V. Ruiz, E. Napolitano, S. Seitz, G. Hinds, R. Raccichini, M. Gaberšček, et al. Application of electrochemical impedance spectroscopy to commercial li-ion cells: A review. *Journal of Power Sources*, 480:228742, 2020.

G. Meyer, R. Bucknall, and D. Breuil. Electrification of the transport system. Technical report, European Commission's Direcorate-General for Research and Innovation, European Commission, B-1049 Brussels, 2017.

Y. Miao, P. Hynan, A. Von Jouanne, and A. Yokochi. Current li-ion battery technologies in electric vehicles and opportunities for advancements. *Energies*, 12(6):1074, 2019.

K. Momidi. What causes battery degradation in electric vehicles and how to avoid it?, 2019. URL https://circuitdigest.com/article/what-causes-battery-degradation-in-electric-vehicles-and-how-to-avoid-it.

S. Mothilal Bhagavathy, H. Budnitz, T. Schwanen, and M. McCulloch. Impact of charging rates on electric vehicle battery life. *Findings*, 2021(March), 2021.

K. Moy, S. B. Lee, S. Harris, and S. Onori. Design and validation of synthetic duty cycles for grid energy storage dispatch using lithium-ion batteries. *Advances in Applied Energy*, 4: 100065, 2021.

I. R. of Shipping. Guidelines on battery powered vessels. Technical report, Indian Register of Shipping, 2019.

M. G. Omran, A. P. Engelbrecht, and A. Salman. An overview of clustering methods. *Intelligent Data Analysis*, 11(6):583–605, 2007.

C. Pillot. Eu battery demand and supply (2019-2030) in a global context. Technical report, Avicenne Energy/EUROBAT, 2020.

M. Qadrdan, N. Jenkins, and J. Wu. Smart grid and energy storage. In *McEvoy's Handbook of Photovoltaics*, chapter 2, pages 915–928. Elsevier, 2018.

Research and Markets. Global marine battery markets report 2021-2030 with focus on battery type, propulsion type, ship type, sales channel, nominal capacity, battery design, battery function. Technical report, Research and Markets, 2021.

D. Rosewater and D. Schoenwald. *U.S. DOE Energy Storage Handbook*, chapter 16: Energy Storage Performance Testing. U.S. DOE, 2020.

V. Ruiz. Standards for the performance and durability assessment of electric vehicle batteries. Technical report, Joint Research Centre (JRC), 2018.

V. Ruiz, A. Kriston, I. Adanouj, M. Destro, D. Fontana, and A. Pfrang. Degradation studies on lithium iron phosphate-graphite cells. the effect of dissimilar charging–discharging temperatures. *Electrochimica Acta*, 240:495–505, 2017.

SAC. Standard administration of china, sac qc/t 743 lithium-ion batteries for electric vehicles, 2006.

SAE. Society of automotive engineers, sae j1798 recommended practice for performance rating of electric vehicle battery modules, 2008.

Safety4Sea. 352 confirmed ships are using battery installations, 2019. URL https://safety4sea.com/352-confirmed-ships-are-using-battery-installations/.

S. Samsung. *Samsung INR21700-40T3 Datasheet*. Samsung, March 2020. Energy Business Division.

C. Secure Power. Ups battery impedance testing, 2023. URL https://securepower.com/impedance-testing/.

X. Seront, R. Fernandez, N. Mandl, and E. Rigler. Annual european union greenhouse gas inventory 1990–2020 and inventory report 2022. Technical report, European Environment Agency and European Commission, DG Climate Action, European Commission, DG Climate Action, BU 5 2/158, B-1049 Brussels, May 2022.

J. Shepard. How to read battery discharge curves. *Battery Power Tips*, July 2021.

I. SparkFun Electronics. Lithium ion rechargeable batteries. Technical report, SparkFun Electronics, 2018. URL https://cdn.sparkfun.com/datasheets/Prototyping/Lithium%20Ion%20Battery%20MSDS.pdf.

A.-I. Stan, M. Świerczyński, D.-I. Stroe, R. Teodorescu, and S. J. Andreasen. Lithium ion battery chemistries from renewable energy storage to automotive and back-up power applications—an overview. In *2014 International Conference on Optimization of Electrical and Electronic Equipment (OPTIM)*, pages 713–720. IEEE, 2014.

Statista. Projections for the electric truck market volume in europe between 2018 and 2026, by truck type. Technical report, 2021. URL https://www.statista.com/statistics/1283443/europe-electric-truck-type-market-forecast/.

T. Sterling, M. Brodowicz, and M. Anderson. *High performance computing: modern systems and practices*. Morgan Kaufmann, 2017.

I. Straits Research. Battery Market Size, Share Trends Analysis Report By Product (Lead Acid, Li-ion, Nickle Metal Hydride, Ni-Cd), By Application, By End-use, By Region, And Segment Forecasts, 2023 - 2030, 2022. URL https://straitsresearch.com/report/battery-testing-equipment-market.

Y. Sun, S. Wang, F. Xiao, and D. Gao. Peak load shifting control using different cold thermal energy storage facilities in commercial buildings: A review. *Energy conversion and management*, 71:101–114, 2013.

Y. Sun, S. Saxena, and M. Pecht. Derating guidelines for lithium-ion batteries. *Energies*, 11 (12):3295, 2018.

N. Sustainable Truck & Van. Electric heavy truck market, 2023. URL https://www.sustainabletruckvan.com/electric-truck-market-2022-volvo-trucks/.

C. Syms. Principal components analysis. Elsevier, 2008.

P. Szymanski, B. Ciuffo, G. Fontaras, G. Martini, and F. Pekar. The future of road transport in europe. environmental implications of automated, connected and low-carbon mobility. *Combustion Engines*, 60, 2021. URL https://www.researchgate.net/publication/354572007_The_future_of_road_transport_in_Europe_Environmental_implications_of_automated_connected_and_low-carbon_mobility.

M. Taljegard. The impact of an electrification of road transportation on the electricity system in scandinavia. Degree thesis, Chalmers University of Technology, Gothenberg, Sweden, 2017. URL https://publications.lib.chalmers.se/records/fulltext/253394/253394.pdf. Department of Space, Earth and Environment.

R. Tian, S.-H. Park, P. J. King, G. Cunningham, J. Coelho, V. Nicolosi, and J. N. Coleman. Quantifying the factors limiting rate performance in battery electrodes. *Nature communications*, 10(1):1933, 2019.

K. Uddin, A. Picarelli, C. Lyness, N. Taylor, and J. Marco. An acausal li-ion battery pack model for automotive applications. *Energies*, 7(9):5675–5700, 2014.

U.S.DoE. Usabc electric vehicle battery test procedure manual. Technical report, Idaho National Laboratory of the U.S. Department of Energy (U.S.DoE, 1996.

J. P. C. U.S.DoE. Battery test manual for electric vehicles. Technical report, U.S. Department of Energy (U.S. DoE, June 2015.

U. UT Austin. Standard potentials. Technical report, Texas University, April 2013.

C. Vartanian, M. Paiss, V. Viswanathan, J. Kolln, and D. Reed. Review of codes and standards for energy storage systems. *Current Sustainable/Renewable Energy Reports*, 8:138–148, 2021.

O. Veneri, editor. *Technologies and Applications for Smart Charging of Electric and Plug-in Hybrid Vehicles*. Springer International Publishing, 2017. doi: 10.1007/978-3-319-43651-7. URL https://doi.org/10.1007%2F978-3-319-43651-7.

B. Veritas. Entering a new era for battery-powered ships, 2021. URL https://marine-offshore.bureauveritas.com/insight/entering-new-era-battery-powered-ships#_ftn1.

J. Verma and D. Kumar. Recent developments in energy storage systems for marine environment. *Materials Advances*, 2(21):6800–6815, 2021.

S. Verma, S. Mishra, A. Gaur, S. Chowdhury, S. Mohapatra, G. Dwivedi, and P. Verma. A comprehensive review on energy storage in hybrid electric vehicle. *Journal of Traffic and Transportation Engineering (English Edition)*, 8(5):621–637, 2021.

C. Volvo Trucks. Volvo trucks leads the electric truck market in europe, 2022. URL https://www.volvotrucks.com/en-en/news-stories/press-releases/2022/feb/volvo-trucks-leads-the-electric-truck-market-in-europe.html.

E. Wikner. *Lithium ion battery aging: Battery lifetime testing and physics-based modeling for electric vehicle applications*. Chalmers Tekniska Hogskola (Sweden), 2017.

H. Zhang, W. Liu, Y. Dong, H. Zhang, and H. Chen. A method for pre-determining the optimal remanufacturing point of lithium ion batteries. *Procedia CIRP*, 15:218–222, 2014.

Q. Zhang, N. Cui, Y. Shang, B. Duan, and C. Zhang. An improved peukert battery model of nonlinear capacity considering temperature effect. *IFAC-PapersOnLine*, 51(31):665–669, 2018.

Y. Zhang, C.-Y. Wang, and X. Tang. Cycling degradation of an automotive lifepo4 lithium-ion battery. *Journal of power sources*, 196(3):1513–1520, 2011.

Appendix

Standard Potentials at 25°C

(v4 : 4-29-13)

Half Reaction	Potential
$F_2 + 2e^- \rightleftharpoons 2F^-$	+2.87 V
$O_3 + 2H^+ + 2e^- \rightleftharpoons O_2 + H_2O$	+2.07 V
$S_2O_8^{2-} + 2e^- \rightleftharpoons 2SO_4^{2-}$	+2.05 V
$H_2O_2 + 2H^+ + 2e^- \rightleftharpoons 2H_2O$	+1.78 V
$PbO_2 + 4H^+ + SO_4^{2-} + 2e^- \rightleftharpoons PbSO_4 + 2H_2O$	+1.69 V
$Au^+ + e^- \rightleftharpoons Au$	+1.69 V
$Pb^{4+} + 2e^- \rightleftharpoons Pb^{2+}$	+1.67 V
$2\,HClO + 2H^+ + 2e^- \rightleftharpoons Cl_2 + 2H_2O$	+1.63 V
$Ce^{4+} + e^- \rightleftharpoons Ce^{3+}$	+1.61 V
$MnO_4^- + 8H^+ + 5e^- \rightleftharpoons Mn^{2+} + 4H_2O$	+1.51 V
$Au^{3+} + 3e^- \rightleftharpoons Au$	+1.40 V
$Cl_2 + 2e^- \rightleftharpoons 2Cl^-$	+1.36 V
$Cr_2O_7^{2-} + 14H^+ + 6e^- \rightleftharpoons 2Cr^{3+} + 7H_2O$	+1.33 V
$O_2 + 4H^+ + 4e^- \rightleftharpoons 2H_2O$	+1.23 V
$MnO_2 + 4H^+ + 2e^- \rightleftharpoons Mn^{2+} + 2H_2O$	+1.21 V
$Pt^{2+} + 2e^- \rightleftharpoons Pt$	+1.20 V
$Br_2 + 2e^- \rightleftharpoons 2Br^-$	+1.09 V
$Pd^{2+} + 2e^- \rightleftharpoons Pd$	+0.915 V
$2Hg^{2+} + 2e^- \rightleftharpoons Hg_2^{2+}$	+0.92 V
$ClO^- + H_2O + 2e^- \rightleftharpoons Cl^- + 2OH^-$	+0.89 V
$Ag^+ + e^- \rightleftharpoons Ag$	+0.80 V
$Hg_2^{2+} + 2e^- \rightleftharpoons 2Hg$	+0.79 V
$Fe^{3+} + e^- \rightleftharpoons Fe^{2+}$	+0.77 V
$MnO_4^- + 2H_2O + 3e^- \rightleftharpoons MnO_2 + 4OH^-$	+0.60 V
$I_2 + 2e^- \rightleftharpoons 2I^-$	+0.54 V
$O_2 + 2H_2O + 4e^- \rightleftharpoons 4OH^-$	+0.40 V
$Cu^{2+} + 2e^- \rightleftharpoons Cu$	+0.34 V
$Hg_2Cl_2 + 2e^- \rightleftharpoons 2Hg + 2Cl^-$	+0.27 V
$AgCl + e^- \rightleftharpoons Ag + Cl^-$	+0.22 V
$Bi^{3+} + e^- \rightleftharpoons Bi$	+0.20 V
$NO_3^- + H_2O + 2e^- \rightleftharpoons NO_2^- + 2OH^-$	+0.01 V
$2H^+ + 2e^- \rightleftharpoons H_2$	**0.000 V**

Half Reaction	Potential
$2H^+ + 2e^- \rightleftharpoons H_2$	**0.000 V**
$Fe^{3+} + 3e^- \rightleftharpoons Fe$	−0.04 V
$Pb^{2+} + 2e^- \rightleftharpoons Pb$	−0.13 V
$Sn^{2+} + 2e^- \rightleftharpoons Sn$	−0.14 V
$Ni^{2+} + 2e^- \rightleftharpoons Ni$	−0.23 V
$V^{3+} + e^- \rightleftharpoons V^{2+}$	−0.26 V
$Co^{2+} + 2e^- \rightleftharpoons Co$	−0.28 V
$In^{3+} + 3e^- \rightleftharpoons In$	−0.34 V
$PbSO_4 + 2e^- \rightleftharpoons Pb + SO_4^{2-}$	−0.36 V
$Cd^{2+} + 2e^- \rightleftharpoons Cd$	−0.40 V
$Cr^{3+} + e^- \rightleftharpoons Cr^{2+}$	−0.41 V
$Fe^{2+} + 2e^- \rightleftharpoons Fe$	−0.44 V
$U^{4+} + e^- \rightleftharpoons U^{3+}$	−0.61 V
$FeCO_3 + 2e^- \rightleftharpoons Fe + CO_3^{2-}$	−0.756 V
$Zn^{2+} + 2e^- \rightleftharpoons Zn$	−0.76 V
$2H_2O + 2e^- \rightleftharpoons H_2 + 2OH^-$	−0.83 V
$Cr^{2+} + 2e^- \rightleftharpoons Cr$	−0.91 V
$Mn^{2+} + 2e^- \rightleftharpoons Mn$	−1.18 V
$V^{2+} + 2e^- \rightleftharpoons V$	−1.19 V
$ZnS + 2e^- \rightleftharpoons Zn + S^{2-}$	−1.44 V
$Al^{3+} + 3e^- \rightleftharpoons Al$	−1.66 V
$Mg^{2+} + 2e^- \rightleftharpoons Mg$	−2.36 V
$Na^+ + e^- \rightleftharpoons Na$	−2.71 V
$K^+ + e^- \rightleftharpoons K$	−2.92 V
$Li^+ + e^- \rightleftharpoons Li$	−3.05 V

Note: all ions are aqueous (aq), many neutral species are solids (s), although some are liquids (l), gases (g), and even aqueous (aq). Use other sources for details on state. They were purposely left off here to save space and keep a cleaner looking table.

Figure 78: Standard Electrode Potential